(12) INTERNATIONAL APPLICATION PUBLISHED UNDER THE PATENT COOPERATION TREATY (PCT)

(19) World Intellectual Property Organization
International Bureau

(43) International Publication Date
21 January 2010 (21.01.2010)

PCT

(10) International Publication Number
WO 2010/009146 A1

(51) International Patent Classification:
A61K 9/26 (2006.01)

(21) International Application Number:
PCT/US2009/050565

(22) International Filing Date:
14 July 2009 (14.07.2009)

(25) Filing Language: English

(26) Publication Language: English

(30) Priority Data:

61/081,034	15 July 2008 (15.07.2008)	US
61/081,037	16 July 2008 (16.07.2008)	US

(71) Applicant *(for all designated States except US)*: **UNIVERSITY OF KANSAS** [US/US]; 2385 Irving Hill Road, Youngberg Hall, Lawrence, KS 66045 (US).

(72) Inventors; and

(75) Inventors/Applicants *(for US only)*: **BERKLAND, Cory, J.** [US/US]; 18329 Northwind Drive, Lawrence, KS 66044 (US). **BAILEY, Mark** [US/US]; 6612 Tenth Street, B2, Alexandria, VA 22307 (US). **EL GENDY, Nashwa** [EG/EG]; 29 El-Galaa Street, #5, El-Naam, Helmiate El-Zaiyoun, Cairo (EG). **PLUMLEY, Carl** [US/US]; 11717 Elmridge Circle, Little Rock, AR 72211 (US).

(74) Agent: **LECOINTE, Michelle, M.**; Baker Botts L.L.P., 98 San Jacinto Blvd., 1500 San Jacinto Center, Austin, TX 78701-4039 (US).

(81) Designated States *(unless otherwise indicated, for every kind of national protection available)*: AE, AG, AL, AM, AO, AT, AU, AZ, BA, BB, BG, BH, BR, BW, BY, BZ, CA, CH, CL, CN, CO, CR, CU, CZ, DE, DK, DM, DO, DZ, EC, EE, EG, ES, FI, GB, GD, GE, GH, GM, GT, HN, HR, HU, ID, IL, IN, IS, JP, KE, KG, KM, KN, KP, KR, KZ, LA, LC, LK, LR, LS, LT, LU, LY, MA, MD, ME, MG, MK, MN, MW, MX, MY, MZ, NA, NG, NI, NO, NZ, OM, PE, PG, PH, PL, PT, RO, RS, RU, SC, SD, SE, SG, SK, SL, SM, ST, SV, SY, TJ, TM, TN, TR, TT, TZ, UA, UG, US, UZ, VC, VN, ZA, ZM, ZW.

(84) Designated States *(unless otherwise indicated, for every kind of regional protection available)*: ARIPO (BW, GH, GM, KE, LS, MW, MZ, NA, SD, SL, SZ, TZ, UG, ZM, ZW), Eurasian (AM, AZ, BY, KG, KZ, MD, RU, TJ, TM), European (AT, BE, BG, CH, CY, CZ, DE, DK, EE, ES, FI, FR, GB, GR, HR, HU, IE, IS, IT, LT, LU, LV, MC, MK, MT, NL, NO, PL, PT, RO, SE, SI, SK, SM, TR), OAPI (BF, BJ, CF, CG, CI, CM, GA, GN, GQ, GW, ML, MR, NE, SN, TD, TG).

Declarations under Rule 4.17:

— *as to applicant's entitlement to apply for and be granted a patent (Rule 4.17(ii))*

— *as to the applicant's entitlement to claim the priority of the earlier application (Rule 4.17(iii))*

Published:

— *with international search report (Art. 21(3))*

(54) **Title**: NANOCLUSTERS FOR DELIVERY OF POORLY WATER SOLUBLE DRUG NANOPARTICLES

FIG.1

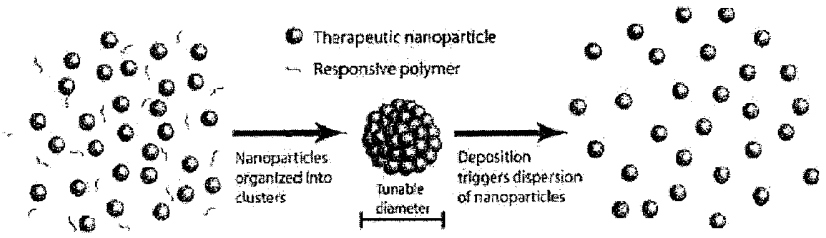

(57) **Abstract**: The present invention discloses compositions and methods for preparing a nanocluster that includes a plurality of nanoparticles that comprise a drug substance. Also disclosed are methods for preventing or treating a disease in a subject by administering a therapeutically effective amount of a composition comprising the nanoclusters of the present invention.

WO 2010/009146 A1

NANOCLUSTERS FOR DELIVERY OF POORLY WATER SOLUBLE DRUG NANOPARTICLES

CROSS-REFERENCE TO RELATED APPLICATIONS

This application claims the benefit of U.S. Provisional Patent Application Serial No. 61/081,034, filed July 15, 2008 and 61/081,037, filed July 16, 2008, the entire disclosure of which is hereby incorporated by reference.

FIELD OF THE INVENTION

The present invention relates generally to delivery vehicles that can be used to transport active ingredients to a subject. In certain aspects, the delivery vehicles can be nanoclusters that can be used in preventative or therapeutic applications.

BACKGROUND

Millions of people worldwide suffer from a wide variety of diseases or conditions that would benefit from the effective delivery of therapeutic and or preventative agents. Examples of these diseases or conditions include pulmonary diseases, circulatory diseases, muscular diseases, bone diseases, cancers, etc.

The use of nanoparticles as drug delivery vehicles has been employed for a variety of indications (John 2003). Nanoparticles, for example, have been shown to improve the dissolution of poorly water-soluble drugs and enhance the transport of drugs both intra- and paracellularly. In addition, literature indicates that plasmid DNA can be effectively delivered by polycantionic polymers that form nanoparticles when mixed with DNA resulting in enhanced gene expression (Kumar 2003). Research efforts on nanoparticle-mediated gene therapy also address treating genetic disorders such as Cystic Fibrosis (Griesenbach 2004).

Most nanoparticle formulations are designed for action at the cellular level. This assumes the efficient delivery of the nanoparticle to the appropriate cellular target. However, current nanoparticle treatment options are limited in the ability to access the cellular target. For example, two research groups are currently investigating microencapsulated nanoparticles as a mode of nanoparticle delivery to the pulmonary epithelium (Sham 2004, Grenha 2005). These efforts are hindered by the common inability to control microparticle size, distribution, and difficulty in

delivering a large payload of therapeutic nanoparticles.

SUMMARY OF THE INVENTION

The present invention overcomes the deficiencies in the art by providing effective drug delivery systems that can: (1) formulate nanoparticles as a nanocluster to facilitate handling, administering, or targeting, for example; and (2) maintain the cluster or disperse the nanoparticles at the targeted site.

In one aspect of the present invention, there is disclosed a nanocluster comprising a plurality of nanoparticles. In certain non-limiting aspects, the nanocluster is maintained at the targeted site (e.g., the nanocluster does not disperse into separate nanoparticles). In other aspects, the nanoparticles disperse in response to an environmental cue. The nanocluster, in certain non-limiting embodiments, can have a size of about 1 to about 200 microns. In certain aspects, the nanocluster size is 1, 2, 3, 4, 5, 6, 7, 8, 9, 10, 11, 12, 13, 14, 15, 16, 17, 18, 19, 20, 21, 22, 23, 24, 25, 26, 27, 28, 29, 30, 31, 32, 33, 34, 35, 36, 37, 38, 39, 40, 45, 50, 55, 60, 65, 70, 75, 80, 85, 90, 95, 100, 110, 120, 130, 140, 150, 160, 170, 180, 190, or 200 microns. In other aspects, the size of the nanocluster can be greater than 200 microns (e.g., 210, 220, 230, 240, 250, 300, 350, 400, 450, 500, 600, 700, or more microns in size.) The nanocluster of the present invention can also have a variety of shapes (e.g., spherical and non-spherical shapes). In certain embodiments, the nanocluster can be solid or hollow. A person of ordinary skill in the art will recognize that a solid nanocluster can be completely solid throughout or can have spaces, such as pores or a hollow core, that are created by the packing of the nanoparticles within the nanocluster. The size of these packing spaces can be from about 1 nm to about 1000 nm, in non-limiting aspects. In certain aspects, the size of the packing spaces can be about 1, 2, 3, 4, 5, 6, 7, 8, 9, 10, 20, 30, 40, 50, 60, 70, 80 , 90, 100, 150, 200, 250, 300, 350, 400, 450, 500, 550, 600, 650, 700, 750, 800, 850, 900, 950, 1000 or more nanometers, in non-limiting aspects. Hollow nanoclusters can have an empty space or cavity. The size of the cavity can vary, for example, from about 50 m to about 20 μm, in non limiting aspects. The size of the cavity, for example, can be 50, 100, 150, 200, 250, 300, 3500, 400, 450, 500, 550, 600, 650, 700, 750, 800 . . . 20 μm, and any range derivable therein.

The nanoparticles that are included in the nanocluster, in some embodiments, are not held (e.g., adhered or chemically bound (e.g., covalent bond, non-covalent bond, van der waals forces)) together by a functional group on the nanoparticles. The nanoparticles can be in direct contact

with one another in some aspects. In other aspects, the nanoparticles are not in direct contact with one another. In certain embodiments of the present invention, the nanoparticles are not encapsulated. In other embodiments, the nanoparticles do not include a functional group. In other aspects, however, the nanoparticles can include a functional group such as, for example, a carboxyl, sulhydryl, hydroxyl, or amino group. All types of functional groups that can be used to bind other nanoparticles together, active ingredients to the surface of nanoparticles, or other compounds are contemplated as being useful with the present invention.

In certain embodiments, the nanocluster can include an active ingredient. Non-limiting examples of active ingredients that are contemplated as being useful in the context of the present invention include those known to a person of ordinary skill and those described throughout this specification. By way of example only, active ingredients can include medical pharmaceuticals and specialties such as preventive agents, for example vaccines, diagnostic agents, for example tracers of various types and imaging enhancers, therapeutic agents, for example small molecules (e.g., nucleic acids, proteins, peptides, polypeptides, etc.), drugs, peptides, and radiation, immuno-modulators, vaccine and virus vectors, and combinations of these classes. The nanoparticles can include particular embodiments, respirable non-medical specialties such as physiochemical agents, for example gas antidotes, biophysical modulators, for example paramagnetics, emitters, for example electromagnetic wave emitters, and imaging enhancers. The active ingredients, in certain embodiments, can be associated with the nanoparticles. For example, the active ingredients can be entangled, embedded, incorporated, encapsulated, bound to the surface (e.g., covalently or non-covalently bonded), or otherwise associated with the nanoparticle. In certain preferred aspects, the active ingredient is the nanoparticle. In other aspects, the nanoparticles can include a polymer material (including, for example, biodegradable and non-biodegradable polymers). Non-limiting examples of polymer materials that can be used include those known to a person of ordinary skill and those described throughout this specification. In certain embodiments, the nanoparticles can include a mixture of a polymer and an active ingredient.

In other non-limiting embodiments, the nanocluster or nanoparticles, or both, can include at least one, two, three, four, five, six, seven, or more different active ingredients. In a preferred embodiment, the nanocluster or nanoparticles include a first drug on its surface, and a second active ingredient encapsulated within the nanocluster or nanoparticles or other incorporated into the nanocluster or nanoparticle material. It is contemplated that a nanocluster can release the

active ingredients in a given environment, or after a given period of time in a controlled manner. For example, a nanocluster having at least one active ingredient can be released in response to an environmental cue or after a pre-determined amount of time. Also by way of example only, a nanocluster having at least two different active ingredients can be released in response to different environmental cues or after pre-determined periods of time. For example, active ingredient 1 can be released first and then active ingredient 2 can be released second. In certain non-limiting aspects, the release of the first active ingredient can improve the performance of the second active ingredient.

In other particular aspects, the nanoclusters of the present invention can include a dispersing material that holds the plurality of nanoparticles together and/or disperses the nanoparticles in response to an environmental cue. The dispersing materials that can be used with the present invention include those materials that are known to a person of skill in the art and those that are disclosed throughout this specification. Non-limiting examples of dispersing material include liquid sensitive materials (e.g., water-soluble materials (e.g., polymers)), biodegradable polymers, polyelectrolytes, metals, surfactants, polymeric cross-linkers, small molecule cross-linkers, pH sensitive materials, pressure sensitive materials, enzymatic sensitive materials, and temperature sensitive materials. Non-limiting examples of environmental cues that can be used with the present invention include liquid (e.g., water, blood, mucous, solvent, etc.), a selected pH range, a selected temperature range, an electric current, a selected ionic strength, pressure, the presence of a selected enzyme, protein, chemical, electromagnetic wavelength range (e.g., visible light, UV light, infrared, ultraviolet light, microwaves, X-rays, and gamma-rays), or the presence of an external force (e.g., vibration, shearing, shaking, etc.). In certain aspects, the dispersing material can be coated onto the surface of the nanoparticles before or after nanocluster formation. In certain embodiments, the dispersing material can be between the nanoparticles or link the nanoparticles together (e.g., covalently or non-covalently couple a first nanoparticle to a second nanoparticle). The dispersing material can be adhered to or covalently or non-covalently coupled to the nanoparticles.

In particular embodiments of the present invention, the nanocluster can include from about 1% to about 99% by weight or volume of the nanoparticles or dispersing materials. The nanocluster can also be completely made up of nanoparticles (i.e., 100%). In preferred embodiments, the nanocluster includes from about 10% to about 90%, 15% to about 80%, 20% to about 70%, 30% to about 60%, and about 40% to about 50% of nanoparticles or dispersing

materials. In certain embodiments, the nanocluster includes at least 50% of the nanoparticles or dispersing material.

Another embodiment to the present invention is a composition comprising a nanocluster of the present invention. The composition in certain non-limiting aspects can have a plurality (e.g., at least 2, 3, 4, 5, 6, 7, 8, 9, 10, 20, 30, 40, 50 , 60, 70, 80, 90, 100, 200, 300, 400, 500, or more nanoclusters. The composition can further include an active ingredient. As discussed throughout this specification, the composition can be formulated into a dry powder, an aerosol, a spray, a tablet, or a liquid. The compositions of the present invention can include at least about 1%, 2%, 3%, 4%, 5%, 6%, 7%, 8%, 9%, 10%, 15%, 20%, 25%, 30%, 35%, 40%, 45%, 50%, 55%, 60%, 65%, 70%, 75%, 80%, 85%, 90%, 95%, or 100% of the nanoclusters of the present invention. In certain aspects, the compositions of the present invention can include a plurality of identical or similar nanoclusters. In other aspects, the compositions of the present invention can include at least 2, 3, 4, 5, 6, 7, 8, 9, 10, or more nanoclusters that have different characteristics (e.g., different active ingredients attached, different shapes, hollow or solid, etc.). The compositions of the present invention can be formulated into a pharmaceutically acceptable carrier.

In another embodiment, there is disclosed a method of preventing or treating a disease or condition in a subject comprising administering a therapeutically effective amount of a composition comprising a nanocluster of the present invention to a subject (e.g., human, pigs, horses, cows, dogs, cats, mouse, rat, rabbit, or any other mammal and non-mammals) in need of the composition. The method can further include a method for determining whether a subject is in need of the prevention or treatment. The disease or condition can include all types of diseases or conditions known to a person of skill in the art and discussed throughout this specification. In certain preferred aspects, the disease or condition can be a pulmonary associated disease or condition (e.g., common cold, flu, cystic fibrosis, emphysema, asthma, tuberculosis, severe acute respiratory syndrome, pneumonia, lung cancer, etc.), a circulatory disease or condition, a muscular disease or condition, a bone disease or condition, an infection, a cancer, etc. In certain embodiments, the method can include the administration of a second therapy used to treat or prevent the disease (e.g., combination therapy). In preferred embodiments, the compositions of the present invention are administered nasally. Other modes of administration known to those of skill in the art or discussed in this specification are also contemplated. In particular aspects, the nanoclusters within the composition are delivered to the deep lung (e.g., bronchiole or alveolar regions of the lung).

In certain preferred aspects of the present invention, the nanoclusters of the present invention can be used to deliver vaccines or components of vaccines. For instance, cells of the immune system, especially macrophages and dendrocytes, are targets for immunization. These "professional" antigen-presenting cells (APCs) can elicit a desired T-cell response to vaccine components. APCs are typically capable of phagocytosis of particles in the range of 1 to 10 μm. By generating in this size range nanoclusters or nanoparticles containing vaccine components, one can passively target delivery of the vaccine to APCs. U.S. Pat. No. 6,669,961, for example, provides a non-limiting explanation of this process.

The nanoclusters of the present invention can also have a particular mass density. In certain preferred embodiments, for example, the mass density can be greater than, equal to, or less than 0.1 g/cm^3. In particular embodiments, the mass density of the nanoclusters of the present invention can be about 0.01, 0.02, 0.03, 0.04, 0.05, 0.06, 0.07, 0.08, 0.09, 0.1, 0.2, 0.3, 0.4, 0.5, 0.6, 0.7, 0.8, 0.9, 1.0, 1.1, 1.2, 1.3, 1.4, 1.5, 1.6, 1.7, 1.8, 1.9, 2.0 g/cm^3, or greater.

Also disclosed is a method of preparing a nanocluster comprising: (i) obtaining a plurality of nanoparticles; (ii) obtaining a dispersion material (when desired); and (iii) admixing (i) and (ii), wherein the admixture is formulated into a nanocluster. In certain aspects, obtaining a plurality of nanoparticles comprises: (i) obtaining an aqueous suspension of nanoparticles; (ii) emulsifying the suspension into a non-aqueous phase; (iii) allowing water in the aqueous suspension to absorb into the non-aqueous phase; (iv) allowing the nanoparticles to aggregate together; and (v) retrieving the aggregated nanoparticles. In other non-limiting embodiments, obtaining a plurality of nanoparticles includes: (i) obtaining a non-aqueous suspension of nanoparticles; (ii) emulsifying the suspension into an aqueous phase; (iii) allowing liquid in the non-aqueous suspension to absorb into the aqueous phase; (iv) allowing the nanoparticles to aggregate together; and (v) retrieving the aggregated nano particles. The disclosed method represents a non-limiting method with other methods being evident by one skilled in the art (e.g. Emulsion/solvent evaporation, extraction, spray-drying, spray freeze-drying, self-assembly in solution, etc.). In certain aspects, it is contemplated that the nanoclusters can be prepared in a solution without using spray and/or freeze dry techniques. It is also contemplated that the nanoclusters can be recovered from the solution by using freeze dry or spray dry techniques that are known to those of skill in the art. As noted throughout this specification, the nanocluster can be included within a composition. The composition can be formulated into a liquid, a spray, an aerosol, or a dry powder in non-limiting embodiments.

Also disclosed is a method of delivering an active ingredient to a subject in need comprising obtaining composition comprising a nanocluster of the present invention and an active ingredient and administering the composition to the subject. In non-limiting aspects, the active ingredient is encapsulated in the nanoparticle, incorporated within the nanoparticle material, conjugated to the nanoparticle, absorbed or coupled to the nanoparticle.

In yet another embodiment of the present invention, there is disclosed a method of preparing a nanocluster comprising: (i) obtaining a first nanoparticle and a second nanoparticle; and (ii) admixing the first and second nanoparticles, wherein the nanoparticles self assemble to form a nanocluster. The first and second nanoparticles, for example, can have hydrophobic properties, hydrophilic properties, or a mixture of both. In other aspects, the first or second nanoparticles can have an electrostatic charge. For example, the first nanoparticle can be positively charged and the second nanoparticle negatively charged, and vice versa. The self-assembly, in particular embodiments can be based on an electrostatic interaction between the first and second nanoparticles. In other non-limiting aspects, the self-assembly can be based on a hydrophobic or hydrophilic interaction between the first and second nanoparticles. The first and second nanoparticles can self assemble in solution to form the nanocluster in certain embodiments. In particular aspects, preparation of the nanoclusters does not require the use of spray and/or freeze dry techniques; rather nanocluster formation can occur in solution. The nanoclusters can be recovered from the solution by using freeze dry or spray dry techniques that are known to those of skill in the art. In other aspects, the method of preparing the nanocluster can further comprise obtaining a dispersion material and admixing the dispersion material with the first and second nanoparticles.

As disclosed is a method of storing nanoparticles comprising forming the nanoparticles into a nanocluster. The nanoparticles, for instance, can be stored as a liquid, a spray, and aerosol, or a dry powder. The method of storing the nanoparticles can further comprise returning the nanocluster to nanoparticles. In certain aspects, returning the nanocluster to nanoparticles can include subjecting the nanocluster to an environmental cue. As noted above and throughout this specification, non-limiting examples of environmental cues include water, a selected pH, a selected temperature, a selected enzyme, a selected chemical, a selected electromagnetic wavelength range, vibration, or shearing. In certain particular aspects, the nanocluster can include a dispersing material that holds the nanoparticles together and/or disperses the nanoparticles in response to an environmental cue. Non-limiting examples of dispersing materials include a water

soluble polymer, a biodegradable polymer, a polyelectrolyte, a metal, a polymeric cross-linker, a small molecule cross-linker, a pH sensitive material, a surfactant, or a temperature sensitive material.

It is contemplated that any embodiment discussed in this specification can be implemented with respect to any method or composition of the invention, and vice versa. Furthermore, compositions of the invention can be used to achieve methods of the invention.

The terms "inhibiting," "reducing," or "prevention," or any variation of these terms, when used in the claims and/or the specification includes any measurable decrease or complete inhibition to achieve a desired result.

The term "effective," as that term is used in the specification and/or claims, means adequate to accomplish a desired, expected, or intended result.

The use of the word "a" or "an" when used in conjunction with the term "comprising" in the claims and/or the specification may mean "one," but it is also consistent with the meaning of "one or more," "at least one," and "one or more than one."

The term "about" or "approximately" are defined as being close to as understood by one of ordinary skill in the art. In one non-limiting embodiment the terms are defined to be within 10%, preferably within 5%, more preferably within 1%, and most preferably within 0.5%.

The use of the term "or" in the claims is used to mean "and/or" unless explicitly indicated to refer to alternatives only or the alternatives are mutually exclusive, although the disclosure supports a definition that refers to only alternatives and "and/or."

As used in this specification and claim(s), the words "comprising" (and any form of comprising, such as "comprise" and "comprises"), "having" (and any form of having, such as "have" and "has"), "including" (and any form of including, such as "includes" and "include") or "containing" (and any form of containing, such as "contains" and "contain") are inclusive or open-ended and do not exclude additional, unrecited elements or method steps.

Other objects, features and advantages of the present invention will become apparent from the following detailed description. It should be understood, however, that the detailed description and the examples, while indicating specific embodiments of the invention, are given by way of illustration only. Additionally, it is contemplated that changes and modifications within the spirit and scope of the invention will become apparent to those skilled in the art from this detailed description.

DRAWINGS

Illustrative embodiments of the invention are illustrated in the drawings, in which:

FIG. 1. Therapeutic nanoparticles are organized into a nanocluster having a defined (and tunable) diameter. Upon contact with an environmental cue, the dispersive material triggers dispersion of the nanoparticles.

FIG. 2. Electron micrographs of (A) ~100 nm silica particles that compose the (B) ~6 μm nanocluster. (C) Represents typical nanocluster distribution. Scale bar in (C) represents 10 μm.

FIG. 3. Nanoclusters can be fabricated with a broad or narrow size distribution (left top and bottom). Adjusting fabrication conditions and/or dispersing material used allows for the formation of a solid (top right) or hollow (bottom right) clusters.

FIG. 4. Uniform (~75 μm) nanoclusters composed of polystyrene nanoparticles.

FIG. 5. Electron micrographs of (A) 225 nm silica nanoparticles coated with a dispersion material (light gray corona) and (B) a 9 μm nanocluster of the silica nanoparticles coated with dispersion material.

FIG. 6. The dispersion of nanoclusters over time composed of nanoparticles coated with a hydrolysable polymer was a function of pH as determined by (A) absorption of light at 480 nm and (B) visual inspection. (C) Size analysis of the dispersion shows polydisperse agglomerates are liberated from the nanoclusters, which then break down into monodisperse nanoparticles.

FIG. 7A, FIG. 7B, FIG. 7C. The (FIG. 7A) geometric and (FIG. 7B) aerodynamic size distributions of PLGA nanoclusters produced by increasing the concentration of nanoparticles (black=0.68 mg/ml, red=1.36 mg/ml, green=2.16 mg/ml, blue=2.72 mg/ml). FIG. 7C Scanning electron micrograph of nanocluster structure. Scale bar=5 μm.

FIG. 8A, FIG. 8B, FIG. 8C, FIG. 8D, FIG. 8E, FIG. 8F. Laser scanning confocal micrographs of PLGA nanoparticle nanoclusters. FITC-labeled PVAm-coated nanoparticles (FIG. 8A and FIG. 8D) and rhodamine-labeled PEMA-coated nanoparticles (FIG. 8B and FIG. 8E) are both identified within the nanocluster structure. FIG. 8C and FIG. 8F Overlays of the micrographs reveal the diffuse structure of the nanoclusters. Scale bar=5 μm.

FIG. 9. Scanning electron microscope (SEM) image of a population of nifedipine nanoparticles.

FIG. 10. SEM image of nifedipine nanoparticle clusters.

FIG. 11. Illustration of the geometric diameter of the nanoclusters comprising

DOTAP/PLGA nanoparticles and ovalbumin.

FIG. 12. SEM images of the nanoclusters comprising DOTAP/PLGA nanoparticles and ovalbumin.

FIG. 13. The particle size distributions of paclitaxel nanoparticle agglomerates in suspension after flocculation and resuspended after lyophilization.

FIG. 14. Aerodynamic size distributions of paclitaxel nanoparticle agglomerates after lyophilization.

FIG. 15. The distribution of Paclitaxel powder as received and nanoparticle agglomerate formulations deposited on the stages of a cascade impactor at a flow rate of ~30 L/min.

FIG. 16. In-vitro dissolution profiles of paclitaxel in PBS (pH 7.4) from pure paclitaxel powder and two different nanoparticle (NP) and nanoparticle agglomerate formulations (NA).

FIG 17. Viability of A549 cells in the presence of formulation components as determined by an MTS assay.

FIG. 18. The particle size distributions of budesonide nanoparticle agglomerates in suspension after flocculation and resuspended after lyophilization.

FIG. 19. Aerodynamic size distributions of budesonide nanoparticle agglomerates after lyophilization.

FIG. 20. The distribution of budesonide nanoparticle agglomerate formulations (A) F1, (B) F2, and (C) F3 deposited on the stages of a cascade impactor. (D) Formulations were compared with stock budesonide at a flow rate of ~30 L/min.

FIG. 21. Transmission electron micrographs of A) F1 nanoparticles and B) F1 nanoparticle agglomerates.

FIG. 22. 13C CP/MAS spectra of budesonide, excipients, and budesonide formulations. The nanoparticle agglomerates spectrum was expanded 8 times vertically to produce the nanoparticle agglomerates x8 spectrum to aid the interpretation of the budesonide peaks.

FIG. 23. Structure of budesonide with carbon numbering.

FIG. 24. 13C CP/MAS spectra from spectral editing experiment.

All = all carbon types are shown, C+CH3 = only unprotonated and methyl carbons are shown, C = only unprotonated carbons are shown, CH = only methine carbons are shown, and CH2 = only methylene carbons are shown.

FIG. 25. In-vitro dissolution profiles of budesonide in PBS (pH 7.4) from budesonide stock and three different nanoparticle (NP) and nanoparticle agglomerate formulations (NA).

FIG. 26. Viability of A549 cells in the presence of formulation components as determined by an MTS assay.

FIG. 27. Percent volume as a function of particle diameter for a flocculated solution of NIF/SA nanoparticles in water (421.7 +/- 26.2 nm, -32.16 +/- 3.75 mV) after addition of NaCl to 0.1M. Also shown is the same solution after homogenization at 25000 RPM for 30 seconds.

FIG. 28. Aerodynamic Diameter size distribution for the sample of nanoparticle flocculates shown in Figure 1.

FIG. 29. A collection of SEM images for nanoparticles directly after sonication (A), newly prepared flocculates (B), flocculate powders after residing under room conditions and devoid of light for 1 month (C), and pure nifedipine crystals as received (D).

FIG. 30. DSC outputs for the optimal formulation of nanoparticles, pure nifedipine, and flocculated nanoparticles.

FIG. 31. Percent drug dissolution vs. Time as deduced via HPLC UV spectroscopy for the nifedipine/stearic acid nanoparticles, flocculates, and the drug in pure crystalline form.

FIG. 32. Cascade impactor readings for nifedipine/stearic acid nanoparticles, flocculates, and drug as received in pure form.

FIG. 33. Particle size distributions for a flocculate sample and portions of the sample after three homogenization regimes. A nanoparticle solution (Before) was allowed to flocculate to completion without homogenization for 4 hours. Portions of the sample were then subject to increasingly powerful homogenization regimes (Low, Mid, High) from 5, 15, and 25 kRPM for 30 seconds, respectively.

FIG. 34. Particle size distributions for the flocculation of a nanoparticle suspension (336.1 +/- 5.9 nm, -34.42 +/- .73 mV) under a range of NaCl molarities (0.01, 0.1, 1, and 10 Molar) marked from lowest to highest. Salt was added with homogenization at 15 kRPM for 30 seconds.

FIG. 35. Particle size distributions for a nanoparticle solution and portions of the solution with MgSO4 added to vary molarities (0.1, 0.25, 0.5) marked as low, mid, high, respectively. Salt was added with homogenization at 15 kRPM for 30 seconds.

FIG. 36. The effects of sonication and homogenization on a flocculated suspension of nanoparticles. A solution of nanoparticles was allowed to flocculate to completion under 0.1M CaCl2. Portions of the solution were then subject to vary shear stresses. Hom refers to 2 minutes of homogenization at 15 kRPM, and Son refers to subsequent sonication at 60% amplitude for 10 seconds.

FIG. 37. Schematic of a typical Anderson cascade impactor. Adapted from Reference: Pharacotherapy, copyright 2003 Pharmacotherapy Publications.

FIG. 38. Outline of insulin processing method.

FIG. 39. Mass fraction of insulin in pellet vs. PH. Each value represents mean ± S.D of three experiments.

FIG. 40. Microparticle size vs. Nanoparticle size. Each value represents mean ± S.D of three experiments.

FIG. 41. SEM micrographs of insulin particles; (A) and (B) are unprocessed insulin particles (scale bars 30 pm and 10 pm, respectively); (C) and (D) are insulin microparticles after processing (scale bars 10 pm and 2 pm, respectively).

FIG. 42. Tap density of insulin powders. Each bar shows mean ± S.D. of three experiments.

FIG. 43. Circular dichroism of dissolved insulin powders. The top panel shows isothermal spectra, and the bottom panel shows variable temperature scan at a wavelength of 210 nm. Each value of the variable temperature scan represents mean ± S.D. of three experiments.

FIG. 44. 13C CP/MAS NMR spectra for insulin powders; (A) Unprocessed; (B) Insulin microparticles; (C) Lyophilized insulin nanoparticles; (D) Centrifuged and dried insulin nanoparticles.

FIG. 45. Percent crystallinity of insulin particles, as determined by the HPLC dissolution method described in the U.S. Pharmacopeia and National Formulary. Each bar shows mean ± S.D. of three experiments.

FIG. 46. Dissolution of insulin powders over time. Each value represents mean ± S.D. of three experiments.

DESCRIPTION

Current drug delivery treatment options can often be ineffective due to inefficient delivery of an active ingredient to a targeted site. Many of the current drug delivery systems are limited in their ability or efficiency to access a specifically targeted site. Although nanoparticles offer several advantages for delivering drugs (e.g. Improved dissolution of low solubility API, intracellular and transcellular transport, etc.), the use of nanoparticles, for example, can be hindered by the inability to deliver nanoparticles to the site of drug action (e.g. Dried nanoparticles are too small to deposit efficiently in the lungs, can avoid detection by APCs, etc.).

In addition, nanoparticles are often difficult to handle at an industrial scale and a controlled clustering process may ease handling and allow facile reconstitution and formulation of nanoparticles or nanoclusters for delivering drugs.

The nanoclusters of the present invention can be used to deliver active ingredients to a targeted site. The size and distribution of the disclosed nanoclusters and nanoparticles can be designed for a desired route of administration and/or for the treatment of a particular disease or condition. In one aspect, for example, the nanoclusters provide an effective and efficient drug delivery system that can carry nanoparticles to a targeted site via the nanocluster. In certain aspects, the nanocluster is maintained at the targeted site. In other aspects, the nanocluster can disperse the nanoparticles at the targeted site. Additionally, the nanoclusters can be formulated with the appropriate physicochemical properties to carry and controllably release therapeutic nanoparticles or active ingredients to a targeted site.

Another aspect of the invention is that the nanoclusters can be prepared in a solution without using standard spray and/or freeze dry techniques known to those of ordinary skill in the art.

These and other aspects of the present invention are described in further detail in the following sections.

A. Nanoclusters

In certain non-limiting aspects, a nanocluster of the present invention can include a plurality of nanoparticles with or without a dispersing material that holds the plurality of nanoparticles together. The dispersing material can also be used to disperse the nanoparticles in response to an environmental cue. An active ingredient can also be incorporated into the nanocluster. In other aspects, the nanoparticle can be the active ingredient. FIG. 1, for example, illustrates a nanocluster having a therapeutic nanoparticle and a dispersing material. This delivery system provides the advantage of particle clusters appropriately sized for delivery (e.g., lung, nasal passage, M-cells in the digestive tract, uptake by antigen presenting cells, etc.) with the benefits of nanoparticles, such as improvements in drug solubility, bioavailability, transport through biological barriers, intracellular delivery, etc. As described in more detail throughout this specification, changing the nature of the dispersing material allows for the development of an environmentally responsive nanoparticle delivery system and/or biosensors. In addition, the special arrangement of nanoparticles within the cluster can allow discrete control over the duration

and concentration of an active ingredient, a concept that can also be facilitated by the independent formulation of each nanoparticle type before cluster formation.

The inventors have successfully formulated nanoclusters from a variety of nanoparticulate materials and have controlled the dispersion of clusters into constituent nanoparticles in aqueous solution (see Examples 1-3 below). In a non-limiting aspect, the inventors obtained a colloidal suspension of nanoparticles in deionized water which is subsequently emulsified into octanol. Water in the dispersed droplets then absorbs into the octanol phase. Nanoparticles can pack together as water is extracted from individual droplets until an aggregate of nanoparticles remains (FIG. 2). The size of the droplet, in certain non-limiting embodiments, can serve as a template for controlling the size of the resulting nanoclusters depending on the concentration of nanoparticles within the droplet. In other aspects, the clustered nanoparticles in FIG. 2 can be held together by hydrophobic, coulombic, and/or Van der Waals forces and can resist dispersion into aqueous media.

These and other aspects of the nanoclusters of the present invention are described in further detail in the following subsections.

1. Nanoparticles

A nanoparticle is a microscopic particle whose size is measured in nanometers. In preferred embodiments, the nanoparticles of the present invention have a size of from about 1 to about 3000 nanometers. In more particular aspects, the nanoparticle has a size of 2, 3, 4, 5, 6, 7, 8, 9, 10, 11, 12, 13, 14, 15, 16, 17, 18, 19, 20, 25, 30, 35, 40, 45, 50, 55, 60, 65, 70, 75, 80, 85, 90, 95, 100, 110, 120, 130, 140, 150, 175, 200, 225, 250, 275, 300, 325, 350, 375, 400, 425, 450, 475, 500, 550, 600, 650, 700, 750, 800, 850, 900, 950, 1000, 1100, 1200, 1300, 1400, 1500, 1600, 1700, 1800, 1900, 2000, 2100, 2200, 2300, 2400, 2500, 2600, 2700, 2800, 2900, 3000, or more nanometers, or any range derivable therein.

It is contemplated that all types of materials and structures, including inorganic and organic materials, can be used for the nanoparticles of the present invention. Non-limiting examples of these materials and structures include active ingredients (see specification), polymersomes, liposomes, and polyplexes. Additional non-limiting materials include poly(orthoesters), poly(anhydrides), poly(phosphoesters), poly(phosphazenes) and others. In preferred aspects, the material is the biodegradable polymer poly(lactic-co-glycolic acid) (PLGA). PLGA is a well-studied polymer for drug delivery and is FDA-approved for a number of in vivo

applications. Other non-limiting materials include, for example, polyesters (such as poly(lactic acid), poly(L-lysine), poly(glycolic acid) and poly(lactic-co-glycolic acid)), poly(lactic acid-co-lysine), poly(lactic acid-graft-lysine), polyanhydrides (such as poly(fatty acid dimer), poly(fumaric acid), poly(sebacic acid), poly(carboxyphenoxy propane), poly(carboxyphenoxy hexane), copolymers of these monomers and the like), poly(anhydride-co-imides), poly(amides), poly(ortho esters), poly(iminocarbonates), poly(urethanes), poly(organophasphazenes), poly(phosphates), poly(ethylene vinyl acetate) and other acyl substituted cellulose acetates and derivatives thereof, poly(caprolactone), poly(carbonates), poly(amino acids), poly(acrylates), polyacetals, poly(cyanoacrylates), poly(styrenes), poly(vinyl chloride), poly(vinyl fluoride), poly(vinyl imidazole), chlorosulfonated polyolefins, polyethylene oxide, copolymers, polystyrene, and blends or co-polymers thereof. In certain preferred aspects, the nanoparticles include hydroxypropyl cellulose (HPC), N-isopropylacrylamide (NIPA), polyethylene glycol, polyvinyl alcohol (PVA), polyethylenimine, chitosan, chitin, dextran sulfate, heparin, chondroitin sulfate, gelatin, etc. And their derivatives, co-polymers, and mixtures thereof. A non-limiting method for making nanoparticles is described in U.S. Publication 2003/0138490, which is incorporated by reference.

In certain embodiments, the nanoparticles can be associated with an active ingredient (e.g., entangled, embedded, incorporated, encapsulated, bound to the surface, or otherwise associated with the nanoparticle). In certain preferred aspects, the active ingredient is the nanoparticle. In a preferred but non-limiting aspect, the active ingredient is a drug such as a pure drug (e.g., drugs processed by crystallization or supercritical fluids, an encapsulated drug (e.g., polymers), a surface associated drug (e.g., drugs that are absorbed or bound to the nanoparticle surface), a complexed drugs (e.g., drugs that are associated with the material used to form the nanoparticle).

The nanoparticles of the present invention, in certain embodiments, do not include a functional group. In other aspects, however, the nanoparticles can include a functional group such as, for example, a carboxyl, sulhydryl, hydroxyl, or amino group. All types of functional groups that can be used to bind other nanoparticles together, active ingredients to the surface of nanoparticles, or other compounds are contemplated as being useful with the present invention. For instance, the functional groups can be available for drug binding (covalent or electrostatic).

2. Dispersing Material

In certain aspects of the present invention, the dispersing material can serve several

functions. For example, it can be used to hold (e.g., adhere or chemical bind (e.g., covalent bond, no-covalent bond, van der wall forces) the nanoparticles to one another via the dispersing material. In other aspects, the dispersing material can disperse the nanoparticles at a targeted site in response to an environmental cue. This dispersing can occur, for example, when the dispersing material breaks-down, disintegrates, or other changes in such a way that it is no longer capable of holding the nanoparticles together.

Non-limiting examples of dispersing materials that are contemplated as being useful with the present invention include liquid sensitive materials (e.g., water-soluble materials) such as polyoxyethylene sorbitan fatty acid esters, polyglycerol fatty acid esters, polyoxyethylene derivatives, and analogues thereof, sugar esters, sugar ethers, sucroglycerides, (e.g. Sucrose, xylitol and sorbitol) etc., biodegradable polymers (see list of polymers for nanoparticle preparation), polyelectrolytes such as dextran sulfate, polyethylenimine, chitosan, chondroitin sulfate, heparin, heparin sulfate, poly(L-lysine), etc., metals (calcium, zinc, etc.), polymeric cross-linkers (polymethacrylate or similar derivatives with this functionality, poly(glutamic acid), poly(phosphorothioates), poly(propylene fumarate)-diacrylate, etc. And/or polymers with appropriate terminal or side chain reactive groups, small molecule cross-linkers (di-expoxies, di-acids, di-amines, etc.) such as 2-methylene-1,3-dioxepane, gluteraldehyde, dithiobis succinimidyl propionate, pH sensitive materials such as poly(γ-glutamic acid), enzymatic sensitive materials such as poly(amino acids) (peptides, proteins, etc.) like poly(N-substituted alpha/beta-asparagine)s, polysaccharides, lipids, oils, etc., and temperature sensitive material such as (2-hydroxyethyl methacrylate), poly(N-isopropylacrylamide), poly(2-ethylacrylic acid-co-N-[4-(phenylazo)phenyl]methacrylamide), polymers of acrylic acid or acrylamide and related polymers including and co-polymers or blends of these in addition to those previously mentioned as nanoparticle forming materials, and surfactants (e.g., nonionic, cationic, anionic, cryptoanionic, and zwitterionic surfactants (See McCutcheon's Emulsifiers & Detergents (2001); U.S. Pat. Nos. 5,011,681; 4,421,769; 3,755,560, 6,117,915)). Non-limiting examples of surfactants include esters of glycerin, esters of propylene glycol, fatty acid esters of polyethylene glycol, fatty acid esters of polypropylene glycol, esters of sorbitol, esters of sorbitan anhydrides, carboxylic acid copolymers, esters and ethers of glucose, ethoxylated ethers, ethoxylated alcohols, alkyl phosphates, polyoxyethylene fatty ether phosphates, fatty acid amides, acyl lactylates, soaps, TEA stearate, DEA oleth-3 phosphate, polyethylene glycol 20 sorbitan monolaurate (polysorbate 20), polyethylene glycol 5 soya sterol, steareth-2, steareth-20, steareth-21, ceteareth-20, PPG-2

methyl glucose ether distearate, ceteth-10, cetyl phosphate, potassium cetyl phosphate, diethanolamine cetyl phosphate, polysorbate 20, polysorbate 60, polysorbate 80, glyceryl stearate, PEG-100 stearate, tyloxapol, cetyltrimethylammonium bromide (CTAB), pluronic-68, and mixtures thereof.

Non-limiting examples of environmental cues that can cause the dispersing material to no longer be capable of holding the nanoparticles together include liquid (e.g., water, blood, mucous, solvent, etc.), a selected pH range, a selected temperature range, an electric current, a selected ionic strength, pressure, the presence of a selected enzyme, protein, DNA, chemical, electromagnetic wavelength range (e.g., visible light, UV light, infrared, ultraviolet light, microwaves, X-rays, and gamma-rays), or the presence of an external force (e.g., vibration, shearing, shaking, etc.).

3. Active Ingredients

In certain non-limiting aspects, the nanoclusters of the present invention can include an active ingredient. Active ingredients include, but are not limited to, any component, compound, or small molecule that can be used to bring about a desired effect. Non-limiting examples of desired effects of the present invention include diagnostic and therapeutic effects. For example, a desired effect can include the diagnosis, cure, mitigation, treatment, or prevention of a disease or condition. An active ingredient can also affect the structure or function of body part or organ in a subject.

Active ingredients which can be used by the present invention include but are not limited to nucleic acids, proteins and peptides, hormones and steroids, chemotherapeutics, NSAIDs, vaccine components, analgesics, antibiotics, anti-depressants, etc. Non-limiting examples of nucleic acids that can be used include DNA, cDNA, RNA, iRNA, siRNA, anti-sense nucleic acid, peptide-nucleic acids, oligonucleotides, or nucleic acids that are modified to improve stability (e.g., phosphorothioates, aminophosphonates or methylphosphonates).

Proteins and peptides that can be used with the present invention include but are not limited to human growth hormone, bovine growth hormone, vascular endothelial growth factor, fibroblast growth factors, bone morphogenic protein, tumor necrosis factors, erythropoietin, thrombopoietin, tissue plasminogen activator and derivatives, insulin, monoclonal antibodies (e.g., anti-human epidermal growth factor receptor2 (Herceptin), anti-CD20 (Rituximab), anti-CD 18, anti-vascular endothelial growth factor, anti-IgE, anti-CD 11a) and their derivatives,

single-chain antibody fragments, human deoxyribonuclease I (domase alfa, Pulmozyme), type-1 interferon, granulocyte colony-stimulating factor, leuteinizing hormone releasing hormone inhibitor peptides, leuprolide acetate, endostatin, angiostatin, porcine factor VIII clotting factor, interferon alfacon-1, pancrelipase (pancreatic enzymes), ovalbumin, nifedipine, loratadine, etc.

Non-limiting examples of hormones and steroids (e.g., corticosteroids) that can be used include norethindrone acetate, ethinyl estradiol, progesterone, estrogen, testosterone, prednisone and the like.

Chemotherapeutics that can be used include but are not limited to taxol (Paclitaxel), vinblastine, cisplatin, carboplatin, tamoxifen and the like.

Non-limiting examples of NSAIDs include piroxicam, aspirin, salsalate (Amigesic), diflunisal (Dolobid), ibuprofen (Motrin), ketoprofen (Orudis), nabumetone (Relafen), piroxicam (Feldene), naproxen (Aleve, Naprosyn), diclofenac (Voltaren), indomethacin (Indocin), sulindac (Clinoril), tolmetin (Tolectin), etodolac (Lodine), ketorolac (Toradol), oxaprozin (Daypro), and celecoxib (Celebrex).

Vaccine components that can be used include but are not limited to Hepatitis B, polio, measles, mumps, rubella, HIV, hepatitis A (e.g., Havrix), tuberculosis, etc.

Non-limiting examples of analgesics include but are not limited to aspirin, acetaminophen, ibuprofen, naproxen sodium and the like.

Antibiotics include but are not limited to amoxicillin, penicillin, sulfa drugs, erythromycin, streptomycin, tetracycline, clarithromycin, tobramycin, ciprofloxacin, terconazole, azithromycin and the like.

Anti-depressants include but are not limited to Zoloft, fluoxetine (Prozac), paroxetine (Paxil), citalopram, venlafaxine, fluvoxamine maleate, imipramine hydrochloride, lithium, nefazodone and the like.

Other active ingredient that can be used with the present invention include but are not limited to sildenafil (Viagra), acyclovir, gancyclovir, fexofenidine, celecoxib (Celebrex), rofecoxib, androstenedione, chloroquine, diphenhydramine HCl, buspirone, doxazocin mesylate, loratadine, clomiphine, zinc gluconate, zinc acetate, hydrocortisone, warfarin, indinavir sulfate, lidocaine, novacaine, estradiol, norethindrone acetate, medroxyprogesterone, dexfenfluramine, dextroamphetamine, doxycycline, thalidomide, fluticasone, fludarabine phosphate, etanercept, metformin hydrochloride, hyaluronate, tetrazocin hydrochloride, loperamide, ibogaine, clonazepam, ketamine, lamivudine (3TC), isotretinoin, nicotine, mefloquine, levofloxacin,

atorvastatin (Lipitor), miconazole nitrate (Monistat), ritonavir, famotidine, simvastatin (Zocor), sibutramine HCl monohydride, ofloxacin, lansoprozole, raloxifene (Evista), zanamivir (Relenza), oseltamivir phosphate, 4-phenylbutyric acid sodium salt, chlorpromazine, nevirapine, zidovudine, and cetirizine hydrochloride (Zyrtec).

Non-limiting examples of additional active ingredients can be found in Physician's Desk Reference 2000, 54th Edition, ISBN: 1563633302, AHFS 99 Drug Information, Amer. Soc. Of Health System, ISBN: 1879907917 and U.S. Pat. No. 5,019,400, all of which are incorporated by reference.

B. Nanocluster Formulation Variables and Tunability

Varying nanoparticle type or size, dispersion properties, dispersing materials, and processing conditions, for example, can be used to tune the nanocluster to a targeted size, density, and/or dispersability. For example, FIGS. 3 and 4 illustrate that varying processing conditions can be used to create nanoclusters with a broad or narrow size range and also allows for the formation of solid or hollow nanoclusters. Controlling the droplet size in an emulsion or sprayed from a nozzle can facilitate the formation of uniform nanoclusters. Varying the solvent and extraction phase, temperature, humidity, etc. As well as the properties of the nanoparticles can control the morphology of the nanocluster. For example, rapid extraction of the nanoparticle-carrying solution may result in a core/shell structure while slow remove of this phase allows time for nanoparticles to diffuse from the interface and form a more dense nanocluster structure. In another example, controlling nanoparticle physicochemical properties can provide a driving force for the nanoparticle towards or away from the droplet interface, thus, leading to a core/shell structure or solid matrix, respectively. Additionally, based on an adaptation of the inventors' reported precision particle fabrication methodology (Berkland 2001, Berkland 2001, Berkland 2002, Berkland 2004) or similar technologies, the inventors can produced a wide range of monodisperse nano clusters (FIG. 4).

A variety of techniques can be used to characterize nanoclusters that have been created by varying nanoparticle type or size, dispersion properties, dispersing materials, and processing conditions. These techniques can be used to mechanistically determine how processing parameters affect particle physicochemical properties. For example, the aerodynamic diameter of a dried nanocluster powder can be determined by an Aerosizer LD (available at the Center for

Drug Delivery Research, KU), which will also provide supportive data on dry particle geometric diameter, size distribution, aggregation and density. A helium pycnometer (Micromeritics AccuPyc 1330 helium gas pycnometer) located in Dr. Eric Munson's lab (Pharmaceutical Chemistry, KU) can be used to more accurately determine the density of different nanocluster formulations. For example, a sample of nanocluster powder is measured into a 1 cm^3 sample and weighed. The density of the sample is determined by helium displacement of the sample compared to a secondary empty chamber. Measurements are conducted in triplicate for each of three samples and the average and standard deviation calculated. Particle exterior and interior morphology (interior viewed via cryo-fracturing (Berkland 2004)) can be investigated via scanning electron microscopy (LEO 1550).

C. Pharmaceutical Compositions and Routes of Administration

One embodiment of this invention includes methods of treating, preventing, or diagnosing a particular disease or condition by administering the disclosed nanoclusters to a subject. In many instances, the nanoclusters are administered alone or can be included within a pharmaceutical composition. An effective amount of a pharmaceutical composition, generally, is defined as that amount sufficient to ameliorate, reduce, minimize or limit the extent of the disease or condition. More rigorous definitions may apply, including elimination, eradication or cure of the disease or condition.

1. Pharmaceutical Compositions

Pharmaceutical compositions of the present invention can include a nanocluster of the present invention. The phrases "pharmaceutical or pharmacologically acceptable" can include but is not limited to molecular entities and compositions that do not produce an adverse, allergic or other untoward reaction when administered to a subject, such as, for example, a human. The preparation of a pharmaceutical composition is generally known to those of skill in the art. Remington's Pharmaceutical Sciences, 18th Ed. Mack Printing Company, 1990. Moreover, for animal (e.g., human) administration, it is preferred that the preparations meet sterility, pyrogenicity, general safety and purity standards as required by FDA Office of Biological Standards.

"Therapeutically effective amounts" are those amounts effective to produce beneficial results in the recipient. Such amounts may be initially determined by reviewing the published literature, by conducting in vitro tests or by conducting metabolic studies in healthy experimental

animals. Before use in a clinical setting, it may be beneficial to conduct confirmatory studies in an animal model, preferably a widely accepted animal model of the particular disease to be treated. Preferred animal models for use in certain embodiments are rodent models, which are preferred because they are economical to use and, particularly, because the results gained are widely accepted as predictive of clinical value.

"Pharmaceutically acceptable carrier" includes any and all solvents, dispersion media, coatings, surfactants, antioxidants, preservatives (e.g., antibacterial agents, antifungal agents), isotonic agents, absorption delaying agents, salts, preservatives, drugs, drug stabilizers, gels, binders, excipients, disintegration agents, lubricants, sweetening agents, flavoring agents, dyes, such like materials and combinations thereof, as would be known to one of ordinary skill in the art (Remington's, 1990).

The actual dosage amount of a composition of the present invention administered to a subject can be determined by physical and physiological factors such as body weight, severity of condition, the type of disease being treated, previous or concurrent therapeutic interventions, idiopathy of the patient and on the route of administration. The practitioner responsible for administration will, in any event, determine the concentration of active ingredient(s) in a composition and appropriate dose(s) for the individual subject.

In certain non-limiting embodiments, pharmaceutical compositions may comprise, for example, at least about 0.1% of an active ingredient or a nanocluster, for example. In other embodiments, the an active ingredient or nanocluster may comprise between about 2% to about 75% of the weight of the unit, or between about 25% to about 60%, for example, and any range derivable therein. In other non-limiting examples, a dose may also comprise from about 1 microgram/kg/body weight, about 5 microgram/kg/body weight, about 10 microgram/kg/body weight, about 50 microgram/kg/body weight, about 100 microgram/kg/body weight, about 200 microgram/kg/body weight, about 350 microgram/kg/body weight, about 500 microgram/kg/body weight, about 1 milligram/kg/body weight, about 5 milligram/kg/body weight, about 10 milligram/kg/body weight, about 50 milligram/kg/body weight, about 100 milligram/kg/body weight, about 200 milligram/kg/body weight, about 350 milligram/kg/body weight, about 500 milligram/kg/body weight, to about 1000 mg/kg/body weight or more per administration, and any range derivable therein. In non-limiting examples of a derivable range from the numbers listed herein, a range of about 5 mg/kg/body weight to about 100 mg/kg/body weight, about 5 microgram/kg/body weight to about 500 milligram/kg/body weight, etc., can be administered,

based on the numbers described above.

The composition may also include various antioxidants to retard oxidation of one or more active ingredient or nanocluster. The prevention of the action of microorganisms can be brought about by preservatives such as various antibacterial and antifungal agents, including but not limited to parabens (e.g., methylparabens, propylparabens), chlorobutanol, phenol, sorbic acid, thimerosal or combinations thereof.

The compositions of the present invention may include different types of carriers depending on whether it is to be administered in solid, liquid or aerosol form, and whether it need to be sterile for such routes of administration as injection.

The compositions may be formulated into a composition in a free base, neutral or salt form. Pharmaceutically acceptable salts, include the acid addition salts, e.g., those formed with the free amino groups of a proteinaceous composition, or which are formed with inorganic acids such as for example, hydrochloric or phosphoric acids, or such organic acids as acetic, oxalic, tartaric or mandelic acid. Salts formed with the free carboxyl groups can also be derived from inorganic bases such as for example, sodium, potassium, ammonium, calcium or ferric hydroxides; or such organic bases as isopropylamine, trimethylamine, histidine or procaine.

In embodiments where the composition is in a liquid form, a carrier can be a solvent or dispersion medium comprising but not limited to, water, ethanol, polyol (e.g., glycerol, propylene glycol, liquid polyethylene glycol, etc.), lipids (e.g., triglycerides, vegetable oils, liposomes) and combinations thereof. The proper fluidity can be maintained, for example, by the use of a coating, such as lecithin; by the maintenance of the required particle size by dispersion in carriers such as, for example liquid polyol or lipids; by the use of surfactants such as, for example hydroxypropylcellulose; or combinations thereof such methods. In many cases, it will be preferable to include isotonic agents, such as, for example, sugars, sodium chloride or combinations thereof.

In other embodiments, one may use eye drops, nasal solutions or sprays, aerosols or inhalants in the present invention. Such compositions are generally designed to be compatible with the target tissue type. In a non-limiting example, nasal solutions are usually aqueous solutions designed to be administered to the nasal passages in drops or sprays. Nasal solutions are prepared so that they are similar in many respects to nasal secretions, so that normal ciliary action is maintained. Thus, in preferred embodiments, the aqueous nasal solutions usually are isotonic or slightly buffered to maintain a pH of about 5.5 to about 6.5. In addition, antimicrobial

preservatives, similar to those used in ophthalmic preparations, drugs, or appropriate drug stabilizers, if required, may be included in the formulation. For example, various commercial nasal preparations are known and include drugs such as antibiotics or antihistamines.

In certain embodiments, the compositions are prepared for administration by such routes as oral ingestion. In these embodiments, the solid composition may comprise, for example, solutions, suspensions, emulsions, tablets, pills, capsules (e.g., hard or soft shelled gelatin capsules), sustained release formulations, buccal compositions, troches, elixirs, suspensions, syrups, wafers, or combinations thereof. Oral compositions may be incorporated directly with the food of the diet. Preferred carriers for oral administration comprise inert diluents, assimilable edible carriers or combinations thereof. In other aspects of the invention, the oral composition may be prepared as a syrup or elixir. A syrup or elixir, and may comprise, for example, at least one active agent, a sweetening agent, a preservative, a flavoring agent, a dye, a preservative, or combinations thereof.

In certain embodiments, an oral composition may comprise one or more binders, excipients, disintegration agents, lubricants, flavoring agents, and combinations thereof. In certain embodiments, a composition may comprise one or more of the following: a binder, such as, for example, gum tragacanth, acacia, cornstarch, gelatin or combinations thereof; an excipient, such as, for example, dicalcium phosphate, mannitol, lactose, starch, magnesium stearate, sodium saccharine, cellulose, magnesium carbonate or combinations thereof; a disintegrating agent, such as, for example, corn starch, potato starch, alginic acid or combinations thereof; a lubricant, such as, for example, magnesium stearate; a sweetening agent, such as, for example, sucrose, lactose, saccharin or combinations thereof; a flavoring agent, such as, for example peppermint, oil of wintergreen, cherry flavoring, orange flavoring, etc.; or combinations thereof the foregoing. When the dosage unit form is a capsule, it may contain, in addition to materials of the above type, carriers such as a liquid carrier. Various other materials may be present as coatings or to otherwise modify the physical form of the dosage unit. For instance, tablets, pills, or capsules may be coated with shellac, sugar or both.

Sterile injectable solutions are prepared by incorporating the active compounds in the required amount in the appropriate solvent with various of the other ingredients enumerated above, as required, followed by filtered sterilization. Generally, dispersions are prepared by incorporating the various sterilized active ingredients into a sterile vehicle which contains the basic dispersion medium and/or the other ingredients. In the case of sterile powders for the

preparation of sterile injectable solutions, suspensions or emulsion, the preferred methods of preparation are vacuum-drying or freeze-drying techniques which yield a powder of the active ingredient plus any additional desired ingredient from a previously sterile-filtered liquid medium thereof. The liquid medium should be suitably buffered if necessary and the liquid diluent first rendered isotonic prior to injection with sufficient saline or glucose. The preparation of highly concentrated compositions for direct injection is also contemplated, where the use of DMSO as solvent is envisioned to result in extremely rapid penetration, delivering high concentrations of the active agents to a small area.

The composition should be stable under the conditions of manufacture and storage, and preserved against the contaminating action of microorganisms, such as bacteria and fungi. It will be appreciated that exotoxin contamination should be kept minimally at a safe level, for example, less that 0.5 ng/mg protein.

In another aspect of the present invention, a person of ordinary skill will recognize that the compositions of the present invention can include any number of combinations of nanoparticles, dispersion materials, active ingredients, and other components. It is also contemplated that that the concentrations of these ingredients can vary. For example, in one-non-limiting aspect, a composition of the present invention can include at least about 0.0001% to about 0.001%, 0.001% to about 0.01%, 0.01% to about 0.1%, 0.2%, 0.3%, 0.4%, 0.5%, 0.6%, 0.7%, 0.8%, 0.9%, 1.0%, 1.1%, 1.2%, 1.3%, 1.4%, 1.5%, 1.6%, 1.7%, 1.8%, 1.9%, 2.0%, 2.1%, 2.2%, 2.3%, 2.4%, 2.5%, 2.6%, 2.7%, 2.8%, 2.9%, 3.0%, 3.1%, 3.2%, 3.3%, 3.4%, 3.5%, 3.6%, 3.7%, 3.8%, 3.9%, 4.0%, 4.1%, 4.2%, 4.3%, 4.4%, 4.5%, 4.6%, 4.7%, 4.8%, 4.9%, 5.0%, 5.1%, 5.2%, 5.3%, 5.4%, 5.5%, 5.6%, 5.7%, 5.8%, 5.9%, 6.0%, 6.1%, 6.2%, 6.3%, 6.4%, 6.5%, 6.6%, 6.7%, 6.8%, 6.9%, 7.0%, 7.1%, 7.2%, 7.3%, 7.4%, 7.5%, 7.6%, 7.7%, 7.8%, 7.9%, 8.0%, 8.1%, 8.2%, 8.3%, 8.4%, 8.5%, 8.6%, 8.7%, 8.8%, 8.9%, 9.0%, 9.1%, 9.2%, 9.3%, 9.4%, 9.5%, 9.6%, 9.7%, 9.8%, 9.9%, 10%, 11%, 12%, 13%, 14%, 15%, 16%, 17%, 18%, 19%, 20%, 21%, 22%, 23%, 24%, 25%, 26%, 27%, 28%, 29%, 30%, 35%, 40%, 45%, 50%, 60%, 65%, 70%, 75%, 80%, 85%, 90%, 95%, or 99% or any range derivable therein, of at least one of the nanoparticles, dispersion materials, active ingredients, or other components that are mentioned throughout the specification and claims. In non-limiting aspects, the percentage can be calculated by weight or volume of the total composition. A person of ordinary skill in the art would understand that the concentrations can vary depending on the addition, substitution, and/or subtraction of nanoparticles, dispersion materials, active ingredients, and other components.

2. Routes of Administration

The present invention can be administered intravenously, intradermally, intraarterially, intraperitoneally, intralesionally, intracranially, intraarticularly, intraprostaticaly, intrapleurally, intratracheally, intranasally, intravitreally, intravaginally, intrauterinely, intrarectally, intrathecally, topically, intratumorally, intramuscularly, intraperitoneally, subcutaneously, subconjunctival, intravesicularlly, mucosally, intrapericardially, intraumbilically, intraocularally, orally, topically, locally, inhalation (e.g., aerosol inhalation), injection, infusion, continuous infusion, localized perfusion bathing target cells directly, via a catheter, via a lavage, in cremes, in lipid compositions (e.g., liposomes), or by other method or any combination of the forgoing as would be known to one of ordinary skill in the art (Remington's, 1990).

D. Combination Therapies

In order to increase the effectiveness of a treatment with the nanoclusters of the present invention, it may be desirable to combine these nanoclusters with other therapies effective in the treatment of a particular disease or condition.

The compositions of the present invention, for example, can precede or follow the other agent treatment by intervals ranging from minutes to weeks. It is contemplated that one may administer both modalities within about 12-24 h of each other and, more preferably, within about 6-12 h of each other. In some situations, it may be desirable to extend the time period for treatment significantly, where several days (2, 3, 4, 5, 6 or 7), several weeks (1, 2, 3, 4, 5, 6, 7 or 8) or even several months (1, 2, 3, 4, 5, 6, or more) lapse between the respective administrations.

Various combinations may be employed where a compositions including a nanocluster is "A" and the secondary agent, is "B": A/B/A B/A/B B/B/A A/A/B A/B/B B/A/A A/B/B/B B/A/B/B B/B/B/A B/B/A/B A/A/B/B A/B/A/B A/B/B/A B/B/A/A B/A/B/A B/A/A/B A/A/A/B B/A/A/A A/B/A/A A/A/B/A.

E. Source of Nanoparticles, Dispersion Materials, Active Ingredients, and Other Components

The nanoparticles, dispersion materials, active ingredients, and other components described in the claims and specification can be obtained by any means known to a person of ordinary skill in the art. In a non-limiting embodiment, for example, these ingredients can be isolated by obtaining the source of such nanoparticles, dispersion materials, active ingredients,

and other components. Additionally, the ingredients can be purified by any number of techniques known to a person of ordinary skill in the art. Non-limiting examples of purification techniques include Polyacrylamide Gel Electrophoresis, filtration, centrifugation, dialysis, High Performance Liquid Chromatography (HPLC), Gel chromatography or Molecular Sieve Chromatography, and Affinity Chromatography. In other aspects, the compounds, agents, and active ingredients can be obtained by chemical synthesis or by recombinant means by using conventional techniques. See, for example, Stewart and Young, (1984); Tam et al., (1983); Merrifield, (1986); and Barany and Merrifield (1979), Houghten (1985).

F. Kits

In further embodiments of the invention, there is a provided a kit. The kit can include, in non-limiting aspects, the nanoparticles, dispersion materials, active ingredients, and other components described in the claims and the specification. In preferred embodiments, the kit can include a composition that includes a nanocluster. The nanocluster can include, for example, a plurality of nanoparticles and a dispersing material that holds the plurality of nanoparticles together and/or disperses the nanoparticles in response to an environmental cue.

Containers of the kits can include a bottle, dispenser, package, compartment, or other types of containers, into which a component may be placed. The container can include indicia on its surface. The indicia, for example, can be a word, a phrase, an abbreviation, a picture, or a symbol.

The containers can dispense a pre-determined amount of the component (e.g. Compositions of the present invention). The composition can be dispensed in a spray, an aerosol, or in a liquid form or semi-solid form. The containers can have spray, pump, or squeeze mechanisms. In certain aspects, the kit can include a syringe for administering the compositions of the present invention.

Where there is more than one component in the kit (they may be packaged together), the kit also will generally contain a second, third or other additional containers into which the additional components may be separately placed. The kits of the present invention also can include a container housing the components in close confinement for commercial sale. Such containers may include injection or blow-molded plastic containers into which the desired bottles, dispensers, or packages are retained.

A kit can also include instructions for employing the kit components as well the use of any other compositions, compounds, agents, active ingredients, or objects not included in the kit.

Instructions may include variations that can be implemented. The instructions can include an explanation of how to apply, use, and maintain the products or compositions, for example.

EXAMPLES

The following examples are included to demonstrate certain non-limiting aspects of the invention. It should be appreciated by those of skill in the art that the techniques disclosed in the examples which follow represent techniques discovered by the inventor to function well in the practice of the invention. However, those of skill in the art should, in light of the present disclosure, appreciate that many changes can be made in the specific embodiments which are disclosed and still obtain a like or similar result without departing from the spirit and scope of the invention.

Example 1

Nanoclusters with Responsive Dispersion

Nanocluster Formation: Nanoclusters of the present invention can be prepared by the following procedure: Two syringe pumps (Harvard Apparatus 4400 and Isco) are connected to the inner and outer ports of a coaxial nozzle to pass a colloidal suspension of nanoparticles (see above formulation) in aqueous solution and 1-octanol (Fisher Scientific) as droplet carrying liquid, respectively. The two immiscible liquids are injected at appropriate flows to produce monodisperse aqueous droplets, which contain the colloidal suspension of nanoparticles, in the octanol phase. The nanoclusters are formed after water in the droplets dissolves into 1-octanol resulting in packing of the nanoparticles into a spherical structure (FIG. 4). Nanoclusters are then washed with ethanol to remove residual 1-octanol and can be freeze dried for analysis. Similar results were achieved by simply adding the nanoparticle suspension to the octanol phase and stirring to form a primary emulsion.

In one non-limiting embodiment, the inventors coated silica nanoparticles with poly(N-vinylformamide) and cross-linked this polymer with a hydrolyzable cross-linker (2-bis[2,2'-di(N-vinylformamido)ethoxy]propane) to form nanoclusters that dispersed in response to a decrease in pH (FIG. 5). This set-up was used to determine the ability to disperse nanoclusters in response to environmental cues.

The clustered nanoparticles were slightly different in appearance due to the presence of the polymer, but the size distribution remained consistent with previous experiments. The

nanoclusters were dispersed into aqueous solution as a function of time and pH (FIG. 6). A turbidity assay was used to measure optical density at 480 nm over time, the opacity of the solution indicating the relative dispersion of the clusters into constituent nanoparticles. The dispersion of the nanoclusters could also be visually tracked over time (FIG. 6B). Size analysis of the solution phase of dispersed nanoclusters via laser light scattering indicated that polydisperse agglomerates of nanoparticles were liberated. These agglomerates further dispersed into individual nanoparticles over time (FIG. 6C).

Example 2

Self-Assembled Nanoclusters

Nanoparticle Formation: PLGA nanoparticles were prepared by a modified emulsion/solvent extraction method using different polyelectrolyte coating materials to control surface charge (Table 1). Polyvinylamine (PV Am) was used as a cationic coating material and was synthesized in house (see Experimental). Polyethylene-alt-maleic acid (PEMA) was synthesized by hydrolysis of the anhydride from of this polymer as adapted from methods reported previously. The resulting polyelectrolyte-coated PLGA nanoparticles possessed excellent uniformity and high surface charge (Table 1). Each nanoparticle formulation was analyzed for size and zeta potential using dynamic light scattering and conductivity measurements (Brookhaven ZetaPALS), respectively, in the appropriate media (water or organic). Studies confirmed the maintenance of particle surface charge upon lyophilization and after more than one week of incubation at 37° C., pH 7.4 (data not shown). PVAm-coated nanoparticles were notably larger than PEMA-coated nanoparticles for this experiment; however, this size is readily controlled. Nanoparticles can be made by using reported techniques, for example; emulsion polymerization, emulsion solvent extraction, reverse emulsions of the same, precipitation, crystallization, freeze drying, spray freeze drying, salting out, etc. (Wittaya-Areekul et al. 2002).

Table 1. PLGA nanoparticle properties

PLGA Nanoparticle Size (nm)	Size (nm)	Zeta potential (mV)
PVAm-coated	498.5 ± 8.4	+30.7 ± 1.0
PEMA-coated	262.7 ± 11.3	-52.3 ± 1.2

Nanocluster Formation: Nanoparticle clusters were produced by slow addition of 3 mL of

PVAm-coated nanoparticles into 10 mL of PEMA-coated nanoparticles under gentle stirring. Nanocluster formation was induced by electrostatic self-assembly of the oppositely charged nanoparticles. Increasing the concentration of mixed nanoparticles resulted in a corresponding increase in the cluster diameter (FIG. 7). The geometric size distribution of nanoclusters was determined in aqueous solution (Isoton) using a Coulter Multisizer III. Geometric size distributions were relatively broad exhibiting standard deviations that were 60-70% of the average geometric diameter. The aerodynamic size distributions were determined from freeze dried nanoclusters using time of flight measurements obtained by an Aerosizer LD. Nanocluster aerodynamic size distributions were narrower than the geometric size distributions as indicated by the increased volume percent (FIG. 7B) and decreased standard deviations (35-60% of the mean; Table 2). Free PEMA-coated nanoparticles were detected as a rising tail in the geometric size distributions, but were not detected in the aerodynamic size distributions. In addition, few free nanoparticles were observed in scanning electron micrographs (FIG. 7C) indicating that nanoparticles that were not associated with nanoclusters in solution bound to nanoclusters during lyophilization.

Table 2. Dependence of the size of nanocluster on the concentration of PLGA nanoparticles.

	PLGA NP conc. (mg/ml)							
	(-)* 0.68	(+)** 0.72	(-) 1.36	(+) 1.44	(-) 2.04	(+) 2.16	(-) 2.72	(+) 2.82
d_{geo} (μm)	7.4 ± 5.1		8.7 ± 5.6		9.4 ± 5.6		13.7 ± 8.3	
d_{aero} (μm)	2.4 ± 1.5		3.0 ± 1.6		3.4 ± 1.6		4.4 ± 1.6	
d_{geo}/d_{aero}	0.33 ± 0.29		0.35 ± 0.29		0.36 ± 0.29		0.32 ± 0.19	
Calculate d ρ (g/cm^3)	0.11 ± 0.09		0.12 ± 0.08		0.13 ± 0.08		0.10 ± 0.04	
Fine Particle Fraction	1.00		0.80		0.75		0.50	

*(-): PLGA nanoparticles with negative surface charge (PEMA-coated)

**(+): PLGA nanoparticles with positive surface charge (PVAm-coated)

[1]Density calculated from Equation 1 using $d_{geo} = d_p$, $\rho_{ref} = 1$ g/cm^3 and $\gamma = 1$.

[2]Fine Particle Fraction defined as the fraction of dry particles with d_{aero} (μm) < 5 μm.

Structural analysis of nanoclusters revealed a low density, web-like morphology. Scanning

electron micrographs showed that freeze dried nanoparticle clusters possessed a large amount of porosity (FIG. 7C). The density of each nanocluster formulation was calculated from the geometric and aerodynamic diameters according to equation 1 (Table 2). Although nanocluster size increased with increasing nanoparticle concentration, the calculated density was essentially the same for each. The calculated densities of nanoclusters were quite low (~0.15 g/cm^3) and yielded a very high fine particle fraction (d_{aero}<5 μm) for most formulations. The use of a hydrated geometric diameter, dehydrated aerodynamic diameter, and the assumed shape factor of γ=1 (i.e. A sphere) should be noted when interpreting this density calculation.

Laser scanning cofocal microscopy was utilized to gain more insight into the nanocluster structure and formation mechanism. PVAm-coated nanoparticles were labeled with a green fluoroisothiocyanate (FITC) dye and PEMA-coated nanoparticles were labeled with a red rhodamine dye. Detailed analysis of two nanocluster particles indicated that both PVAm-coated (FIG. 8A and FIG. 8D) and PEMA-coated (FIG. 8B and FIG. 8E) nanoparticles were present throughout the entire nanocluster structure.

Example 3

Preparation of Nifedipine and Loratadine Nanoparticles

The following includes examples of preparing various non-limiting nifedipine and loratadine nanoparticles.

1020 nm Nifredipine nanoparticle--Nifedipine (50 mg) was dissolved in 3 ml of methylene chloride. Dumped nifedipine solution into 0.125% Cetyltrimethylammonium bromide (CTAB) solution (30 mL) and sonicated for 60 s. The particle suspension was placed into a hood for two hours to evaporate the methylene chloride. The resulting nanoparticle had a particle size of 1020 nm and a polydispersity of 0.24.

660 nm Nifedipine nanoparticle--Nifedipine (50 mg) was dissolved in 3 ml of methylene chloride. Dumped nifedipine solution into 0.5% CTAB solution (30 mL) and sonicated for 60 s. The particle suspension was placed into a hood for two hours to evaporate the methylene chloride. The resulting nanoparticle had a particle size of 660 nm and a polydispersity of 0.17.

480 nm Nifedipine nanoparticle--Nifedipine (50.2 mg) was dissolved in 3 ml of ethanol. Dumped nifedipine solution into 0.5% CTAB solution (30 mL) and sonicated for 60 s. The particle suspension was placed into a hood for two hours to evaporate the ethanol. The resulting nanoparticle had a particle size of 480 nm and a polydispersity of 0.12.

2373 nm Nifedipine nanoparticle--Nifedipine (30 mg) was dissolved in 2 ml of ethanol. Dumped nifedipine solution into 0.3% Pluronic F-68 solution (30 mL) and homogenized at 15,000 rpm for 60 s. The particle suspension was placed into a hood for two hours to evaporate the ethanol. The resulting nanoparticle had a particle size of 2373 nm and a polydispersity of 0.09.

897 nm Nifedipine nanoparticle--Nifedipine (30 mg) was dissolved in 2 ml of ethanol. Dumped nifedipine solution into 0.6% Pluronic F-68 solution (30 mL) and homogenized at 15,000 rpm for 60 s. The particle suspension was placed into a hood for two hours to evaporate the ethanol. The resulting nanoparticle had a particle size of 897 nm and a polydispersity: 0.07.

639 nm Nifedipine nanoparticle--Nifedipine (30 mg) was dissolved in 2 ml of ethanol. Dumped nifedipine solution into 0.9% Pluronic F-68 solution (30 mL) and homogenized at 15,000 rpm for 60 s. The particle suspension was placed into a hood for two hours to evaporate the ethanol. Resulting nanoparticle had a particle size of 639 nm and a polydispersity of 0.005.

391 nm Loratadine nanoparticle--Loratadine (10 mg) was dissolved in 1 ml of ethanol. Dumped loratadine solution into 0.9% Pluronic F-68 solution (10 mL) and homogenized at 15,000 rpm for 60 s. The particle suspension was placed into a hood for two hours to evaporate the ethanol. The resulting nanoparticle had a particle size of 391 nm and a polydispersity of 0.005.

Example 4

Preparation of Nifedipine Nanoparticle Clusters

This example provides a non-limiting embodiment of the present invention where the nanoparticle is pure nifedipine (a calcium channel blocker that treats high blood pressure). The nanoparticle is coated with a cationic surfactant (CTAB). A polyanion (sodium alginate) couples with the CTAB which induces nanocluster formation.

Preparation of nifedipine nanoparticles: Nifedipine (50 mg) was dissolved in methylene chloride (3 ml). The solution was poured completely into a CTAB concentration-known aqueous solution (Table 3). The solution was sonicated for 60 s. Subsequently, the particle suspension was placed into a hood for two hours to evaporate the methylene chloride. The suspension was diluted to 1 mg/ml. FIG. 9 is a scanning electron microscope (SEM) image of a population of nifedipine nanoparticles.

Table 3. Geometric size and aerodynamic diameters of clusters*

Conc. of CTAB (wt %)	$V_{nifedipine}$ / $V_{algenic\ acid}$	Geometric size (μm)	Dynamic diameter (before	Dynamic diameter (after

			grinding) (μm)	grinding) (μm)
0.125	2:1	28.11 ± 8.33	3.313 ± 1.868	3.321 ± 1.763
	1:1	22.84 ± 11.64	3.814 ± 1.811	4.133 ± 1.829
	1:2	29.27 ± 11.47	4.219 ± 1.597	4.234 ± 1.836
	1:3	23.31 ± 13.4	3.397 ± 1.858	3.702 ± 1.844
0.25	2:1	27.24 ± 11.42	3.775 ± 1.804	3.467 ± 2.025
	1:1	29.49 ± 12.36	3.98 ± 1.868	4.135 ± 1.803
	1:2	23.36 ± 13.48	4.217 ± 1.874	4.312 ± 1.926
	1:3	23.82 ± 10.50	3.520 ± 1.989	4.006 ± 1.903
0.4	2:1	26.39 ± 12.76	3.819 ± 1.786	4.715 ± 1.397
	1:1	33.74 ± 13.85	4.156 ± 1.769	3.840 ± 1.942
	1:2	30.97 ± 14.31	3.793 ± 1.866	3.973 ± 1.876
	1:3	23.72 ± 15.70	/	/

*Concentration: particle suspension: 1 mg/ml; Algenic acid: 1 mg/ml $V_{nifedipine}$ / $V_{algenic\ acid}$

Preparation of nifedipine nanoparticle clusters: Algenic acid aqueous solution (10 ml, 1 mg/ml) was poured into nifedipine nanoparticle aqueous suspension (10 ml, 1 mg/ml) and the mixture was homogenized with a homogenizer (about 2000 rpm) for 2 min. Dry Nifedipine nanoparticle clusters were obtained by freeze-drying. FIG. 10 is a SEM image of nifedipine nanoparticle clusters.

Example 5

Nanocluster Comprising Ovalbumin

This example provides a non-limiting embodiment of the present invention where the nanoparticle is a biodegradable polymer (PLGA) coated with a cationic lipid (DOTAP). Ovalbumin couples to the surface of the coated nanoparticle which induces nanocluster formation.

Preparation of nanoparticles: PLGA nanoparticles were prepared using a modified emulsion-solvent evaporation technique (Kazzaz et al., 2000; Mainardes et al., 2005, both of which are incorporated by reference). A cationic surface charge was incorporated using the lipid 1,2-dioleoyl-3-trimethylammonium-propane (DOTAP; Avanti Polar Lipids, Inc.; Alabaster, Ala.) as the coating material. 3 mL PLGA (0.41 dL/g inherent viscosity; Lactel; Pelham, Ala.) dissolved in an acetone/methanol mixture (5/1) at 1.67% (w/v) was added to 25 mL DOTAP (50 μM) and sonicated at 50% power using a sonic dismembrator (Fisher Scientific; Pittsburgh, Pa.) for 60 s on ice. This was repeated for a total of 6 batches. The batches were combined and stirred at moderate speed in the hood overnight to evaporate the solvent. The particles were crudely filtered through a KimWipe and washed three times with ~15 mL distilled, deionized water using an Amicon

Ultra-15 centrifugal filter unit (Millipore; Billerica, Massachusetts; F=863 g). The washed nanoparticles were sonicated in a water bath for 15 min and again filtered through a Kim Wipe to remove any large agglomerates. The resulting particles were then characterized using a Zeta Potential Analyzer (Brookhaven Instruments; Holtsville, N.Y.) to measure particle size and surface charge (.zeta.): the nanoparticles had an average size of 343.0±8.6 (nm), a polydispersity of 0.232±0.022, and a zeta potential of 36.44±0.56 (mV). The nanoparticle suspension was diluted in 1 mM sodium nitrate solution for surface charge measurements.

Spontaneous nanocluster formation of nanoparticles with ovalbumin: Ovalbumin was used as a model protein. Three solutions containing approximately 0.4, 1.5 and 2.5 mg/mL ovalbumin were prepared in phosphate buffered saline (PBS), and the exact concentration of each solution was determined using UV absorbance spectroscopy (Table 4). Three labeled, 15 mL centrifuge tubes, 6 mL DOTAP nanoparticles and 1 mL ovalbumin solution were added. The samples were tumbled gently on an end-over-end tube rotator for 45 min at 4° C. The resulting nanoclusters were analyzed using a Multisizer 3 Coulter Counter (Beckman Coulter, Inc.; Fullerton, Calif.) to measure their geometric diameter. The nanoclusters were lyophilized using a Labconco bench-top lyophilizer (Kansas City, Mo.) and further characterized to determine the aerodynamic diameter (Aerosizer; Amherst Process Instruments Inc.) and morphology (SEM) (Table 5). FIG. 11 illustrates the geometric diameter of the DOTAP/PLGA nanoparticles with ovalbumin.

Table 4. Concentration of ovalbumia solutions as determined by UV absorbance spectroscopy

Target Concentration (mg/mL)	Actual Concentration (mg/mL)
0.4	0.371 ± 0.001
1.5	1.374 ± 0.003
2.5	2.236 ± 0.040

Table 5. Nanocluster sizes

Target concentration of ovalbumin (mg/mL)	Mode Geometric Diameter* (μm)	Mean Aerodynammic Diameter (μm)
0.4	6.25	2.384 ± 1.775
1.5	5.15	2.468 ± 1.931
2.5	5.10	2.447 ± 1.918

*See FIG. 11 for size distribution.

Scanning electron microscopy (SEM): The size and morphology of the nanoclusters were

evaluated using a LEO 1550 field emission scanning electron microscope with secondary electron detection. The nanoclusters were coated on a platform and sputtered with gold prior to imaging at 4000 and 10,000.times.0 magnification. FIG. 12 includes SEM images of the nanoclusters comprising DOTAP/PLGA nanoparticles and ovalbumin.

Example 6

Assessment of Dry Powder Performance In Vitro

A multi-stage liquid impactor (MSLI) fitted with a mouthpiece and throat assembly (el-Araud et al. 1998) can be used to evaluate the deposition performance of various particle formulations administered from a dry powder inhaler. For administration through a dry powder inhaler (DPI) such as the Spinhaler®. Or Rotahaler®, particles are first encapsulated in a large, two-piece gelatin capsule. The capsule is placed into a small compartment in the DPI, which is then twisted to either separate or rupture the capsule immediately prior to breath actuation. Since no propellants or compressed gases are used for these DPIs, the breathing force of the patient, or in our case the volumetric flow rate through the MSLI, disperses the powder.

Using this experimental set-up, several important performance parameters can be evaluated, including the respirable fraction of a particle formulation, the mass depositing in the mouthpiece and throat assembly and the fractions of particles depositing at different stages throughout the MSLI (assessed by removing each section and weighing the collected particle mass). Particle batches depositing with high efficiency to the lower stages (~1-5 μm cut-off) of the MSLI will be deemed as "deep lung" formulations suitable for ciprofloxacin encapsulation experiments.

Example 7

Identification of Nanocluster Formulations that Can Entrap, Deposit, and Release Ciprofloxacin

Nanoclusters can be formulated for controlled release of ciprofloxacin for ~1 week. A complete analysis of nanocluster physicochemical properties, dispersion and release of the drug can be prepared by the methods described throughout this specification. The nanoclusters, in one embodiment, can be made with nanoparticles of pure ciprofloxacin or ciprofloxacin encapsulated in PLGA nanoparticles.

Ciprofloxacin is a broad spectrum antibiotic, especially effective against gram negative bacteria (Geller 2002, Geller 2003, Marier 2003) having the following formula:

Nanocluster dispersability and ciprofloxacin release kinetics: Nanocluster formulations can be reformulated to determine controlled release of ciprofloxacin, taking care to maintain the same fabrication procedure and resulting structure designed for deep lung deposition. Ciprofloxacin (Sigma, Inc.) can be encapsulated by co-dissolving with the polymer phase and will be partially suspended in the polymer phase or dissolved in a co-solvent if low solubility in the polymer phase is an issue. Dissolution studies ascertain the release kinetics of ciprofloxacin. These studies are performed in phosphate buffered saline solution (pH 7.4) at physiological temperature (37° C.). Approximately 10-20 mg of each particle formulation is placed in 2 mL microcentrifuge tubes shaken at 150 rpm. Release samples will be tested by intermittently centrifuging samples to separate nanoparticles (15,000 rpm), collecting 1-1.5 mL of supernatant, replacing supernatant with fresh buffer and resuspending the samples. The supernatant will then be analyzed by spectrophotometry at ~350 nm to determine the concentration of ciprofloxacin at each time point while avoiding detection of polymer dissolution products. The release of ciprofloxacin from the various nanocluster formulations will be conducted in triplicate and the average and standard deviation is calculated. The initial loading of ciprofloxacin in nanocluster formulations is determined by dissolving ~10 mg of each formulation in triplicate in dimethylsulfoxide and measuring the absorbance at ~350 nm. Absorbance values for formulations of nanoclusters without ciprofloxacin are used as blanks. The calculated amount of ciprofloxacin per mass of polymer is termed the drug loading. This number can be divided by the mass of ciprofloxacin per mass of polymer entered into the experiment to calculate the drug encapsulation efficiency. The summed mass of ciprofloxacin released over time is then divided by the drug loading to arrive at the cumulative percent released. Analogous samples of nanoclusters can be prepared to determine the dispersion kinetics based on measuring the turbidity of the sample solution at 480 nm (see preliminary data above).

Reformulation and optimization of controlled release: Generating a near constant release of ciprofloxacin for ~1 week may include reformulation of nanoclusters. If drug "bursting" (rapid initial release) occurs or increased duration of release is desired, higher molecular weight PLGA or PLGA with a higher lactide content will be used as each of these prolong degradation of the polymer phase. In addition, increasing the size of constituent nanoparticles to decrease the rate of ciprofloxacin release can be used. The maintenance of small (e.g., <200 nm) nanoparticles can be used as a way to avoid phagocytosis or other clearance mechanisms from the lung epithelium.

Example 8

Paclitaxel nano-agglomerates as dry powder for pulmonary delivery

Paclitaxel (PX), L-a-phosphatidylcholine (lecithin; Lec), cetyl alcohol (CA), L-leucine (Leu), polyvinylpyrrolidone (PVP K90, Mw ~36,000) and sodium chloride were purchased from Sigma Chemicals Co, USA. Pluronic F-127 (PL, Mw ~12,220) was purchased from BASF, The Chemical Company, USA. Polyvinyl alcohol (PVA; Mw = 22,000, 88% hydrolyzed) was purchased from Acros Organics, New Jersey, USA. Potassium dihydrogen phosphate, disodium hydrogen phosphate, acetone, ethanol and acetonitrile were purchased through Fisher Scientific. Floatable dialysis membrane units (Mw cut-off = 10,000 Da) were obtained from Spectrum Laboratories Inc., USA. A549 cells were obtained from the American Type Culture Collection (ATCC, Rockville, MD). The cell culture medium (Ham's F-12 Nutrient Mixture, Kaighn's modified with L-glutamine) was purchased through Fisher Scientic. Fetal bovine serum (FBS) was purchased from Hyclone. Penicillin-streptomycin was purchased from MB Biomedical, LLC. Trypsin- EDTA was purchased through Gibco. MTS reagent [tetrazolium compound; 3-(4,5-dimethylthiazol-2-yl)-5-(3-carboxymethoxyphenyl)-2-(4-sulfophenyl)-2H-tetrazolium, inner salt] was purchased from Promega, USA. Double-distilled water was used throughout the study, provided by an EASYpure® RODI (Barnstead International, Model # D13321).

A. Fabrication and characterization of paclitaxel nanoparticles.

Nanosuspensions were prepared using a precipitation technique. The drug was precipitated by direct injection of acetone solution of paclitaxel, 0.1% w/v, in waters at a rate of 1 mL/min under sonication (Fisher Scientic, Sonic Dismembrator) with an amplitude of 46%. The chosen surfactants for the study included hydrophobic (cetyl alcohol), hydrophilic (PL, PVA and PVP K90) and amphoteric (lecithin). The hydrophobic and amphoteric surfactants were added to the drug organic solvent solution and the contents were allowed to stand at room temperature for 30 to 45 minutes with occasional vortexing to allow complete solubilization of the drug and the surfactants. Hydrophilic surfactants were added to the aqueous phase. Surfactants were used individually or in combination as reported.

The particle size and zeta potential of the nanosuspensions were determined by dynamic light scattering (Brookhaven, ZetaPALS). Zeta potential measurements were performed using 1 mM KCl solution. All measurements were performed in triplicate.

B. Preparation of paclitaxel nano-agglomerates

The paclitaxel nanoparticle agglomerates were prepared by addition of L-leucine powder to agglomerate nanoparticle suspensions followed by homogenization at 25,000 rpm for 30 sec. The amount of L-leucine added was adjusted to a drug:leucine ratio equal to 1:1. The size of paclitaxel nanoparticle agglomerates was measured in Isoton diluent using a Coulter Multisizer 3 (Beckman Coulter Inc.) equipped with a 100 mm aperture after three hours of incubation with the flocculating agent. The suspensions were kept overnight at room temperature to allow evaporation of acetone and then frozen at -80° C and transferred to a freeze dryer (Labconco, FreeZone 1). Drying lasted for 36 hours to remove all appreciable water content. Lyophilized powder was stored at room temperature for further characterization.

C. Characterization of the prepared nanoparticle agglomerates

1. Determination of particle size distribution

The particle size of the dispersed nanoparticle agglomerates as well as the resuspended lyophilized powder was measured using a Coulter Multisizer 3. The particle size distributions are shown in FIG. 13.

2. Flowability characteristics

The flow properties of the nanoparticle agglomerates were assessed by angle of repose (tan θ = height / radius) measurement of the dried powders. The fixed- height cone method was used. A glass funnel with cut stem surface of 5 mm internal diameter was fixed at 2.5 cm height over a flat surface. The powders were allowed to flow gently through the funnel until a cone was formed and reached the funnel orifice. The flow of powder was then stopped and the average diameter of the formed cone (D) was measured. The area of the base of the cone was taken as a measure of the internal friction between the particles. The angle of repose was calculated by the equation: tan θ = height / radius.

In addition, the bulk density, Hausner ratio (Tapped density / bulk density) and Carr's index (Ci) [(Tapped density –bulk density)/ Tapped density X 100%] were also determined for the dried powders. Ten mg of powders were weighed and poured into a 10 mL graduated measuring cylinder. The bulk volume occupied (V_b) was recorded. The measuring cylinder was tapped until a constant value was obtained and the tapped volume was recorded (V_t). The process was repeated at least three times and the average was taken in each case. The bulk and tapped densities of powder were calculated by dividing the weight by the corresponding bulk volume or tapped volume recorded.

3. Measurement of aerodynamic diameter

The aerodynamic size distributions of the agglomerate powders were measured directly from lyophilized powder by time-of-flight measurement using an Aerosizer LD (Amherst Instruments) equipped with a 700 mm aperture operating at 6 psi.

The theoretical mass–mean aerodynamic diameter (d_{aero}) of the nanoparticle agglomerates was determined from the geometric particle size and tapped density using the following relationship:

$$d_{aero} = \frac{d_{geo}}{\gamma}\sqrt{\rho / \rho_a}$$

Where d_{geo} = geometric diameter, γ = shape factor (for a spherical particle, $\gamma = 1$; for aerodynamic diameter calculations, the particles in this study were assumed to be spherical), ρ = particle bulk density and ρa = water mass density (1 g/cm^3). Aerodynamic size distributions of paclitaxel nanoparticle agglomerates is shown in FIG. 14. Tapped density measurements underestimate particle bulk densities since the volume of particles measured includes the interstitial space between the particles. The true particle density, and therefore the aerodynamic diameter of a given powder, is expected to be slightly larger than reported.

4. Aerosolization performance of nano-agglomerate dry powders

Aerodynamic characteristics of selected nanoparticle agglomerates were studied in vitro using a Tisch Ambient Cascade Impactor (Tisch Environmental, Inc., Ohio). The study was carried out by applying ~20 mg powder manually into the orifice of the instrument at an air flow rate of ~30 L/min. Cut-off particle aerodynamic diameters for each stage of the impactor were: pre-separator (10.00 mm), stage 0 (9.00 mm), stage 1 (5.8 mm), stage 2 (4.7 mm), stage 3 (3.3 mm), stage 4 (2.1 mm), stage 5 (1.1 mm), stage 6 (0.7 mm), stage 7 (0.4 mm) and filter (0 mm). Nanoparticle agglomerates deposited on each stage of the impactor were determined by measuring the difference in weight of filters placed on the stages. The mass median aerodynamic diameter, MMAD, and geometric standard deviation, GSD, were obtained by a linear fit of the cumulative percent less-than the particle size range by weight plotted on a probability scale as a function of the logarithm of the effective cut-off diameter. FIG. 15 shows the distribution of Paclitaxel powder as received and nanoparticle agglomerate formulations deposited on the stages of a cascade impactor at a flow rate of ~30 L/min.

D. Imaging of particles by Transmission Electron Microscopy

Image data was used to corroborate the size of nanoparticles and nanoparticle agglomerates and to observe their morphological aspects. Transmission electron micrographs (TEM) were obtained for paclitaxel nanoparticles and nanoparticle agglomerates using a JEOL 1200 EXII transmission electron microscope. Initially, carbon-coated grids (Electron Microscopy Sciences) were floated on a droplet of the suspensions on a flexible plastic film (Parafilm), to permit the adsorption of the particles onto the grid. After this, the grid was blotted with a filter paper and air dried for 1 hr.

E. Determination of process yield and loading efficiency

The lyophilized powder for the prepared nanoparticle agglomerates was weighed and the yield was calculated using the following expression:

Paclitaxel loading efficiency was assessed by dispersing one mg of the lyophilized powder in 10 mL ethanol. The dispersion was sonicated in a bath-type sonicator (Branson 3510) for 30 min. Then the solution was centrifuged (Beckman, Avanti TM) at ~15,000 rpm for 30 min to remove insoluble ingredients and the amount of drug in the supernatant was determined spectrophotometrically (Agilent C) at 228 nm. Drug loading was defined as follows:

F. Dissolution studies

The dissolution of the prepared nanoparticles and nanoparticle agglomerates was determined and compared with the dissolution characteristics of the drug powder as received. The dissolution of paclitaxel was carried out at 37 ± 0.5° C in a 1 liter beaker. A known amount (~10 mg) of the lyophilized powder was suspended in 10 mL phosphate buffered saline (PBS, pH 7.4) and was placed into a floatable dialysis membrane unit (Mw cut-off = 10,000 Da), and the unit was allowed to float in a 500 mL of PBS. The solution was stirred at a constant speed (100 rpm) using a magnetic stirrer (Barnstead, Thermolyne MIRAKTM). At predetermined time intervals for a total period of 8 hours, serial samples (1 mL) of the medium were withdrawn from the dialysis bag and centrifuged for 30 minutes at ~13,000 rpm. The nanoparticles-free supernatant was removed and extracted with 3 mL of ethanol. The ethanol extract was analyzed for paclitaxel concentration using a reverse-phase HPLC method. Studies were conducted in triplicate. A Shimadzu HPLC system including a solvent delivery pump (Shimadzu LC-10AT), a controller (Shimadzu SCL-10A), an autoinjector (Shimadzu SIL-10AxL), and a UV detector (Shimadzu SPD-10A) was used in this study. The peak areas were integrated using Shimadzo Class VP (Version 4.3). A 4.6 mm x 100 mm long Zorbax SB C-8 column (Agilent C) with a particle diameter of 3.5 μm was

used. During the assay, paclitaxel was eluted isocratically at a mobile phase flow rate of 0.9 mL/minute and monitored with a UV detector operating at 228 nm. The mobile phase for the assay consisted of an acetonitrile and water mixture (50:50 v/v). The run time for the assay was 20 minutes, and the retention time for paclitaxel was 10.7 minutes. FIG. 16 shows the in-vitro dissolution profiles of paclitaxel in PBS (pH 7.4) from pure paclitaxel powder and two different nanoparticle (NP) and nanoparticle agglomerate formulations (NA).

G. Cytotoxicity assay

The cytotoxicity of selected nanoparticles and nanoparticle agglomerates was assessed using the CellTiter 96® Aqueous Cell Proliferation Assay (Promega) and compared with paclitaxel powder as received, lecithin, PVP K90, L-leucine, physical mixtures of these ingredients and blank nanoparticle agglomerates. In this experiment, 8 x 104 A549 cells / well were seeded in 96-well microtiter plates. At the end of the incubation period (12 h), 20 ml of MTS reagent solution was added to each well and incubated for 3 h at 37 °C. The absorbance was measured at 490 nm using a microtiter plate reader (SpectraMax, M25, Molecular Devices Corp., CA). The percentage of viable cells with all tested concentrations was calculated relative to untreated cells. FIG. 17 shows the viability of A549 cells in the presence of formulation components as determined by an MTS assay.

Table 6. IC50 for Paclitaxel Formulations

Formulation	IC_{50}
Pure paclitaxel powder	1.8 mg/ml
F1NP	2.1 mg/ml
F1NA	1.9 mg/ml
PM1	1.5 mg/ml
Blank1	0.88 mg/ml
F2NP	1.6 mg/ml
F2NA	2.1 mg/ml
PM2	1.5 mg/ml
Blank2	1.8 mg/ml

Table 7. Paclitaxel formulations used in the studies.

Formulation	Paclitaxel (% w/v)	Lecithin (% w/v)	PVP K90 (% w/v)	Cetyl alcohol (% w/v)

F1	0.1	0.02	0.01	
F2	0.1	0.02		
F3	0.1	0.02		0.01

Table 8. Physical properties of Paclitaxel nanoparticles (values = average ± S.D.).

Formulation	Nanoparticle size (nm)	Zeta-potential (mV)	Polydispersity
F1[a]	298.7 ± 10.3	25.1 ± 0.7	0.04 ± 0.03
F2[b]	339.1 ± 13.6	24.7 ± 1.5	0.18 ± 0.1
F3[c]	358.5 ± 8.1	22.4 ± 1.02	0.31 ± 0.1

[a] F1 = 0.1: 0.02: 0.01; PX: Lec: PVP K90

[b] F2 = 0.1: 0.02; PX: Lec

[c] F3 = 0.1: 0.02: 0.01; PX: Lec: CA

Table 9. Characteristics of Paclitaxel nanoparticle agglomerates (values = average ± S.D.).

Characteristics	Formulations	
	F1[a]	F2[b]
Geometric particle size (μm) of NA[c] before lyophilization	2.8 ± 0.5	3.7 ± 0.9
Geometric particle size (μm) of lyophilized NA[c]	4.8 ± 1.3	5.4 ± 1.6
$MMAD_A$[d] of lyophilized NA[c]	1.5 ± 0.08	1.7 ± 0.4

[a] F1 = 0.1: 0.02: 0.01; PX: Lec: PVP K90

[b] F2 = 0.1: 0.02; PX: Lec

[c] NA: Nanoparticle agglomerates.

[d] MMAD: Mass median aerodynamic diameter obtained from Aerosizer.

Table 10. Yield, loading and dissolution behavior of Paclitaxel nanoparticle agglomerates (values = average ± S.D.).

Characteristics	Formulations	
	F1[a]	F2[b]
% Process yield of lyophilized NA[c]	85.9 ± 2.7	89.8 ± 3.1
Drug loading of lyophilized NA[c]	85.1 ± 3.9	85.9 ± 8.7

Q_{8h}[e]NP[d]	66.4 % ± 2.4	60.7 % ± 13.04
Q_{8h}[e] NA[c]	43.6 % ± 4.3	40.4 % ± 2.9

[a] F1 = 0.1: 0.02: 0.01; PX: Lec: PVP K90

[b] F2 = 0.1: 0.02; PX: Lec

[c] NA: Nanoparticle agglomerates.

[d] NP: Nanoparticles.

[e]Q_{8h}: %Paclitaxel dissolved after 8 hours.

Table 11. Cascade impaction results of lyophilized paclitaxel nanoparticle agglomerates (values = average ± S.D.).

Characteristics of the lyophilized NA[c]			**Formulations**		
			F1[a]	**F2[b]**	**Paclitaxel as received**
At flow rate of ~30 L//min	% EF[d]		71.9 ± 4.9	71.6 ± 15.4	68.3 ± 6.1
	% RF[e]	< 5.7	95.7 ± 3.01	95.3 ± 4.1	0.39 ± 0.3
		< 3.3	83.8 ± 2.8	79.55 ± 4.8	0
	MMAD[f]		1.5 ± 0.1	1.9 ± 0.4	0.08 ± 0.02
	GSD[g]		2.26 ± 0.09	2.29 ± 0.05	2.2 ± 0.03

[a] F1 = 0.1: 0.02: 0.01 ; Px: Lec: PVP K90

[b] F2 = 0.1: 0.02; Px: Lec

[c] NA: Nanoparticle agglomerates.

[d] % EF: Percent emitted fraction.

[e] RF: Percent respirable fraction.

[f] MMAD: Mass median aerodynamic diameter.

[g] GSD: Geometric standard deviation.

Example 9

Application of Budesonide Nanoparticles

Nanoparticle technology represents an attractive approach for formulating poorly water soluble pulmonary medicines. Unfortunately, nanoparticle suspensions used in nebulizers or metered dose inhalers often suffer from physical instability in the form of uncontrolled

agglomeration or Ostwald ripening. In addition, processing such suspensions into dry powders can yield broad particle size distributions. To address these encumbrances, a controlled nanoparticle flocculation process has been developed. Nanosuspensions of the poorly water soluble drug budesonide were prepared by dissolving the drug in organic solvent containing surfactants followed by rapid solvent extraction in water. Different surfactants were employed to control the size and surface charge of the precipitated nanoparticles. Selected budesonide nanoparticle suspensions exhibited an average particle size ranging from ~160-230 nm, high yield and high drug content. Nanosuspensions were flocculated using leucine, which produced micron-sized agglomerates. Freeze-drying the nanoparticle agglomerates yielded dry powders with desirable aerodynamic properties for inhalation therapy. In addition, the dissolution rates of dried nanoparticle agglomerate formulations were significantly faster than that of stock budesonide. The results of this study suggest that nanoparticle agglomerates possess the microstructure desired for lung deposition and the nanostructure to facilitate rapid dissolution of poorly water soluble drugs.

Pulmonary dosage forms have established an important role in the local treatment of lung diseases. Systemic treatments delivered through the lungs are also emerging since this route offers access to a well blood-supplied surface area, avoids first-pass metabolism, and reduces drug degradation that may occur in the gastrointestinal tract. Pulmonary drug delivery approaches continue to develop rapidly in an effort to improve product stability and efficacy for local and systemic treatment of diseases. One problem with pulmonary drug delivery is the poor deposition efficiency as, in some cases, only approximately 10% of the inhaled drug powder reaches the alveoli. In addition, many current and emerging formulations would benefit from improved drug dissolution rate, which often enhances drug bioavailability.

In recent years, significant effort has been dedicated to expand nanotechnology for drug delivery since it offers a potential means of improving the delivery of small molecule drugs, as well as macromolecules such as proteins, peptides or genes to the tissue of interest. The increase in the percentage of poorly water-soluble molecules being identified as active pharmaceutical ingredients beckons new approaches to bring these molecules to the market place in a timely fashion. Nanoparticles, whether amorphous or crystalline, offer an interesting way of formulating drugs having poor water solubility. By presenting drugs at the nanoscale, dissolution can be rapid and as a result the bioavailability of poorly soluble drugs can be significantly improved. Nanoparticles have been disregarded to some extent in dry powder dosage forms because particles

< 1 mm have a high probability of being exhaled before deposition, are prone to particle growth due to Ostwald ripening and can suffer from uncontrolled agglomeration. Conversely, particles exhibiting an aerodynamic diameter from 1 to 5 mm are more likely to bypass the mouth and throat, resulting in augmented deposition in the lung periphery.

Budesonide is a potent nonhalogenated corticosteroid with high glucocorticoid receptor affinity, airway selectivity and prolonged tissue retention. It inhibits inflammatory symptoms, such as edema and vascular hyperpermeability. Budesonide is already applied through dry powder inhalers (DPI, Pulmicort), metered dose inhalers (pMDI, Rhinocort) or ileal-release capsules (Entocort). This drug is considered one of the most valuable therapeutic agents for the prophylactic treatment of asthma despite its poor solubility in water (21.5 mg/ml under constant agitation).

The objective of this study was to translate budesonide nanosuspensions into dry powder formulations capable of effective deposition and rapid dissolution. Different surfactants were used to create surface charge on the nanoparticles and charge interactions were leveraged to flocculate nanoparticles into nanoparticle agglomerates exhibiting a particle size range of ~2-4 mm. Nanoparticle suspensions were evaluated by measuring particle size, polydispersity and zeta potential. Nanosuspensions were then flocculated and lyophilized to obtain dry powders composed of micron-sized agglomerates. Nanoparticle agglomerates were characterized by the determination of particle size, aerolization efficiencies, flowability characteristics, process yield and loading efficiency. Finally, dissolution studies were performed for the selected nanoparticles and nanoparticle agglomerates, which were compared with the stock drug. The present work represents an approach to harmonize the features of micro- and nanostructure for developing novel dry powder aerosols.

A. Materials and methods

Budesonide (Bud), L-a-phosphatidylcholine (lecithin; Lec), cetyl alcohol (CA), L-leucine (Leu), polyvinylpyrrolidone (PVP), sorbitan tri-oleate (Span 85) and sodium chloride were purchased from Sigma Chemicals Co, USA. Pluronic F-127 (PL, Mw ~12,220) was purchased from BASF, The Chemical Company, USA. Polyvinyl alcohol (PVA; Mw = 22,000, 88% hydrolyzed) was purchased from Acros Organics, New Jersey, USA. Potassium dihydrogen phosphate, disodium hydrogen phosphate, acetone, ethanol and acetonitrile were purchased through Fisher Scientic. Floatable dialysis membrane units (Mw cut-off = 10,000 Da) were

obtained from Spectrum Laboratories Inc., USA. A549 cells were obtained from the American Type Culture Collection (ATCC, Rockville, MD). The cell culture medium (Ham's F-12 Nutrient Mixture, Kaighn's modified with L-glutamine) was purchased through Fisher Scientic. Fetal bovine serum (FBS) was purchased from Hyclone. Penicillin-streptomycin was purchased from MB Biomedical, LLC. Trypsin- EDTA was purchased through Gibco. MTS reagent [tetrazolium compound; 3-(4,5-dimethylthiazol-2-yl)-5-(3-carboxymethoxyphenyl)-2-(4-sulfophenyl)-2H-tetrazolium, inner salt] was purchased from Promega, USA. Double-distilled water was used throughout the study, provided by an EASYpure® RODI (Barnstead International, Model # D13321).

1. Preparation of budesonide nanosuspensions

Nanosuspensions were prepared using a precipitation technique. Briefly, solutions of budesonide in acetone were prepared at concentrations of 0.1 and 0.2% w/v and water was used as nonsolvent. To precipitate the drug, the solution of budesonide was directly injected into the non-solvent at a rate of 1 mL/min under sonication (Fisher Scientic, Sonic Dismembrator) with an amplitude of 46% in an ice bath. The selected surfactants for the study included hydrophobic (cetyl alcohol and Span 85), hydrophilic (PL, PVA and PVP) and amphoteric (lecithin). The hydrophobic and amphoteric surfactants were added to the drug organic solvent solution and the contents were allowed to stand at room temperature for 30 to 45 minutes with occasional vortexing to allow complete solubilization of the drug and the surfactants. Hydrophilic surfactants were added to the aqueous phase. Surfactants were used individually or in combination as reported.

2. Flocculation of budesonide nanoparticles

The budesonide nanoparticle agglomerates were prepared by slow addition of L-leucine solution (1 % w/v) in water to flocculate nanoparticle suspensions during homogenization at 25,000 rpm for 30 sec. The amount of L-leucine added was adjusted to a drug:leucine ratio equal to 1:1. The size of budesonide nanoparticle agglomerates was measured in Isoton diluent using a Coulter Multisizer 3 (Beckman Coulter Inc.) equipped with a 100 mm aperture after three hours of incubation with the flocculating agent. The flocculated suspensions were kept overnight at room temperature to allow evaporation of acetone and then frozen at -80° C and transferred to a freeze dryer (Labconco, FreeZone 1). Drying lasted for 36 hours to remove all appreciable water content. Lyophilized powder was stored at room temperature for further characterization.

B. Characterization of the prepared nanoparticles and nanoparticle agglomerates.

1. Particle size analysis and Zeta potential measurement of the selected nanosuspensions.

The size and zeta potential of the nanosuspensions were determined by dynamic light scattering (Brookhaven, ZetaPALS). Zeta potential measurements were performed using 1 mM KCl solution. All measurements were performed in triplicate.

2. Determination of particle size distribution and aerodynamic diameter of the prepared nanoparticle agglomerates.

The particle size of the dispersed nanoparticle agglomerates as well as the resuspended lyophilized powder was measured using a Coulter Multisizer 3. The aerodynamic size distributions of the agglomerate powders were measured directly from lyophilized powder by time-of-flight measurement using an Aerosizer LD (Amherst Instruments) equipped with a 700 mm aperture operating at 6 psi.

3. Aerosolization of nanoparticle agglomerates

Aerodynamic characteristics of selected nanoparticle agglomerates were studied in vitro using a Tisch Ambient Cascade Impactor (Tisch Environmental, Inc., Ohio). The study was carried out by applying ~20 mg powder manually into the orifice of the instrument at three air flow rates; ~15 L/min, ~30 L/min and ~60 L/min. Cut-off particle aerodynamic diameters at 30 L/min for each stage of the impactor were: pre-separator (10.00 mm), stage 0 (9.00 mm), stage 1 (5.8 mm), stage 2 (4.7 mm), stage 3 (3.3 mm), stage 4 (2.1 mm), stage 5 (1.1 mm), stage 6 (0.7 mm), stage 7 (0.4 mm) and filter (0 mm). Nanoparticle agglomerates deposited on each stage of the impactor were determined by measuring the difference in weight of filters placed on the stages. The mass median aerodynamic diameter, MMAD, and geometric standard deviation, GSD, were obtained by a linear fit of the cumulative percent less-than the particle size range by weight plotted on a probability scale as a function of the logarithm of the effective cut-off diameter.

4. Transmission electron microscopy (TEM)

Image data was used to corroborate the size of nanoparticles and nanoparticle agglomerates and to observe their morphological aspects. Transmission electron micrographs (TEM) were obtained for budesonide nanoparticles and nanoparticle agglomerates using a JEOL 1200 EXII transmission electron microscope. Initially, carbon-coated grids (Electron Microscopy Sciences) were floated on a droplet of the suspensions on a flexible plastic film (Parafilm), to permit the adsorption of the particles onto the grid. After this, the grid was blotted with a filter

paper and air dried for 1 hr.

5. SSNMR analysis.

All 13C spectra were collected using a Chemagnetics CMX-300 spectrometer using ramped amplitude cross-polarization (RAMP), magic-angle spinning (MAS), and SPINAL-64 decoupling. Samples were packed in 7 mm zirconia rotors using Teflon® end caps, and spun at 4 kHz in a 7 mm spin module from Revolution NMR.

All spectra are the sum of 2,000–48,000 transients collected using a 1–1.5 s pulse delay, a contact time of 0.5–2 ms, and a 1H 90° pulse width of 3–4.5 □s. The free induction decays consisted of 512–2048 points with a dwell time of 33.3 □s. The spectra were externally referenced to tetramethylsilane using the methyl peak of 3-methylglutaric acid at 18.84 ppm.

The assignment of the peaks in the 13C spectrum of the "as received" budesonide was performed using the modified spectral editing methods of Hu et al. 23 and the 13C solution predictions from ChemBioDraw Ultra (version 11.0) from CambridgeSoft and ACD/CNMR Predictor (version 7.09) from ACD/Labs. The spectral editing subspectra were collected using the parameters given in Table 12. These parameters were optimized using 3-methylglutaric acid.

Table 12. Parameters used to collect ^{13}C spectral editing subspectra.*

Subspectra	Pulse Sequence	t_{CP} (μs)	t_{PI} (μs)	t_{DD} (μs)	t_{SL} (μs)	Number of Transients
All	(+)	1500	0.2	—	133	800
C+CH_3	(+)	1500	0.2	130	3	800
C	(-)	400	135	130	3	8,000
CH	(+)	40	24	—	133	6,000
	(-)	37	0.2	130	1	6,000
CH_2	(+)	80	39	—	133	6,000
	(-)	78	0.2	147	1	6,000

* = All subspectra were collected with a 1.5 s pulse delay, a ^1H 90° pulse width of 3.1 μs, 1024 acquisition points with a dwell time of 33.3 μs, and a magic-angle spinning rate of 4 kHz.

6. Determination of process yield

The lyophilized powder for the prepared nanoparticle agglomerates was weighed and the yield was calculated using the following expression:

$$\%\ \text{Process yield} = \frac{\text{Recovered mass}}{\text{Mass entered into the experiment}} \times 100$$

7. Budesonide loading efficiency measurement

Budesonide loading efficiency was assessed by dispersing one mg of the lyophilized

powder in 10 mL ethanol. The dispersion was sonicated in a bath-type sonicator (Branson 3510) for 2 hours and then kept overnight at room temperature to allow complete dissolution of the drug by ethanol. Then the solution was centrifuged (Beckman, Avanti TM) at ~15,000 rpm for 30 min to remove insoluble surfactants and L-leucine and the amount of drug in the supernatant was determined spectrophotometrically (Agilent C) at 243 nm. Drug loading was defined as follows:

$$\%\,\text{Loading} = \frac{\text{Recovered budesonide mass}}{\text{Total mass}} \times 100$$

8. Flowability characteristics

The flow properties of the nanoparticle agglomerates were assessed by angle of repose (tan θ = height / radius) measurement of the dried powders. The fixed- height cone method was used. A glass funnel with cut stem surface of 5 mm internal diameter was fixed at 2.5 cm height over a flat surface. The powders were allowed to flow gently through the funnel until a cone was formed and reached the funnel orifice. The flow of powder was then stopped and the average diameter of the formed cone (D) was measured. The area of the base of the cone was taken as a measure of the internal friction between the particles. The angle of repose was calculated by the equation: tan θ = height / radius.

In addition, the bulk density, Hausner ratio (Tapped density / bulk density) and Carr's index (Ci) [(Tapped density –bulk density)/ Tapped density X 100%] were also determined for the dried powders. Five mg of powders were weighed and poured into a 10 mL graduated measuring cylinder. The bulk volume occupied (Vb) was recorded. The measuring cylinder was tapped until a constant value was obtained and the tapped volume was recorded (Vt). The process was repeated at least three times and the average was taken in each case. The bulk and tapped densities of powder were calculated by dividing the weight by the corresponding bulk volume or tapped volume recorded.

9. Dissolution studies

The dissolution of the prepared nanoparticles and nanoparticle agglomerates was determined and compared with the dissolution characteristics of the stock drug. The dissolution of budesonide was carried out at 37 ± 0.5oC in a 400 mL beaker. A known amount (~10 mg) of the lyophilized powder was suspended in 10 mL phosphate buffered saline (PBS, pH 7.4) and was placed into a floatable dialysis membrane unit (Mw cut-off = 10,000 Da), and the unit was allowed to float in a beaker containing 300 mL of PBS. The solution was stirred at a constant speed (100

rpm) using a magnetic stirrer (Barnstead, Thermolyne MIRAKTM). At predetermined time intervals for a total period of 8 hours, aliquots (5 ml) of the medium were removed and fresh medium was immediately added to continue the dissolution study. Studies were conducted in triplicate. The budesonide concentration was analyzed using a reverse-phase HPLC method. A Shimadzu HPLC system including a solvent delivery pump (Shimadzu LC-10AT), a controller (Shimadzu SCL-10A), an autoinjector (Shimadzu SIL-10AxL), and a UV detector (Shimadzu SPD-10A) was used in this study. The peak areas were integrated using Shimadzo Class VP (Version 4.3). A 4.6 mm x 100 mm long Zorbax SB C-18 column (Agilent C) with a particle diameter of 3.5 μm was used. During the assay, budesonide was eluted isocratically at a mobile phase flow rate of 0.6 mL/minute and monitored with a UV detector operating at 254 nm. The mobile phase for the assay consisted of an acetonitrile and water mixture (45:55 v/v). The run time for the assay was 20 minutes, and the retention time for budesonide was 14.01 minutes.

10. Cytotoxicity assay

The cytotoxicity of selected nanoparticles and nanoparticle agglomerates was assessed using the CellTiter 96® Aqueous Cell Proliferation Assay (Promega) and compared with stock budesonide, lecithin, leucine, physical mixtures of these ingredients and blank nanoparticle agglomerates. In this experiment, 8 x 104 A549 cells / well were seeded in 96-well microtiter plates. At the end of the incubation period (12 h), 20 ml of MTS reagent solution was added to each well and incubated for 3 h at 37 °C. The absorbance was measured at 490 nm using a microtiter plate reader (SpectraMax, M25, Molecular Devices Corp., CA). The percentage of viable cells with all tested concentrations was calculated relative to untreated cells.

C. Results and discussion

1. Fabrication of budesonide nanoparticles

Various methods have been reported for generating nanoparticles of poorly water soluble drugs. A precipitation method was selected to produce budesonide nanoparticles. Different concentrations of the drug and various types and ratios of surfactants, individually or in combination, were evaluated as a means to control the particle size and surface charge. Surfactants were chosen from excipients regarded as suitable for inhalation that have been designated as safe for human use. Formulations prepared using PVP and PVA in different ratios produced very large particle sizes even when combined with other surfactants. The mean particle size of formulations containing lecithin, cetyl alcohol, Span 85 and/or PL ranged from ~130 to 323 nm. Formulations

containing Span 85 alone or in combination with lecithin yielded the smallest particle size but since Span is liquid at room temperature, it was not suitable for use in dry powder formulations.

Attempts to generate budesonide nanoparticles using PL alone or in combination with lecithin yielded reasonable particle sizes (~129-270 nm) but offered very low nanoparticle yields and high polydispersity values. Selected surfactant combinations for preparing budesonide nanosuspensions in acetone were designated F1 (0.1% w/v Bud + 0.02% w/v Lec), F2 (0.1% w/v Bud + 0.02% w/v CA + 0.01% w/v PL) and F3 (0.2% w/v Bud + 0.04% w/v CA + 0.02% w/v PL) as reported in Table 13. These surfactant combinations demonstrated small particle size and could be used in dry powder formulations. A small change in zeta potential was observed with different types of surfactants and the values ranged from 22.5-25.1 mV (Table 14). The charged surface of the nanoparticles provided the potential for destabilizing this colloid via interaction with a flocculating agent to form nanoparticle agglomerates.

Table 13. Composition of the selected formulations.

Formulation	Budesonide (% w/v)	Lecithin (% w/v)	Cetyl alcohol (% w/v)	Pluronic F127 (% w/v)
F1	0.1	0.02		
F2	0.1		0.02	0.01
F3	0.2		0.04	0.02

Table 14. Physical properties of budesonide nanoparticle (values = average ± S.D.).

Formulation	Nanoparticle size (nm)	Zeta-potential (mV)	Polydispersity
F1[a]	160.9 ± 15.6	25.1 ± 1.3	0.41 ± 0.1
F2[b]	188.8 ± 26.3	24.2 ± 1.1	0.34 ± 0.02
F3[c]	232.2 ± 11.2	22.5 ± 0.5	0.33 ± 0.02

[a] F1 = 0.1: 0.02; Bud: Lec

[b] F2 = 0.1: 0.02: 0.01; Bud: CA: PL

[c] F3 = 0.2: 0.04: 0.02; Bud: CA: PL

2. Agglomerated budesonide nanoparticles yielded desirable aerosol characteristics

The mechanism to control nanoparticle agglomeration is mainly driven by leveraging the competitive processes of attraction (van der Waals force) and repulsion (electrostatic repulsive force or steric hindrance barrier or both). If particles are mainly stabilized electrostatically, disruption of the electrostatic double layer surrounding the particles will result in the

agglomeration of nanoparticles. The addition of flocculating agents has also been speculated to decreases the cohesion between particles. It is thought that these agents may interfere with weak bonding forces between small particles, such as Van der Waals and Coulomb forces. These agents may act as weak links or "chain breakers" between the particles which are susceptible to disruption in the turbulent airstream created during inhalation. The amino acid, L-leucine, used as a flocculating agent in these studies may also act as an anti-adherent material to yield a high respirable fraction of the agglomerated budesonide nanoparticles.

Flocculation of nanoparticles resulted in the formation of agglomerates within the micrometer or sub-micrometer scale consisting of closely-packed nanoparticles. Nanoparticle agglomerates were prepared through the slow incorporation of a flocculating agent (L-leucine) during homogenization (25,000 rpm) for 30 sec. The geometric size distribution of the prepared nanoparticle agglomerates was measured in Isoton diluent using a Coulter Multisizer 3. The size average of the three selected nanoparticle agglomerate formulations ranged from ~2-4 mm (Table 15). The size distributions of resuspended lyophilized powders were slightly broader and the average particle size was slightly increased, when compared to the nanoparticle agglomerates prior to lyophilization (Table 15 and FIG. 18). This may be due to the deposition of nanoparticles on agglomerates during lyophilization or to cohesion between agglomerates as a result of drying. The key physical parameter that predicts the site of aerosol deposition within the lungs for particles larger than several hundred nanometers is the aerodynamic diameter (d_{aero}). The aerodynamic diameter of the flocculated nanoparticles, measured by an Aerosizer LD, was smaller than the geometric diameter and the aerodynamic size distribution was narrower than the geometric size distribution (Table 15 and FIG. 19). When compared to the geometric diameter, the lower aerodynamic diameter was likely due to the low density of nanoparticle agglomerates.

Table 15. Characteristics of budesonide nanoparticle agglomerates (values = average ± S.D.).

Characteristics	**Formulations**		
	F1[a]	**F2**[b]	**F3**[c]
Geometric particle size (μm) of NA[d] before lyophilization	2.8 ± 0.4	2.7 ± 0.4	3.2 ± 0.7
Geometric particle size (μm) of lyophilized NA[d]	3.1 ± 0.6	3.3 ± 0.7	3.9 ± 1.1
MMAD[f] of lyophilized NA[d]	1.4 ± 1.7	2.1 ± 1.8	1.9 ± 1.8
% Process yield of lyophilized NA[d]	95.5 ± 4.9	92.7 ± 3.1	89.7 ± 3.6

Loading Efficiency of lyophilized NA[d]	95.9 ± 3.6	86.5 ± 6.0	92.5 ± 6.6
Q_{8h}[g]NP[e]	61.5 % ± 1.6	75.5 % ± 9.9	88.9 % ± 3.0
Q_{8h}[g]NA[d]	41.8 % ± 4.6	51.2 % ± 5.1	63.1 % ± 5.1

[a] F1 = 0.1: 0.02; Bud: Lec

[b] F2 = 0.1: 0.02: 0.01; Bud: CA: PL

[c] F3 = 0.2: 0.04: 0.02; Bud: CA: PL

[d] NA: Nanoparticle agglomerates.

[e] NP: Nanoparticles.

[f] MMAD: Mass median aerodynamic diameter obtained from Aerosizer.

[g] Q_{8h}: % budesonide dissolved after 8 hours.

The theoretical mass–mean aerodynamic diameters (d_{aero}) of the nanoparticle agglomerates, determined from the geometric particle size and tapped density, was found to be 2, 2.1 and 2.5 mm for F1, F2 and F3, respectively as calculated from the relationship:

$$d_{aero} = \frac{d_{geo}}{\gamma}\sqrt{\rho / \rho_a}$$

Where d_{geo} = geometric diameter, γ = shape factor (for a spherical particle, $\gamma = 1$; for aerodynamic diameter calculations, the particles in this study were assumed to be spherical), ρ = particle bulk density and ρa = water mass density (1 g/cm^3). Tapped density measurements underestimate particle bulk densities since the volume of particles measured includes the interstitial space between the particles. The true particle density, and therefore the aerodynamic diameter of a given powder, is expected to be slightly larger than reported. Particles with a daero between 1 and 5 mm that are inhaled via the mouth are capable of efficient alveolar deposition, whereas daero between 4 and 10 mm are more likely to deposit primarily in the tracheobronchial region of the lungs. Therefore, the budesonide nanoparticle agglomerates with daero in the 2-2.5 mm range are expected to deposit primarily in the alveolar region of the lungs.

Aerosizer results and theoretical MMAD calculations were corroborated by cascade impaction studies at air flow rates of ~15 L/min, ~30 L/min and ~60 L/min (FIG. 20). At these flow rates, most nanoparticle agglomerates were deposited in stages 6 and 7 of the cascade impactor which was suggestive of efficient aerosolization and a high fine particle fraction. The aerosolization efficiency of nanoparticle agglomerates was represented by the percent emitted fraction (%EF), percent respirable fraction (RF), mass-median aerodynamic diameter (MMAD)

and geometrical standard deviation (GSD). The percent emitted fraction was determined from the following equation:

$$\%\,\text{Emitted fraction (\%EF)} = \frac{\text{Total particle mass collected from the stages of the impactor}}{\text{Total particle mass entered into the impactor}} \times 100$$

The high emitted fraction of nanoparticle agglomerates obtained at the tested flow rates suggested efficient aerosolization of the powder (Table 16). The percent respirable fraction (RF), referred to also as the fine particle fraction of the total dose (FPFTD), was calculated as the percentage of aerosolized particles that reached the lower seven stages of the impactor (corresponding to aerodynamic diameters below 5.8 mm), or the lower five stages (corresponding to aerodynamic diameters below 3.3 mm) according to the following equation:

$$\%\,\text{Respirable fraction (RF)} = \frac{\text{Powder mass recovered from terminal stages of the impactor}}{\text{Total particle mass recovered in the impactor}} \times 100$$

The results of the respirable fraction also suggested the efficient aerosolization of nanoparticle agglomerate powders (Table 16). The geometric standard deviation (GSD) of the nanoparticle agglomerates was determined from the following equation:

$$GSD = \left(\frac{d_{84.13\%}}{d_{15.87\%}}\right)^{1/2}$$

Where d_n is the diameter at the nth percentile of the cumulative distribution. The mass–mean geometric size of nanoparticle agglomerates ranged between 3 and 4 mm with a GSD of ~2.3 mm (Table 16). Typical GSD values for aerosol particles are between 1.3–3.0.17 The mass-mean aerodynamic diameter (MMAD) of the selected nanoparticle agglomerates, as calculated from the cascade impaction results (Table 16) was close to that obtained from the Aerosizer (Table 15) although it was slightly smaller than the theoretical density values calculated from the tapped density indicating the suitability of the prepared nanoparticle agglomerate powders for peripheral lung deposition (i.e., < 3 mm).

Table 16. Cascade impaction results of lyophilized budesonide nanoparticle agglomerates (values = average ± S.D.).

Characteristics of the lyophilized NA[d]		**Formulations**		
		F1[a]	**F2[b]**	**F3[c]**
At flow rate	% EF[e]	74.9 ± 6.1	69.3 ± 5.5	86.5 ± 8.6

of ~15 L//min	% RF[f]	< 5.7	96.3 ± 1.8	97.5 ± 1.3	97.9 ± 0.3
		< 3.3	77.6 ± 3.9	81.2 ± 5.2	75.3 ± 1.7
	MMAD[g]		1.7 ± 0.1	1.5 ± 0.1	1.9 ± 0.3
	GSD[h]		2.4 ± 0.2	2.3 ± 0.1	2.3 ± 0.3
At flow rate of ~30 L//min	% EF[e]		75.3 ± 7.3	70.2 ± 4.1	81.2 ± 12.9
	% RF[f]	< 5.7	97.1 ± 0.2	96.8 ± 1.5	96.9 ± 1.4
		< 3.3	84.3 ± 3.9	87.7 ± 1.5	82.3 ± 4.2
	MMAD[g]		1.3 ± 0.2	1.2 ± 0.04	1.6 ± 0.3
	GSD[h]		2.3 ± 0.3	2.3 ± 0.4	2.3 ± 0.1
At flow rate of ~60 L//min	% EF[e]		77.4 ± 6.6	72.2 ± 5.9	82.9 ± 12.7
	% RF[f]	< 5.7	95.8 ± 0.2	95.9 ± 1.5	95.7 ± 1.7
		< 3.3	87.1 ± 2.3	89.3 ± 2.5	83.6 ± 2.8
	MMAD[g]		1.1± 0.2	1.1 ± 0.1	1.3 ± 0.2
	GSD[h]		2.3 ± 0.1	2.3 ± 0.2	2.3 ± 0.1

[a] F1 = 0.1: 0.02; Bud: Lec

[b] F2 = 0.1: 0.02: 0.01; Bud: CA: PL

[c] F3 = 0.2: 0.04: 0.02; Bud: CA: PL

[d] NA: Nanoparticle agglomerates.

[e] % EF: Percent emitted fraction.

[f] RF: Percent respirable fraction.

[g] MMAD: Mass median aerodynamic diameter.

[h] GSD: Geometric standard deviation.

Electron microscopy was used to study the morphology of budesobide nanoparticle and nanoparticle agglomerate formulations. Transmission electron micrographs (TEM) of F1 nanoparticles (FIG. 21A) depicted slightly elongated nanoparticles with smooth surfaces and a particle size around 170 nm. TEM images of F1 nanoparticle agglomerates (FIG. 21B) show that the nanoparticles were flocculated into micron sized agglomerates with irregular structure and some sharp edges.

FIG. 23 shows the 13C spectra of budesonide by itself and in formulations. Both the budesonide as received and the leucine exhibit relatively narrow lines (several tens of hertz), indicating that these samples are crystalline. Lecithin also had narrow lines, which is consistent with it being a crystalline form of phosphatidylcholine; however, it is a semi-solid and therefore cannot be crystalline. Conversely the budesonide that was melt quenched had significantly broader lines (several hundreds of hertz) indicating that the budesonide is consistent with it being

amorphous. In the nanoparticles, the peaks for budesonide are similar to the peaks in the budesonide that was melt quenched, although the peak at ~180 ppm shows that there is a small amount of crystalline budesonide in the nanoparticles. The tall, sharp peaks in the spectrum of the nanoparticle agglomerates align with the peaks in the leucine spectrum and showed that the leucine in the formulation has undergone phase separation and has crystallized to some extent. The peak at 180 ppm showed that the amount of crystalline budesonide had increased in the formulation of the nanoparticle agglomerates. This was consistent with the shape of several other budesonide peaks in the spectrum.

Budesonide consists of 25 carbons (FIG. 23); however, the spectrum of the budesonide as received had at least 27 resolved peaks and several peaks that may be the result of several overlapping peaks. The extra peaks did not seem to be due to splitting, as would be expected if there were more than one molecule in the asymmetric unit cell.

The budesonide is a racemic mixture of both epimers that have been shown to pack differently in the crystal lattice. Therefore, spectral editing was used in an attempt to assign the peaks in the spectrum to determine if the differences in the two epimers could be used to explain the "extra" peaks. The spectral editing experiment allowed the assignment of carbon type (C, CH, CH2, or CH3) to a peak, these assignments could then be combined with predictions to assign the peaks to specific carbons within the molecule. The carbon type of most of the peaks could be assigned from these experiments (FIG. 24) with the exception of a few of the aliphatic peaks (particularly ~30–40 ppm). These results were then compared with predictions of the solution state chemical shifts from two different software programs and the resulting assignments are shown in Table 17.

Table 17. ^{13}C peak assignments for budesonide as received.

Assignment	As Received	ACD/Labs*	ChemBioDraw*
20	209.0	207.0	211.2
3	185.4	186.2	185.7
5	170.6	170.3	168.1
1	156.7	156.5	158.4
2	122.5 and 128.2	127.5	128.3
4		122.1	124.2
22	104.5 and 107.3**	105.1	102.0
17	99.8	94.4	105.0
16	83.0	77.3	86.7
11	67.4 and 70.7	68.0	69.0
21		67.0	66.6

9	49.7 and 53.6	54.1	59.0
14		48.8	44.0
13	44.6 and 47.4	47.0	44.7
10		42.6	44.1
12		41.0	40.4
23	32.2, 33.9, 34.7, 38.1, 39.0, and 40.2	35.3	36.5
7		33.4	32.0
6		31.9	32.9
15		31.9	32.7
8	31.6	32.3	34.6
19		21.0	19.0
18	15.6, 18.7, and 22.5	16.3	17.3
25		14.0	14.4
24	17.2	18.4	13.1

* = Software predictions of chemical shifts in solution.

** = See text for explanation.

Chemical shifts for a compound in the solution and solid state can vary by as much as 10 ppm. For this reason, some assignments can be narrowed down to a few possibilities but an exact assignment was not possible with this data. For example, carbons 2 and 4 can be assigned to the peaks at 122.5 and 128.2, but it was not possible to definitively determine which carbon was associated with which peak. The solution predictions placed carbon 22 at ~103 ppm, while the spectral editing experiment showed that there are two peaks at 104.5 and 107.3 ppm that can be assigned to CH carbons. Additionally, carbon 22 is the chiral center of the epimers. Based on these observations and the fact that the two epimers have been shown to pack in different conformations, both peaks were assigned to carbon 22 with the interpretation that each peak represents one of the epimers. It is important to note that this interpretation assumes the budesonide is pure, which we have not confirmed. Additionally, there is always the possibility that these are different polymorphs; however, reports of polymorphism in budesonide have not been identified.

The process of agglomerating nanoparticles was evaluated to determine their yield. The results (Table 15) have shown that the process was efficient providing a high yield (~90-95%) and minimum batch variability. The loading efficiency of the drug in the prepared nanoparticle agglomerates was found to be between 85-95% (Table 16), thus demonstrating minimal loss of drug during formation.

The flow characteristics of the selected nanoparticle agglomerates were also determined (Table 18). Angle of repose, Hausner ratio and Carr's index are considered to be indirect methods

for quantifying powder flowability. Budesonide nanoparticle agglomerates generally exhibited similar bulk densities and lower tapped densities than that of the stock drug powder. Nanoparticle agglomerates also demonstrated improved flow properties. This may be attributed to the reduced density of the nanoparticle agglomerates. In addition, L-leucine has been reported to reduce surface energy in dry powders and may improve flowability in this case. Formula F3 showed slightly better flowability compared to the others according to the Carr's index; however, all nanoparticle agglomerate powders possessed acceptable flowability.

Table 18. Flowability characteristics of budesonide nanoparticle agglomerates (values = average ± S.D.).

Formula No.	Angle of repose (θ) (flowability)	Bulk density (g/cm3)	Tapped density (g/cm3)	Carr's index (C_i %)	Hausner ratio
F1 [a]	37.1 ± 2.6	0.34 ± 0.1	0.42 ± 0.03	21.8 ± 0.5	1.2 ± 0.03
F2 [b]	39.1 ± 1.1	0.31 ± 0.1	0.40 ± 0.1	23.6 ± 0.6	1.3 ± 0.03
F3 [c]	37.8 ± 2.1	0.29 ± 0.1	0.38 ± 0.1	18.6 ± 0.4	1.2 ± 0.1
Stock budesonide	43.5 ± 0.7	0.30 ± 0.04	0.47 ± 0.1	35.4 ± 2.1	1.5 ± 0.1

[a] F1 = 0.1: 0.02; Bud: Lec

[b] F2 = 0.1: 0.02: 0.01; Bud: CA: PL

[c] F3 = 0.2: 0.04: 0.02; Bud: CA: PL

3. Budesonide nanoparticle and nanoparticle agglomerates showed improved dissolution rates

A dissolution study of budesonide was conducted for the prepared nanoparticles and nanoparticle agglomerates and compared to the unprocessed drug. The cumulative percentage of drug dissolved after 8 hours (Q8h) was found to be slower than that of the nanoparticles and faster than that of the stock budesonide (Table 15). This finding was the expected result of increasing the surface area by decreasing the particle size. F2 and F3 nanoparticle and nanoparticle agglomerate formulations showed faster drug dissolution than F1 which may be due to the incorporation of the hydrophilic surfactant, PL (FIG. 25). In addition, increasing the concentration of this surfactant (F3) led to even faster dissolution. Linear regression analysis of the dissolution data concluded that the drug was released by the Higuchi diffusion mechanism in all cases. A two-way Analysis of Variance (ANOVA) was performed to determine the significance of differences in dissolution kinetics. Significant differences ($\alpha = 0.05$) existed between nanoparticles, nanoparticle

agglomerates and stock budesonide. No significant differences existed between different nanoparticles or nanoparticle agglomerate formulations. A significant improvement ($P<0.05$) in the dissolution behavior of the nanoparticles and nanoparticle agglomerates was also observed when these were individually compared to the stock budesonide.

4. Formulation components exhibited minimal cytotoxicity

The cytotoxicity of the different budesonide formulations were compared to stock budesonide, lecithin, leucine, physical mixtures of F1 components and blank F1 nanoparticle agglomerates (FIG. 26). Stock budesonide, excipients and physical mixtures of F1 components up to 5 mg/mL did not show any significant cytotoxicity in A549 cells at the end of 12 hours. Blank F1 nanoparticle agglomerates did induce a very low level of cytotoxicity where the IC50 was found to be 0.97 mg/mL. Additionally, F1 nanoparticles and nanoparticle agglomerates also induced very low level of cytotoxicity with IC50 values equal to 1.67 mg/mL and 1.91 mg/mL, respectively. The IC50 values occurred at higher concentrations than the maximum daily dose of inhaled budesonide currently prescribed. These results may suggest that lecithin was responsible for the cytotoxic effect.

Many current techniques to generate dry powder aerosols have a major disadvantage of poor control over the particle shape, size and size distribution. In addition, many pulmonary formulations may benefit from the improved bioavailability and rapid onset of action that may be achieved by using drug nanoparticles. In this work, budesonide nanosuspensions were successfully prepared yielding nanoparticles in the range of ~160-230 nm. This was accomplished by using surfactants proven to be safe for human use such as lecithin. Nanosuspensions were flocculated using L-leucine and the resulting nanoparticle agglomerates were analyzed. Nanoparticle agglomerates were efficiently aerosolized and offered a high fine particle fraction suitable for accessing the peripheral lung. Nanoparticle agglomerates also exhibited significantly faster budesonide dissolution when compared to the stock powder. In conclusion, budesonide nanoparticle agglomerates demonstrated a desirable microstructure for efficient lung deposition and nanostructure for rapid dissolution of poorly water soluble drugs.

Example 10

Application of Nifedipine Nanoparticles

Pulmonary administration of poorly water soluble drugs represents a leading challenge in

the drug delivery industry. These drugs are generally not suitable for delivery to the aqueous lumen of the GI tract, and are often susceptible to enzymatic degradation. This thesis investigates a general method for producing micron sized dry powders of a general class of drugs, poorly water soluble small molecule drugs, for their use in pulmonary drug delivery. These drugs are stable at room conditions in crystalline form, and typically soluble in ethanol. Our model drug in this body of work was Nifedipine, a well known calcium channel blocker used to treat various symptoms of hypertension. Formulation methods already exist for some drugs that fall into this category, but the resulting powders show limited performance.

Particulates for Pulmonary Drug Delivery

Drug delivery is a rapidly growing field of research, and the pulmonary route has not been neglected throughout this process. As technologies become more adept at characterizing and manipulating the microscopic and submicron world, our ability to reliably produce entities on this scale continually improves, and drug delivery science has rapidly sought to put these improvements to application. The ideal drug nanoparticle is equipped with a milieu of targets and sensors; everything it needs to seek and destroy the pathogen, or rebuild the damaged tissue. Indeed, we are many years from this idealized super particle, but more simple particles on this scale still yield enormous benefits. In the past few decades, it has become clear that nanoparticles and microparticles are a benchmark design strategy for drug delivery scientists, and possibly the only strategy for those interested in pulmonary delivery.

Pulmonary Physiology and Molecular Transport

Many barriers exist in the goal of delivering drugs locally and systemically via the pulmonary route. Poor deposition of particulates is a main concern. If particles are not able to be deposited into the farthest reaches of the pulmonary bed, then it is most likely that the drug will be cleared via the mucociliary transport mechanism and be deposited into the stomach and degraded and/or delivered via traditional mechanisms in the gastrointestinal tract. If the drugs are able to deposit along the terminal bronchioles and within the alveoli, there are still potential difficulties to consider. Hydrophobic drugs may not be transport efficiently in the lung surfactant that resides along these regions. The drugs may get caught on the surface, or within the surfactant mixture, never reaching the epithelial cell membranes where they can traverse the lipid bilayers. Hydrophilic drugs bear the opposite challenge. Even though they may readily disperse throughout the surfactant layers, they still may not be provided with a suitable pathway to the capillaries just

beyond the tightly grouped epithelial barrier. The surface cells in this region of the lungs are characterized by their minute morphologies and lack of interstitial spacing between cells.

A Brief History of Pulmonary Drug Delivery

Pulmonary delivery stands out among the various delivery schemes for many reasons. Inhalers can be stored and used for isolated emergency events, such as those that may arise through such diseases as diabetes and chronic bronchitis. Drug entities delivered via the lungs are able to avoid first pass metabolism in the liver and this may increase overall bioavailability.

The aim of this study was to investigate the synthesis and performance of nanoparticle flocculations in the formulation of micron sized particulates for aerosolized pulmonary drug delivery. Nanoparticles (~700 nm, -30mV) of the hypertension drug Nifedipine were synthesized via known solvent anti-solvent precipitation techniques. The resulting colloids were destabilized via ionic charge interactions using common salts at different solution molarities to achieve a final particle size distribution suitable for delivery of particulates to the deep lung. The flocculated solutions were freeze dried and collected as dry powders for further characterization. Synthesis and separation techniques were optimized for nanoparticle size, flocculate size, overall yield, and flowability. Performance of the final powders was found suitable for delivery of Nifedipine to the deep lung.

Introduction

Pulmonary drug delivery represents a rapidly growing sector in the field of drug delivery. With characteristically fast onset of action, high bioavailability and relative ease of administration, this delivery route presents potential advantages to many traditional dosage forms. Nifedipine is one such drug that bears complicated pharmacodynamics in the traditional oral dosage form. Nifedipine shows limited systemic bioavailability via the oral route due to a combination of enzymatic effects in the stomach and small intestine, primarily from P450 reductase and CYP3A mediated drug metabolism. Though it is effective in easing symptoms of sever hypertension, it sometimes can not be used for this reason due to elevated vasodilation and extreme hypotension. It is particularly useful in treating pulmonary hypertension, but hypotensive side affects hinder the drug in this case, as well. Given orally, the concentrations that are needed to achieve beneficial effects to the heart may cause unwanted side affects, including an increase in mortality rate for patients with coronary heart disease. For these reasons, current forms of Nifedipine bear a largely untapped therapeutic effect that could be harnessed if it were effectively administered at lower

dosages to the heart and lung tissues. Pulmonary administration of Nifedipine is one such strategy that might help alleviate the aforementioned difficulties.

Nifedipine is a dihydropyridine and resides in a class of calcium antagonists known as calcium channel blockers. It is a small molecule poorly water soluble drug with the site of action at the calcium channels residing on the surface of all cells and primarily acts upon smooth muscle cells and heart muscle cells. Many different drugs bear similar physical and chemical properties to nifedipine, such as its hydrophobicity and cyclic structure, so the methods contained in this paper may be applicable to formulating a host of drugs for pulmonary delivery.

In designing our formulation, it was of great importance to control the surface charge of the nanoparticles, so as to promote a destabilization of the colloid upon introduction of the salt ions. To this end, we introduced stearic acid into the initial drug solution, which is found native in the surfactant layer that rests above the lung epithelium, and also bears a minimal penetration enhancing effect, at least for protein delivery.

Nifedipine (NIF), stearic acid (SA), arachidonic acid (AA), sodium chloride and calcium chloride were purchased from Sigma Chemicals Co, USA and used as received in solid form. Acetone, methanol, ethanol, and phosphate buffered salts were purchased from Fisher Scientific and used as received. Dialysis membranes (MWCO = 6-8 kDa) were purchased from Fisher Scientific. DI water was used throughout the study as obtained from a Millipore ultrapurification unit present on site.

Preparation of nifedipine nanoparticle suspensions

Nanoparticles were prepared by the rapid mixing of ethanol with dissolved nifedipine and stearic acid into a larger aqueous volume, known as a solvent anti-solvent precipitation technique. Briefly, 10 mg of Nifedipine and 1 mg of stearic acid were completely dissolved in 1 ml of ethanol and allowed to stir overnight. Upon complete dissolution this solution was added to 29 ml of cold deionized water under probe sonication at 60% amplitude for 20 seconds. The resulting colloid was then immediately frozen and lyophilized, or stored in a 4°C refrigerator until further processing into flocculations. At this time, a small sample was taken from the solution for sizing and imaging. All solution vials and reaction vessels were kept covered from any light sources, as Nifedipine exhibits considerable photosensitivity from UV and visible light spectra.

Preparation of nanoparticle flocculations

Nanoparticle colloids were destabilized via a largely understood combination of ionic and

thermodynamic force interactions to produce stable flocculations of nanoparticles. Briefly, 30 ml of the nanoparticle suspension was taken from refrigeration and solid salt crystals were added in various amounts. Directly after addition, the suspensions would be subject to vigorous mixing via a homogenization probe operating at 20,000 RPM. Three different salt species were tested for their ability to form flocculations: sodium chloride, calcium chloride, and magnesium sulfate. Salts were commonly added in a 1:1 ratio of salt to NIF. Colloid stability was also tested under a range of salt molarities and flocculation behaviors were observed under all conditions.

Nanoparticle characterization

Nanoparticle size, polydispersity, and zeta potential were all measured in solution directly after synthesis and prior to flocculation using a zetaPALS dynamic light scattering device. Size and polydispersity were first measured. Briefly, 1ml of the solution was added to a standard cuvette and the remaining volume was filled with deionized water. Data were collected in three runs and combined to arrive at a final size for each solution. Measurements were taken at 90 degrees to the incident light source while assuming a viscosity and refractive index of pure water. After arriving at a combined size, a second cuvette was filled with 1 ml of our colloid solution and the remaining volume was filled with KCl. A known voltage was then applied to this solution and data were analyzed via online software to determine the zeta potential of the particles in solution.

Flocculate characterization

Flocculated nanoparticles were studied in solution and as a dry powder. After the flocculation event was complete, a small volume (~3ml) of the solution was analyzed using a Beckman Colture multisizer III. Data were collected until the output graphs showed a stable shape and particle counts were above 100,000.

After lyophilization, dry powders of the flocculates were first analyzed using an aerosizer. At this point, 5mg of the powder was added to the aerosizer and data were collected until the output graphs showed a stable shape and the particle counts were above 100,000. Measurements were taken under medium shear and no regularization.

A cascade impactor was then used to collect data on powder performance in the lung. Briefly, eight filters were preweighed and set onto collection plates which were housed within eight airtight stages arranged serially and stacked on a level setting. Air was then pumped through the stages at 30 liters per minute via a vacuum pump and 10 mg of sample was introduced at the top of the impactor device. The powders were allowed to deposit amongst the stages for 20

seconds, after which time the air flow was stopped. Filters were then removed from the stages and weighed a second and final time.

Finally, the powders were characterized via two simple tests: a tap density test, and a test for angle of repose. The tap (bulk) density was determined by demarcating a small cuvette with known volumes, and then inserting a small mass of powder into the cuvette and tapping it vertically against a padded bench top 50 times. The density was tested in triplicate. The angle of repose was measured by placing a volume of powder on a glass slide and tilting the slide until the powder began to move down the slide, and recording the angle between the slide and the horizontal. This test was also performed in triplicate for each sample.

Particle Imaging

Nanoparticles, microparticles and pure drug crystals were imaged via a scanning electron microscope. The samples were deposited onto mica slides in solution (or as received for the crystals) and allowed to evaporate over night. The slides were then coated with a 2 nm gold surface using a voltage controlled gold sputtering device and subject to a vacuum chamber whereby image data were subsequently collected.

Dissolution Studies

Dissolution events for the flocculates, nanoparticles, and pure drug were observed and data were recorded using a Shimadzu SPD-10A UV-Vis detector set for detection at 240 nm. 45:55 (water:methanol) mixture buffered to pH 4.5 was used as mobile phase. Flowrates in the column were adjusted to 2 ml/hr and all injections were made at 50ul. All studies were performed via the dialysis method in triplicate and sink conditions were maintained at a 30:1 volume ratio. Solutions were allowed to stir at 200 rpm without heating. Samples were introduced into dialysis bags with a molecular weight cut off of 6-8 kDa.

Results

Table 19. Nanoparticle size, polydispersity, and zeta potential for an optimal formulation from an ethanol solution containing 1% w/v nifedipine and using stearic acid as a stabilizer in a ratio of 10:1 drug:acid.

Effective Diameter (nm)	732.1
Polydispersity	0.012
Zeta Potential (mV)	-26.46
Drug/Acid (mg/mg)	10
Vsolvent (ml)	1
Vantisol (ml)	29

Table 20. Flowability parameters for three samples: Pure drug as received, a selected sample of

nifedipine/stearic acid nanoparticles, and their corresponding flocculates.

Sample	Bulk Density (g/cm^3)	Tapped Density (g/cm^3)	Carr Index	Hausner Ratio
Pure Nif	0.205	0.227	10.00	1.11
Nif/SA NP	0.103	0.123	16.67	1.20
Nif/SA Floc	0.073	0.097	25.00	1.33

The properties of our nanoparticle samples are shown in Table 19. It is hypothesized that including stearic acid in the formulation allows the polar lipids to migrate to the surface of the nanoparticles arranging their carbon chains to the core of the particles while allowing their hydroxyl groups to hydrogen bond with the surrounding water molecules. This behavior is observed from the greatly reduced zeta potential of the particles as compared with the pure drug nanoparticles (data not shown). Nifedipine is a characteristically non polar molecule, so any accumulation of charge on the surface of the nanoparticles may be attributed to the stearic acid. This reasoning is also aided by the observation that stearic acid is slightly more hydrophilic than nifedipine, so it likely acts as a surfactant between the nifedipine and the surrounding water molecules and thus migrates to the surface.

It was observed that a main design constraint, nanoparticle size, could not be easily controlled by manipulating operating conditions during the formation of the colloid (data not shown). This is probably due to dominating thermodynamic force interactions in the suspension. The rate of particle precipitation is strongly dependent on the relative solubilities of the drug in both phases (water and ethanol), and this effect dominates other potential factors in particle formation such as mixing energy and time. As long as there is sufficient mixing of these two solvents, which can be achieved via ultrasonication at low to moderate amplitudes, the nucleation and growth kinetics will be able to proceed as governed by the unique interfacial force balances within the system.

Size distributions for a sample of nanoparticle flocculations are shown in FIG. 28. This data reveals the particle size distribution from a sample of nanoparticles (geometric diameter: 421.7 +/- 26.2 nm, zeta potential: -32.16 +/- 3.75) before and after homogenization at 25,000 RPM for 30 seconds. The data were collected in solution, and as such it is not ideal data for studying the powder characteristics of the flocculates. However, it is important at this stage in the synthesis to verify flocculation, as it is well known that particles can agglomerate upon lyophilization and we wanted to verify that this is not the case in our experiments. The samples reveal a fairly monodisperse distribution of sizes between about 2 and 20 microns, with an average diameter of

about 10 microns. More so, the data reveals very stable microstructure in the flocculates. Their distributions are barely altered after intense homogenization, and they maintain their shape almost entirely.

To begin powder characterization, particle samples were tested on an aerosizer via time of flight measurements. Only flocculates were used in the aerosizer. FIG. 28 shows a typical aerodynamic size distribution as collected via this method. The theoretical mass–mean aerodynamic diameter (d_{aero}) of the nanoparticles was determined from the geometric particle size and tapped density using the following relationship:

$$d_{aero} = \frac{d_{geo}}{\gamma}\sqrt{\rho / \rho_a}$$

Where d_{geo} = geometric diameter, γ = shape factor (for a spherical particle, $\gamma = 1$; for aerodynamic diameter calculations, the particles in this study were assumed to be spherical), ρ = particle density and ρ_a = water mass density (1 g/cm^3). As one can see from the variables, if the particle density is lower than that for water, then the aerodynamic diameter will be some fraction of the geometric diameter. This is the case for our flocculate samples. Their geometric diameters are shown to be much larger, on average, than the aerodynamic diameters. For the samples shown in FIGS. 22 and 23, the average geometric diameter is about five times larger than the average aerodynamic diameter. They are shown to be about 10 and 2 microns, respectively.

FIG. 29 shows SEM micrographs of the nanoparticles, flocculates and pure drug. These images further validate the data collected, thus far. The nanoparticles are shown to bear an elliptical morphology with an average diameter somewhere below one micron, but not as small as 100 nanometers. The flocculate images reveal a highly textured morphology, with many small and similarly shaped lumps protruding from the surface. These features are indicative of the mechanism behind particle formation, as they are probably the result of nanoparticles grouped together during the flocculation step. Also, we can see a somewhat porous assembly in the imaged marked 'C'. Finally, the pure drug is shown to bear a highly crystalline structure, and is received in crystals larger than 100 micrometers in some cases. This crystalline morphology is not seen in any of the other images, thus indicating the potential change in overall crystallinity.

DSC thermographs were used to further investigate the effects of processing on drug crystallinity, and to verify the overall content in each of our formulations. As we can see from FIG. 30, both stearic acid and nifedipine draw sharp endothermic troughs where they undergo a

melting phenomenon upon heating. These troughs show up in all the other graphs, however their extent and exact shape undergo changes. Firstly, it can be seen that the area between the curves and the baseline decrease for all processed samples. This may be due to experimental error, as small samples (< 5mg) were used to collect data for all particles. This was due, in part, to their very low density and the difficulties of handling the powders within the small sampling trays. However, it may be noted that since the particles have such a large surface area per mass, they will be much more susceptible to heating and thus will not require as much heat to induce a state transition. This difference would then show up as smaller troughs in the DSC endotherms. It is also worth noticing the consistently changed shape of the nifedipine peak for the nanoparticle samples. They reveal an exothermic peak indicative of a crystallization event, or some other energy producing phenomena. It may be surmised that the stearic acid and nifedipine interact upon melting of the nifedipine, whereby they arrange with respect to each other into a semi crystalline state of lower energy than just the randomly organized fluids initially present. No other theories for these exotherms have been presented at this point.

Dissolution studies were conducted to measure the relative ease of nifedipine dissolution from the various forms of processed drug as seen in FIG. 31. Drug was mostly dissolved from all samples within 8 hours, or the kinetics simply slowed to a considerable halt, as was the case with the pure nifedipine crystals. We can see here that the nanoparticles released the most drug in the least amount of time. This is to be expected as their smaller size allows for a greater surface area for the dissolution event to take place. The flocculates outperformed the pure drug by a considerable margin, but no samples released 100% of their material into the bulk medium. This was due primarily to difficulties in the experimental apparatus, as nifedipine was inclined to adhere to the air water interfaces within the dissolution membrane and also to the membrane itself. Lack of proper dispersion prevented the pure drug samples from maintaining an optimal contact with the dissolution medium, and the same holds true for the other samples though to a lesser degree.

Finally, cascade impaction studies were performed to formalize our powder characterization for a pharmacological setting. The cascade impactor is a well known instrument devised in the 1950's for simulating aerosol performance in the human lungs. The stages are set up so that each of them (1-7 and F) represents a deeper layer of the pulmonary bed. Our data are shown in FIG. 32. Firstly, it should be noted that stage F is shown here as stage 8, simple to ensure a numerical ordering to the graph. The outputs reveal different behaviors for each of the samples.

The pure drug mostly deposits in the earlier stages, 1-3. These stages prepresent the pharyx and primary bronchi and so it may be assumed that these powders would not enter the lungs whatsoever. The nanoparticles show the bulk of their deposition between stages 4-6 and these represent the secondary, and terminal bronchiolar and alveolar regions. The flocculates show similar deposition patterns. Indeed, these are suitable regions for delivery of particles to the lungs and so it may be shown here that both the nanoparticle samples and their corresponding flocculates are able to deposit efficiently to the lungs. The exact reasons for this similarity, given different processing steps, may be elusive for the time being. However, one may consider that the nanoparticles are able to agglomerate upon lyophilization and hence bear similar structural properties to the flocculates. However, this similarity does not necessarily detract from the advantages of the flocculation since the flocculated particles are more likely able to be harvested directly from solution without the expensive processing step of lyophilization.

Stearic acid stabilized pure drug nanoparticles of nifedipine were synthesized via ultrasonication in a pure aqueous solution. These colloids were destabilized under different salt molarities and/or salt:drug mass ratios to induce particle flocculation and subsequent microstructure formation. Nifedipine changes morphology upon processing with and without stearic acid. Nanoparticles revealed enhanced dissolution kinetics when compared to the pure drug and flocculated samples. The resulting dried powders exhibited suitable flowability characteristics and size distributions for pulmonary drug delivery.

Throughout the course of preparing samples for the primary study, data were collected to help optimize the formulation and gain understanding of the processes at work. The results of these studies are shown here, with a brief discussion concerning their significance.

Table 21. Nanoparticle size, polydispersity, and zeta potential under various operating conditions.

Sample	size (nm)	polydispersity	zeta (mV)	drug/acid	disp. vol. (ml)	cont. vol. (ml)	son. time (s)
A	235.10	0.03	-20.93	50.00	1.50	30.00	90.00
B	259.60	0.01	-27.38	10.00	1.50	25.00	90.00
C	262.90	0.24	-30.44	0.71	5.00	50.00	60.00
D	264.30	0.51	n/a	6.00	5.00	50.00	120.00
E	308.80	0.26	-19.67	5.00	1.50	25.00	60.00
F	317.80	n/a	-46.61	0.30	5.00	50.00	60.00
G	323.30	n/a	-33.64	0.60	5.00	50.00	60.00
H	336.10	n/a	-34.42	0.60	5.00	50.00	60.00
I	472.30	0.15	n/a	6.00	1.00	50.00	20.00
J	584.40	0.01	n/a	6.00	1.00	25.00	60.00
K	598.10	n/a	n/a	6.00	0.10	25.00	40.00
L	635.20	0.46	n/a	6.00	5.00	10.00	60.00
M	653.70	0.23	n/a	6.00	0.10	50.00	60.00

Table 22. Particle sizes under a range of sonication amplitudes. W/O = 25, D/A = 1, Vtot = 30ml,

Prepared with 0.1% nifedipine in ethanol and stearic acid as a stabilizer.

Amplitude (%)	Effective Diameter (nm)	Polydispersity
10	626.1	0.064
20	696.5	0.271
30	947.3	0.289
40	1057.5	0.005
50	1049.3	0.22
60	1303.7	0.005
70	689.8	0.354

Table 23. Particle sizes under a range of sonication times. W/O = 60, D/A = 10, Vtot = 30ml, prepared with 1% nifedipine in ethanol.

Time (seconds)	Effective Diameter (nm)	Polydispersity	Zeta Potential
5	534.3 +/- 28.4	0.091	(14.32) +/- 0.82
10	507.1 +/- 39.0	0.154	(12.47) +/- 0.69
15	553.8 +/- 16.5	0.166	(15.65) +/- 1.25
30	507.0 +/- 20.1	0.184	(17.63) +/- 2.19
60	495.8 +/- 50.2	0.26	(15.61) +/- .64

The dynamics of nanoparticle and flocculate synthesis are somewhat elucidated from the previous tables and figures. It is shown from Tables 21-23 that nanoparticle formation does not show immediate dependence on either sonication amplitude or sonication time. However, it should be noted that both tests were carried out while holding all solution variables constant (solvent/anti-solvent volumes, drug concentration in the solvent phase, drug/acid ratio). It may be the case that our results could have shown stronger sonication amplitude and time dependencies if we had altered our solutions. Even so, our final synthesis routine probably would not have changed, since we fixed our solution variables with in depth reasoning. The drug/acid ratio was minimized since the lungs show sensitivity to stearic acid, and the drug concentration in the solvent phase and the solvent/anti-solvent volumes were maximized to make the synthesis scheme cost effective. Indeed, it remains for future work to compile a comprehensive report of the particle size and zeta potential dependencies under a vast range of operating conditions.

Example 11

Application of Insulin Nanoparticles

Diabetes is a set of diseases characterized by defects in insulin utilization, either through autoimmune destruction of insulin-producing cells (Type I) or insulin resistance (Type II). Treatment options can include regular injections of insulin, which can be painful and inconvenient, often leading to low patient compliance. To overcome this problem, novel

formulations of insulin are being investigated, such as inhaled aerosols. Sufficient deposition of powder in the peripheral lung to maximize systemic absorption requires precise control over particle size and density, with particles between 1 and 5 μm in aerodynamic diameter being within the respirable range. Insulin nanoparticles were produced by titrating insulin dissolved at low pH up to the pI of the native protein, and were then further processed into microparticles using solvent displacement. Particle size, crystallinity, dissolution properties, structural stability, and bulk powder density were characterized. We have demonstrated that pure drug insulin microparticles can be produced from nanosuspensions with minimal processing steps and with suitable properties for deposition in the peripheral lung.

Diabetes mellitus is a set of diseases characterized by defects in insulin utilization, either from autoimmune destruction of insulin-producing cells (Type I) or insulin resistance (Type II). As of 2005, 20.8 million people in the United States (7.0% of the population) suffered from diabetes, and it was the sixth leading cause of death due to the many complications associated with this disease, such as pulmonary hypertension and ischemia. Current treatment methods involve regular injections of insulin, which can be both painful and inconvenient, thus often leading to low patient compliance.

In order to overcome this problem, other routes of insulin administration have been investigated. Inhaled aerosols have been shown to be an effective means to treat local diseases of the lung. Additionally, the large surface area of the lungs (~140 m^2) and their ready access to systemic circulation makes them a possible candidate for noninvasive, systemic drug delivery. This is particularly good for macromolecular drugs such as peptides, proteins, and DNA.

Sufficient deposition of aerosol particles in the peripheral lung requires precise control over particle size and density, which greatly affect the region of deposition in the lungs. Particles possessing an aerodynamic diameter in the range of 1-5 μm are required for suitable terminal bronchiole and alveolar deposition, as a means to access systemic bioavailability. Low-density particles are currently being developed as a means to deliver drugs to the distal regions of the lungs. These particles possess large geometric diameters, but smaller aerodynamic diameters due to their low density, as described by the following equation,

$$d_{aero} = d_{geo}\left[\frac{\left(\rho/\rho_{ref}\right)}{\gamma}\right]^{0.5}$$

Where p_{ref} is a reference density (for example 1 g/cm^3 for water) and γ is the shape factor (equal to 1 for a sphere).

Studies have shown that insulin delivered via the pulmonary route is well tolerated and effective in treating patients with Type I diabetes. Currently, there are several inhaled insulin delivery systems in development. Of these, those employing the Technosphere (Mannkind Corporation) and Spiros technologies (Dura Pharmaceuticals) are dry powder formulations. The Exubera formulation (Nektar Therapeutics and Pfizer) and the formulation using AIR technology (Alkermes and Eli Lilly) are other examples of dry powder formulations that were either FDA approved and discontinued (Exubera), or terminated during Phase III clinical trials (AIR). One potential drawback to these formulations is that they contain excipients, which aid in manufacturing and aerosol performance, but may have unforeseen negative impacts on the long-term respiratory health of the patient. Of particular concern are penetration enhancers, such as polyoxyethylene 9 lauryl ether and sodium glycocholate, which have been shown to induce acute inflammation in the lung. It may therefore be desirable to create an inhalable form of insulin that does not contain excipients so as to avoid any potential complications that might arise.

Additionally, most of the current technologies use a spray drying technique to produce particles, which can subject the insulin to air/water interfaces, high temperatures, and other conditions that can cause the protein to denature.

Here, a dry powder Zn-insulin formulation possessing appropriate microstructure to reach the deep lung that is processed without excipients has been developed (FIG. 38). Factors such as pH and insulin concentration were shown to have an affect on seed nanoparticle size. Circular dichroism (CD) and solid-state nuclear magnetic resonance (ssNMR) were used to show that irreversible secondary structure and crystallinity changes of the insulin did not occur as a result of processing. It has been demonstrated that excipient-free, insulin microparticles that are suitably sized for pulmonary delivery and have a high dissolution velocity can be produced with minimal processing steps. This development may help future researchers develop novel pulmonary

delivery systems for the treatment of diabetes.

A. Materials and Methods.

1. Materials.

Lyophilized insulin powder from bovine pancreas (0.5% zinc content) and phosphate buffered saline premix (PBS) were purchased from Sigma (St. Louis, MO). All other reagents were purchased from Fisher Scientific (Pittsburgh, PA) and used without further purification.

2. Fabrication of insulin nanoparticles.

Approximately 100 mg of insulin stock powder were dissolved in 15 mL of 0.01 N HCI solution. The solution was then titrated drop-wise to a pH just below the isoelectric point (pi) of the native protein (5.3) with 0.01 N NaOH solution, at which point the solution became colloidal without fully precipitating. The mean geometric diameters and polydispersities of the nanoparticle suspension were measured using dynamic light scattering (Brookhaven Instruments Zeta Potential Analyzer, Holtsville, NY). Nanoparticles were diluted in deionized H2O (100X) and three, 1 minute measurements were obtained at 25°C for each sample. Mean size and polydisperity were determined by the method of cumulants. The same instrument was used to determine the zeta potential (ζ) of the nanoparticles in 1mM potassium chloride solution. Three runs of 15 cycles were acquired, and the mean zeta potential was recorded. Some samples were frozen at -80°C and lyophilized using a Labconco bench top lyophilizer (Kansas City, MO) for further analysis.

A range of pH values near the pi of the native protein were determined in which the nanoparticle colloid was preserved. Particle sizes and zeta potentials were measured for each sample. Nanoparticle samples within this pH range (from 4.92 to 5.09) were centrifuged at 13,000 rpm for 10 minutes and the supernatant concentration of insulin was analyzed using UV absorbance spectroscopy (Agilent 8453). All pH values were measured in triplicate. The measured concentration was used to calculate the mass of insulin in the pellet from the original insulin mass and total volume.

3. Agglomeration of insulin microparticles.

5 mL aliquots of insulin nanoparticle suspensions were added to 15 mL of ethanol and stirred for -36 hours at 300 rpm under a fume hood. Nanoparticles with diameters of approximately 200 nm were selected for this step. The geometric diameters of the insulin microparticles were measured using a Coultier MultisizerTM 3 (Beckman Counter, Fullerton,

CA). Samples were then frozen at -80 °C and lyophilized for further analysis.

4. Characterization of aerosol properties.

The aerodynamic diameters of the lyophilized powders were determined using an Aerosizer LD (Amherst Process Instruments Inc.). Data were collected over ~70 seconds under high shear force (-3.4 kPa) using a 700 μm nozzle.

5. Characterization of particle morphology.

The size and morphology of lyophilized samples were evaluated using a LEO 1550 field emission scanning electron microscope (SEM). All samples were sputter-coated with gold for 30 seconds prior to imaging.

6. Conformational stability of processed insulin.

Post-processing secondary structural changes in samples were analyzed by dissolving particles in 0.01 N HCI solution and analyzing using circular dichroism spectroscopy (CD; Jasco J-810, Easton, MD) to determine conformational differences between processed and unprocessed insulin, as well as thermal stability differences between groups. CD spectra were acquired in three accumulations from 260-195 nm with a scanning speed of 50 nm/min and 1.0 nm resolution. Thermal stability was determined at a wavelength of 210 nm from 10-80 °C with a scanning speed of 15 °C/hr. Thermal stability spectra were acquired in triplicate. Insulin concentration in prepared solutions was determined by UV absorbance spectroscopy.

7. Crystallinity of processed insulin.

NMR: Spectra were collected using a Tecmag Apollo spectrometer operating at 300 MHz using ramped amplitude cross-polarization (RAMP), magic-angle spinning (MAS), and SPINAL-64 decoupling. Samples were packed in 4 mm o.d. Zirconia rotors using Teflon® encaps, and spun at 8 kHz in a Chemagnetics™ Triple-Resonance HXY CP/MAS NMR probe configured to run in double-resonance mode using the H and X channels, and fitted with a 4 mm spin module from Revolution NMR. All spectra are the sum of 120,000 transients collected using a 1.5 s pulse delay, a contact time of 2 ms, and a 1H 90° pulse width of 2.3 ps. The free induction decays consisted of 256 points with a dwell time of 33.3 ps. The spectra were externally referenced to tetramethylsilane using the methyl peak of 3-methylglutaric acid at 18.84 ppm.

HPLC: The crystalline insulin content of the materials was determined using the method in the insulin zinc suspension monograph of the 2005 U.S. Pharmacopoeia National Formulary, with minor modifications. Buffered acetone TS was produced by dissolving 8.15 g of sodium

acetate and 42 g of sodium chloride in 100 mL of water, to which 68 mL of 0.1 N hydrochloric acid and 150 mL of acetone were added, the mixture was then diluted with water to make 500 mL. Approximately 0.5 mg of insulin was placed in a 1.5 mL microcentrifuge tube and 33.3 pL of a 1:2 mixture of water and buffered acetone TS was added to the tube to extract any amorphous insulin. The sample was immediately centrifuged at 13,000 rpm for one minute, the supernatant was decanted, and the extraction was repeated. Additionally, ~0.5 mg of insulin was placed in another microcentrifuge tube to be used as a control. Both insulin samples were each dissolved in 33.3 pL of 0.01 N hydrochloric acid and analyzed by HPLC, with each sample being prepared in triplicate.

The HPLC was a Shimadzu system that consisted of an SCL-10A system controller, LC-10AT liquid chromatography pump, SIL-10A auto injector with a sample cooler, and SPD-10A UV-VIS detector with instrument control and data analysis performed through CLASS-VP software. Aqueous mobile phase was prepared by dissolving 28.4 g of anhydrous sodium sulfate in 1000 mL of water, to which 2.7 mL of phosphoric acid was added and the pH was adjusted to 2.3 with ethanolamine. The aqueous mobile phase was then mixed 74:26 with acetonitrile. The separation was performed on a 4.6 x 250 mm Symmetry® C18 column from Waters that was maintained at 40°C. Samples were maintained at 5°C and 20 pL were injected for analysis, with a mobile phase flow rate of 1 mL/min and the detector set to 215 nm. Peak areas were normalized to the mass of insulin used to prepare the sample and the percent crystalline insulin was calculated with the following equation:

8. Dissolution of insulin particles.

Approximately 6 mg of each insulin particle sample was suspended in PBS (pH 7.4). The solution was placed in a 100,000 Dalton biotech grade cellulose ester dialysis tube (Spectrum Labs, Rancho Dominiguez, CA) and placed in PBS solution to a final volume of 45 mL. All samples were incubated at 37°C and shaken at 50 rpm on a shaker table. 1 mL aliquots were taken at various time points up to 8 hours from the bulk solution and replaced with 1 mL of fresh PBS. The insulin concentration was measured using a Coomassie Plus colorimetric protein quantification assay (Thermo Fisher Scientific, Waltham, MA). A calibration curve was used to correlate the insulin concentration with the measured absorbance, with insulin concentrations ranging between 1 and 25 µg/mL being used as the standard. Dissolved mass was calculated from the measured concentration, and was then normalized to the total loaded mass to determine the

percent dissolved. All experiments were performed in triplicate. Analysis of variance (ANOVA) was used to determine statistically significant differences between groups ($p < 0.05$). Comparisons among groups were done using a Fisher's F-test.

9. Estimation of bulk powder density.

The bulk density of the dry powder was estimated using a micro-tap test approach, as defined in the U.S. Pharmacopoeia National Formulary, with slight modifications. Briefly, dry powder samples (unprocessed insulin, nanoparticles, and microparticles) were added to pre-weighed microcentrifuge tubes, and the tubes were weighed again to determine the mass of powder. The tubes were then tapped thirty times on the lab bench to compress the powder. The volume of the powder was approximated by comparing the height of the compressed powder to that of a volume of water in an identical pre-weighed microcentrifuge tube. The tube containing the water was then weighed to determine the volume of water (assuming a density of 1 g/mL). The powder density was calculated by dividing the mass of powder by the volume of water. All samples were analyzed in triplicate. Analysis of variance (ANOVA) was used to determine statistically significant differences between groups ($p < 0.05$). Comparisons among groups were done using a Fisher's F-test.

B. Results

1. Characterization of insulin nanoparticles.

Zn insulin nanoparticles were created by titrating dissolved insulin to the pI of the native protein, which resulted in a colloidal suspension of nanoparticles. Particle sizes and zeta potentials were analyzed over a pH range of 4.92 to 5.09, and ranged from 292.5 nm to 592.1 nm (Table 24. Zeta potentials ranged from 10.86 mV to 18.89 mV. Neither particle sizes nor zeta potentials correlated strongly with the pH of the solution.

Table 24. Characteristics of nanoparticles at various pH values.

pH	Diameter (nm)	Polydisperity	ζ-Potential (mV)
4.92	292.5 ± 42	0.384 ± 0.015	10.86 ± 2.44
4.94	535.5 ± 60.1	0.364 ± 0.008	18.89 ± 1.27
4.97	345.1 ± 15.5	0.342 ± 0.02	15.6 ± 1.05
4.98	439.8 ± 57.6	0.357 ± 0.025	17.95 ± 1.27
5.09	592.1 ± 61.8	0.349 ± 0.012	17.62 ± 0.27

The mass fraction of insulin remaining in solution after nanoparticle precipitation was determined using UV absorbance spectroscopy. These values were used to determine the mass fraction of total insulin contained in the nanoparticles. The results suggest a positive correlation between the particle size and the total mass of the insulin nanoparticles in suspension (FIG. 39).

2. Characterization of insulin microparticles.

Insulin microparticles were produced from insulin nanoparticle suspensions through solvent displacement. This was achieved by adding aliquots of insulin nanoparticle suspension to ethanol and stirring overnight. The geometric diameter of the insulin microparticles was determined to be 3.408 ± 1.35 gm. No correlation was determined to exist between insulin nanoparticle size and microparticle size (FIG. 40). SEM imaging revealed differences in the morphology of the unprocessed insulin and the insulin microparticles (FIG. 41). The unprocessed insulin agglomerates appear to have a more regular structure, while the microparticles have more of a leaf-like morphology. This leaf-like shape could aid in the aerosolizability of the insulin microparticles, and would suggest a shape factor, γ, of less than 1.

3. Aerosol properties of insulin particles.

The aerodynamic diameters of the unprocessed insulin powder, lyophilized insulin nanoparticles, and lyophilized insulin microparticles were measured with an Aerosizer LD and are shown in Table 25. The large aerodynamic diameter of the insulin nanoparticles is most likely due to uncontrolled agglomeration, which probably occurred during lyophilization. The smaller aerodynamic diameter of the insulin microparticles compared to the geometric diameter of the microparticles was expected because of the lower density of the insulin microparticles (FIG. 42).

Table 25. Particle sizes

Sample	d_{geo} (μm)	d_{aero} (μm)
Unprocessed	N/A	4.117 ± 1.852
Nanoparticles	N/A	3.649 ± 2.069
Micropatides	3.408 ± 1.35	2.32 ± 1.874

4. Conformational stability of processed insulin.

Circular dichroism (CD) was employed to analyze the secondary structure and thermal stability of processed insulin powders. Isothermal scans of dissolved, unprocessed insulin powder, dissolved nanoparticles, and dissolved microparticles reveal near-identical spectra with

minima at 210 nm, suggesting that any changes in secondary structure that might occur during processing were reversible upon dissolution (FIG. 43). This overlap was also reflected in the thermal stability CD scans, which show a slight change in molar ellipticity from 10-80°C starting at about 50°C for all samples.

5. Crystallinity of processed insulin.

The crystallinity of the insulin particles was examined using 13C CP/MAS NMR (FIG. 44). The spectra display differences in the aliphatic region (-0 to 75 ppm), although these differences are difficult to correlate with the physical state of insulin. More obvious differences between the samples arise in the carbonyl (-175 ppm) and aromatic (-137 ppm) regions. The peak at -137 ppm in the unprocessed insulin seems to be more narrow and better resolved than peaks at -129 ppm. These same lines in the other samples are broader, to the point where peaks at -129 ppm cannot be resolved. The peak at -175 ppm in the unprocessed insulin is more narrow, with two very clear shoulders at -180 ppm and -173 ppm. Other samples only show one broad peak at -175 ppm.

Crystallinity of the insulin particles was also examined using the buffered acetone method described in the U.S. Pharmacopoeia National Formulary. The results suggest that the unprocessed insulin particles are between 80% and 88% crystalline, which is much greater than both the nanoparticles and microparticles, which were estimated to be between 2% and 8% crystalline, and between 17% and 24% crystalline, respectively (FIG. 45).

6. Dissolution of insulin particles.

The concentration of insulin was measured over time in PBS solution to determine the dissolution rate of the different powders (FIG. 46). The unprocessed insulin follows Higuchi dissolution kinetics, and the nanoparticles and microparticles appear to show a burst dissolution phenomenon after 15 minutes. The dissolved masses of nanoparticles and microparticles were both significantly different from the dissolved mass of unprocessed powder after 15 minutes ($p = 0.0021$ and $p = 0.0054$, respectively). The dissolved masses of neither the nanoparticles nor the microparticles were significantly different from the dissolved mass of the unprocessed insulin after 8 hours.

7. Bulk powder density.

The tap test method was used to determine the bulk density of the insulin powders before and after processing. Density of the unprocessed insulin powder was determined to be 0.48 ± 0.08

mg/μL (FIG. 42). The nanoparticle bulk density was determined to be 0.28 ± 0.04 mg/μL, and the bulk density of the insulin microparticles was determined to be 0.063 ± 0.004 mg/μL. Analysis of variance revealed a p-value of 0.00025 ($p < 0.05$), indicating a statistically significant difference between the bulk densities of each group.

C. Discussion

Pure insulin microparticles with sizes within the respirable range were produced from the solvent-induced agglomeration of insulin nanoparticles. Nanoparticles were produced using titration and were shown to have a strong correlation between pH and particle size (FIG. 39). Microparticles were then produced using ethanol to displace the aqueous solvent and induce nanoparticle agglomeration. The proposed mechanism for this agglomeration is a combination of decreased electrostatic interactions between nanoparticles due to the addition of the organic phase, and the deposition of dissolved insulin onto the surface of the nanoparticles, forming microparticles with a leaf-like morphology. Alternatively, it might be possible that the addition of the organic phase caused a partial "melting" of the nanoparticles, thereby causing their surfaces to fuse together.

The sizes of the microparticles were independent of the size of the nanoparticles used, and had a mean aerodynamic diameter that was roughly between 0.436 gm and 4.294 gm. This range of particle sizes is similar to other dry powder insulin formulations, such as Exubera (3.5 μm), and a formulation based on the Spiros technology (2-3 μm). Additionally, these particles were smaller than those produced using AIR technology (5-30 μm). Based on the relationship between geometric and aerodynamic diameters, our data suggest a mean shape factor equal to 0.135 (assuming a P_{ref} of 1 mg/μL and $p_{tap} = P_{partide}$). This value is much less than 1, indicating that our particles are aspherical and highly irregular in morphology, thus making them good candidates for inhalation. This observation is further corroborated by SEM imaging (FIG. 41).

Circular dichroism was used to determine changes in the secondary structure of insulin that might occur as a result of particle processing. The data suggest that there are no irreversible changes that occur as a result of processing, and that the thermal stability of the insulin processed into microparticles and nanoparticles is neither enhanced nor diminished (FIG. 43).

The crystallinity of the insulin particles was first examined using 13C CP/MAS NMR (FIG. 44). Due to their highly ordered nature, crystalline materials will have relatively narrow lines in a 13C CP/MAS spectrum, while disordered or amorphous materials have relatively broad

lines. Insulin consists of 51 amino acids and therefore the spectrum will be quite complicated because every amino acid will have at least an amide and a carbon, each of which will have slightly different conformations and thus different chemical shifts. Because of this, even the 13C CP/MAS spectrum of a crystalline protein will appear to have broad lines even though it of many narrow lines with slightly different chemical shifts. Therefore, it would be expected that there would be very few differences between the 13C CP/MAS spectra of amorphous and crystalline proteins, and any differences may be subtle. The sharply resolved peaks of the unprocessed insulin would suggest that it is crystalline while all of the other samples appear to be amorphous, which is corroborated by the dissolution testing. However, at this time nothing can be said about the purity of each form because there could be some crystalline insulin in the samples that appears to be amorphous.

Crystallinity was also determined by dissolution testing, as defined by the 2005 U.S. Pharmacopoeia National Formulary, with modifications. Buffered acetone TS was used to dissolve the amorphous insulin from each sample, the concentration of which was then determined and used to estimate the crystallinity of the particles. The unprocessed insulin was shown to be about 17 times more crystalline than the nanoparticles, and 4 times more crystalline than the microparticles (FIG. 45). The dissolution rate of both the microparticles and the nanoparticles exhibited a burst effect over the first few minutes when compared to the unprocessed insulin (FIG. 46). This burst may be due to the rapid dissolution of amorphous material deposited on the surface of the particles during processing or possibly during lyophilization.In the case of the nanoparticles, it is probable that the large total surface area of the particles also plays a significant role in increasing the dissolution rate. This may be beneficial in a pulmonary insulin formulation if the desired therapeutic effect is rapid control of spikes in glucose levels. This type of formulation may be adjusted for sustained control of glucose over long periods of time, or for postprandial glucose control.

One concern with the technique outlined in the U.S. Pharmacopoeia is that it is based on the assumption that amorphous materials dissolve more rapidly than crystalline materials. This assumption might not always apply when using nanoparticles because of the enhanced dissolution velocity of particles at this scale, so interpretation of the results should be approached conservatively. Additionally, it would be prudent to examine the shelf-life of the formulation using an accelerated stability study. Solid-state drug formulations are typically more thermodynamically stable in their crystalline forms than in their amorphous forms, which could

cause the microparticle formulation to crystallize and possibly lose its burst-release properties over time. Future studies should also include examination of the formulation performance in vivo to determine the relative performance of this formulation over intravenous and subcutaneous insulin formulations, as well as other pulmonary insulin formulations.

Pure insulin microparticles produced through agglomeration of insulin nanoparticles may be a potential candidate for a pulmonary insulin formulation. The lack of penetration enhancers and other excipients in this formulation may reduce the occurrence of unforeseen side effects, thus making it potentially safer than existing alternatives. Additionally, the processing steps necessary for this formulation are minimal and did not denature or degrade the peptide, which may be a concern with currently used techniques. A major benefit of this formulation method is the ability to produce pure insulin microparticles, which has not been demonstrated with techniques such as spray drying. The development of a dry powder insulin formulation for the treatment of diabetes may help to reduce, or altogether eliminate, patient dependence on painful injections, and thus may help to increase patient compliance.

All of the compositions and/or methods disclosed and claimed in this specification can be made and executed without undue experimentation in light of the present disclosure. While the compositions and methods of this invention have been described in terms of preferred embodiments, it will be apparent to those of skill in the art that variations may be applied to the compositions and/or methods and in the steps or in the sequence of steps of the method described herein without departing from the concept, spirit and scope of the invention. More specifically, it will be apparent that certain agents which are both chemically and physiologically related may be substituted for the agents described herein while the same or similar results would be achieved. All such similar substitutes and modifications apparent to those skilled in the art are deemed to be within the spirit, scope and concept of the invention as defined by the appended claims.

CLAIMS

What is claimed is:

1. A nanocluster that comprises a plurality of nanoparticles, wherein the nanoparticles comprise a drug substance, and wherein the nanocluster is cluster of nanoparticles arranged such that the surface of the nanoparticles are in contact with one another, and wherein the nanocluster is not hollow.

2. The nanocluster of claim 1, wherein the drug substance has a solubility in water of less than 500 μg/ml.

3. The nanocluster of claim 1, wherein the drug substance has a solubility in water of less than 100 μg/ml.

4. The nanocluster of claim 1, wherein the drug substance comprises a chemo therapeutic.

5. The nanocluster of claim 4, wherein the chemo therapeutic comprises paclitaxel.

6. The nanocluster of claim 1, wherein the drug substance comprises a steroid.

7. The nanocluster of claim 6, wherein the steroid comprises budesonide.

8. The nanocluster of claim 1, wherein the drug substance comprises a hormone.

9. The nanocluster of claim 8, wherein the hormone comprises insulin.

10. The nanocluster of claim 1, wherein the drug substance comprises of a drug substance selected from the group consisting of a tocolytic agent, a vasodilator agent, a calcium channel blocker, and a dihydropyridine.

11. The nanocluster of claim 1, wherein the drug substance is nifedipine.

12. The nanocluster of claim 1, wherein the drug substance comprises of a drug substance selected from the group consisting of analgesics, anti-inflammatory agents, anthelmintics, anti-arrhythmic agents, antibiotics, anticoagulants, antidepressants, antidiabetic agents, antiepileptics, antihistamines, antihypertensive agents, antimuscarinic agents, antimycobacterial agents, antineoplastic agents, immunosuppressants, antithyroid agents, antiviral agents, anxiolytic sedatives, astringents, beta-adrenoceptor blocking agents, contrast media, corticosteroids, cough suppressants, diagnostic agents, diagnostic imaging agents, diuretics, dopaminergics, haemostatics, immuriological agents, lipid regulating agents, muscle relaxants, parasympathomimetics, parathyroid calcitonin, prostaglandins, radio-pharmaceuticals, sex hormones, anti-allergic agents, stimulants, sympathomimetics, thyroid agents, vasodilators and

xanthines.

13. The nanocluster of claim 1, wherein the nanocluster has a size within a range from about 1 to about 200 microns.

14. The nanocluster of claim 1, wherein the nanoparticles are not covalently bonded together.

15. The nanocluster of claim 1, wherein the nanoparticles are not encapsulated.

16. The nanocluster of claim 1, wherein the nanoparticles include a surface modifier comprising a surface modifier selected from the group consisting of gelatin, casein, lecithin, gum acacia, cholesterol, tragacanth, stearic acid, benzalkonium chloride, calcium stearate, glyceryl monostearate, cetostearyl alcohol, cetomacrogol emulsifying wax, sorbitan esters, polyoxyethylene alkyl ethers, polyoxyethylene caster oil derivatives, polyoxyethylene sorbitan fatty acid esters, polyethylene glycols, polyoxyethylene stearates, colloidol silicon dioxide, phosphates, sodium dodecylsulfate, carboxymethylcellulose calcium, carboxymethylcellulose sodium, methylcellulose, hydroxyethylcellulose, hydroxypropylcellulose, hydroxypropylmethycellulose phthalate, noncrystalline cellulose, magnesium aluminum silicate, triethanolamine, polyvinyl alcohol, polyvinylpyrrolidone, a tetrafunctional block copolymer derived from sequential addition of ethylene oxide and propylene oxide to ethylenediamine, gum acacia, a block copolymer of ethylene oxide and propylene oxide, a polyoxyethylene sorbitan fatty acid ester, a sorbitan ester of a fatty acid, a surfactant, a nonionic surfactant, an anionic surfactant, poloxomers, tyloxapol, poloxamines, dextran, a dioctyl ester of sodium sulfosuccinic acid, sodium lauryl sulfate, an alkyl aryl polyether sulfonate, a mixture of sucrose stearate and sucrose distearate, hexyldecyl trimethyl ammonium chloride, bovine serum albumin and C18 H37CH2(CON(CH3)CH2 (CHOH)4 CH2OH)2.

17. The nanocluster of claim 1, wherein the nanoparticles have an effective average particle size of less than about 1000 nm.

18. The nanocluster of claim 1, wherein the nanoparticles have an effective average particle size of less than about 500 nm.

19. The nanocluster of claim 1, wherein the nanoparticles have an effective average particle size of less than about 400 nm.

20. The nanocluster of claim 1, wherein the nanoparticles have an effective average particle size of less than about 300 nm.

21. The nanocluster of claim 1, wherein the nanoparticles have an effective average particle size of less than about 250 nm.

22. The nanocluster of claim 1, wherein the nanoparticles have an effective average particle size of less than about 100 nm.

23. The nanocluster of claim 1, wherein the nanoparticles have an effective average particle size within a range of about 50 nm to about 100 nm.

24. The nanocluster of claim 1, wherein the nanoparticles have an effective average particle size within a range of about 50 nm to about 300 nm.

25. The nanocluster of claim 1, wherein the nanocluster comprises at least 50% nanoparticles by weight.

26. The nanocluster of claim 1, wherein the nanocluster comprises at least 25% nanoparticles by weight.

27. A composition that comprises a nanocluster comprising a plurality of nanoparticles, wherein the nanoparticles comprise a drug substance, and wherein the nanocluster is cluster of nanoparticles arranged such that the surface of the nanoparticles are in contact with one another, and wherein the nanocluster is not hollow.

28. The composition of claim 27, wherein the composition is formulated into a dry powder, an aerosol, a spray, a tablet, or a liquid.

29. The composition of claim 27, wherein the composition is formulated into a pharmaceutically acceptable carrier.

30. A method of preparing a nanocluster in a solution comprising:

(i) obtaining at least a first nanoparticle and a second nanoparticle, and

(ii) admixing the first nanoparticle and the second nanoparticle,

wherein at least one of the first nanoparticle and the second nanoparticle include a drug substance, and wherein the first nanoparticle and the second nanoparticles assemble in a solution to form a nanocluster that is not hollow.

31. The method of claim 30, wherein the drug substance has a solubility in water of less than 500 μg/ml.

32. The method of claim 30, wherein the drug substance has a solubility in water of less than 100 μg/ml.

33. The method of claim 30, wherein the drug substance comprises a chemo therapeutic.

34. The method of claim 33, wherein the chemo therapeutic comprises paclitaxel.

35. The method of claim 30, wherein the drug substance comprises a steroid.

36. The method of claim 34, wherein the steroid comprises budesonide.

37. The method of claim 30, wherein the drug substance comprises a hormone.

38. The method of claim 36, wherein the hormone comprises insulin.

39. The method of claim 30, wherein the drug substance comprises a drug substance selected from the group consisting of a tocolytic agent, a vasodilator agent, a calcium channel blocker, and a dihydropyridine.

40. The method of claim 38, wherein the drug substance comprises nifedipine.

41. The method of claim 30, further comprising the step of including adding a flocculating agent during or subsequent to the admixing the first nanoparticle and the second nanoparticle so as to destabilize a colloidal suspension of the first nanoparticle and the second nanoparticles assemble in a solution.

42. The method of claim 40, wherein the flocculating agent comprises a salt or an amino acid.

43. The method of claim 41 wherein the salt comprises NaCl.

44. The method of claim 41, wherein the amino acid comprises leucine.

45. The method of claim 30, wherein spray and freeze drying techniques are not used to prepare the nanocluster.

46. A method of preventing or treating a disease in a subject comprising: administering a therapeutically effective amount of a composition comprising a nanocluster that comprises a plurality of nanoparticles, wherein the nanoparticles comprise a drug substance, and wherein the nanocluster is cluster of nanoparticles arranged such that the surface of the nanoparticles are in contact with one another, and wherein the nanocluster is not hollow.

47. The method of claim 45, wherein the disease is a pulmonary disease or condition.

48. The method of claim 45, wherein the composition is administered nasally.

49. The method of claim 45, wherein the composition is administered into the lungs.

FIG.1

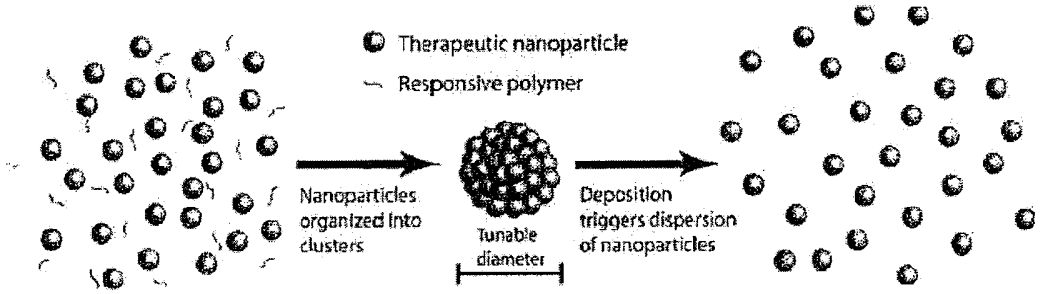
Therapeutic nanoparticle
Responsive polymer
Nanoparticles organized into clusters
Tunable diameter
Deposition triggers dispersion of nanoparticles

FIG. 2

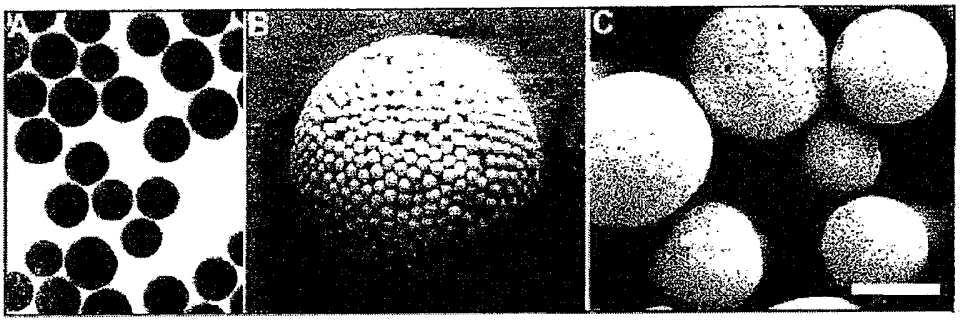
A
B
C

FIG. 3

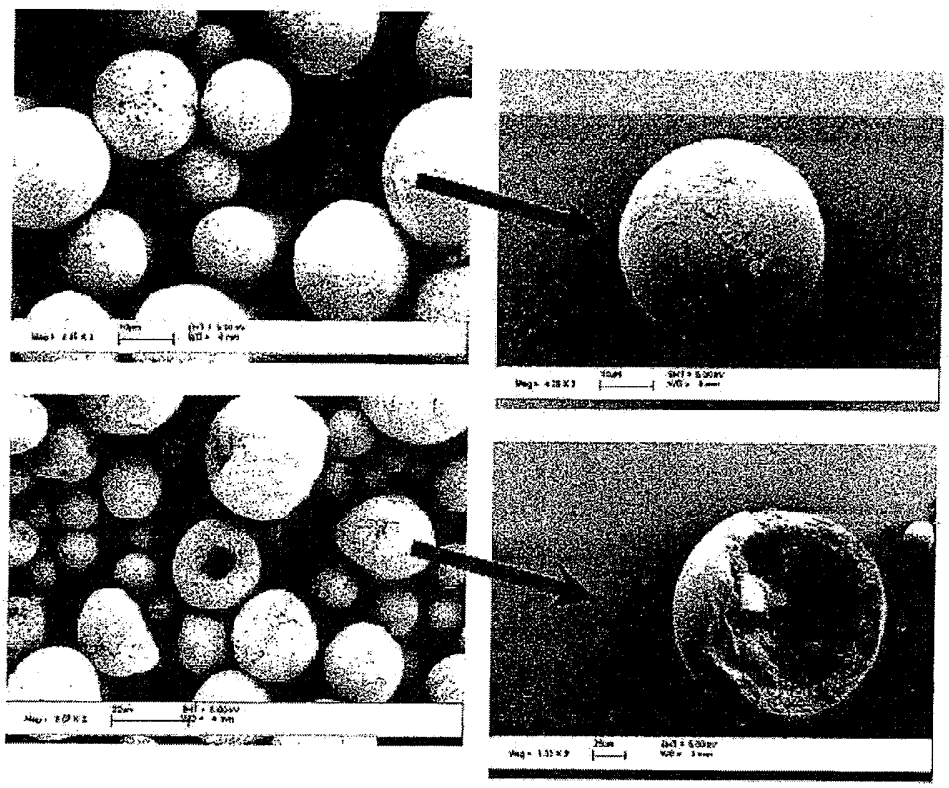

FIG. 4

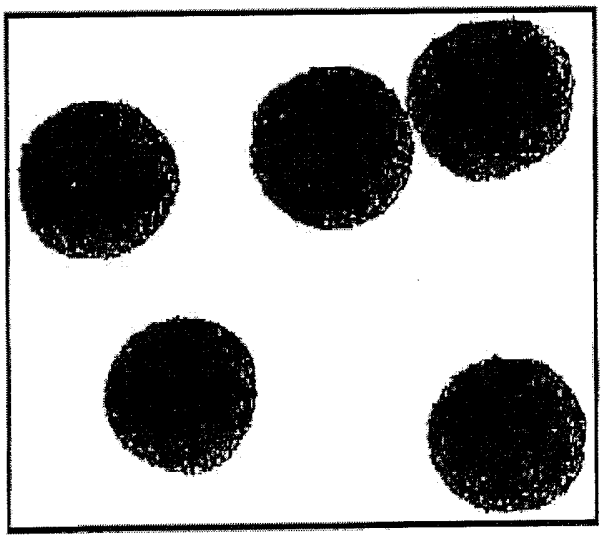

FIG. 5

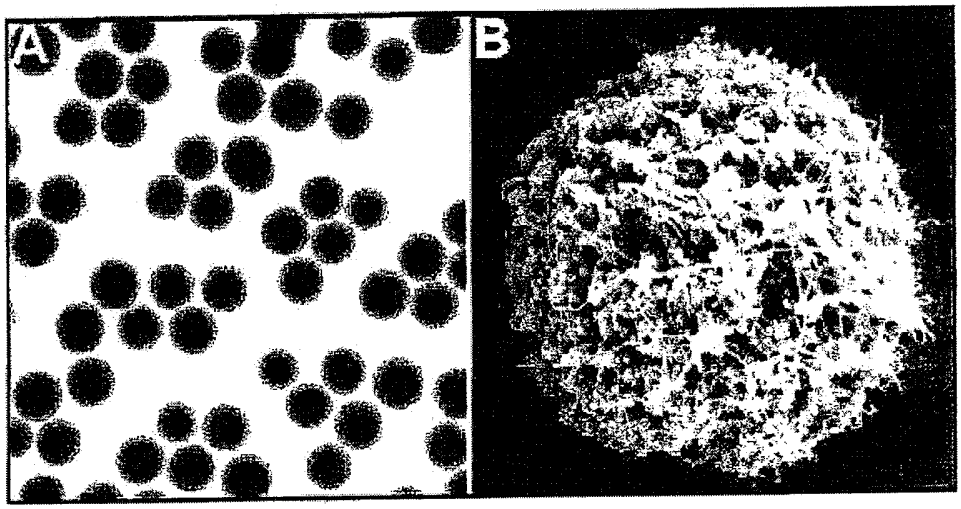

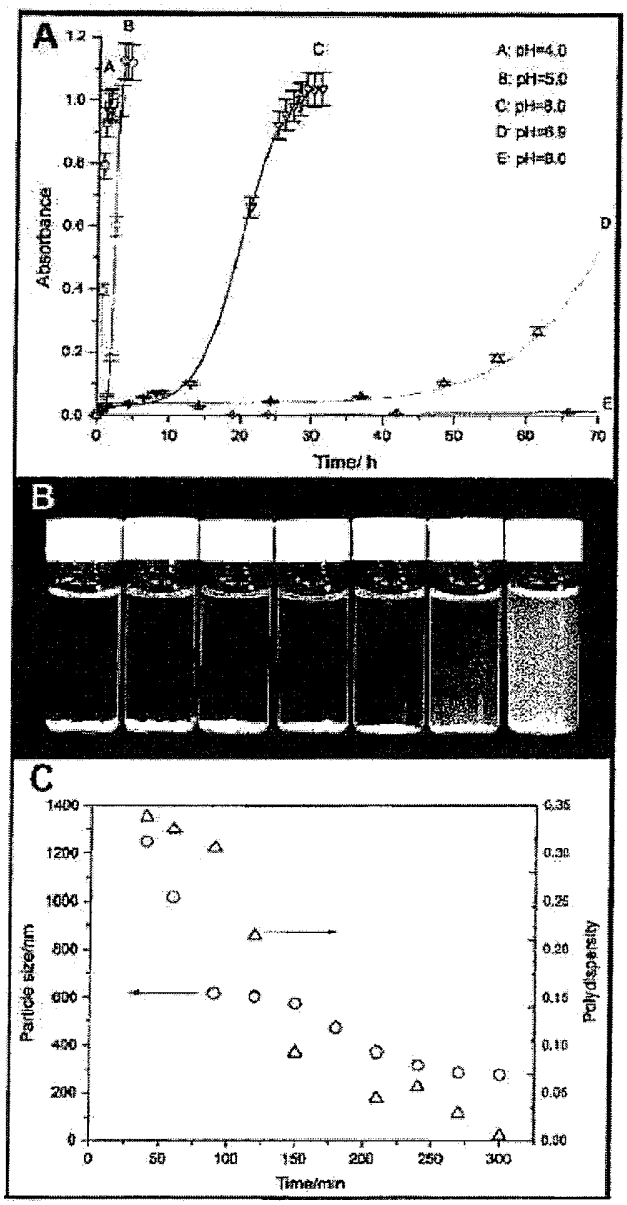
A
B
C
D
E
A: pH=4.0
B: pH=5.0
C: pH=8.0
D: pH=6.9
E: pH=8.0
Absorbance
Time/ h
B
C
Particle size/nm
Polydispersity
Time/min

FIG. 6

FIG. 7A, FIG. 7B, FIG. 7C

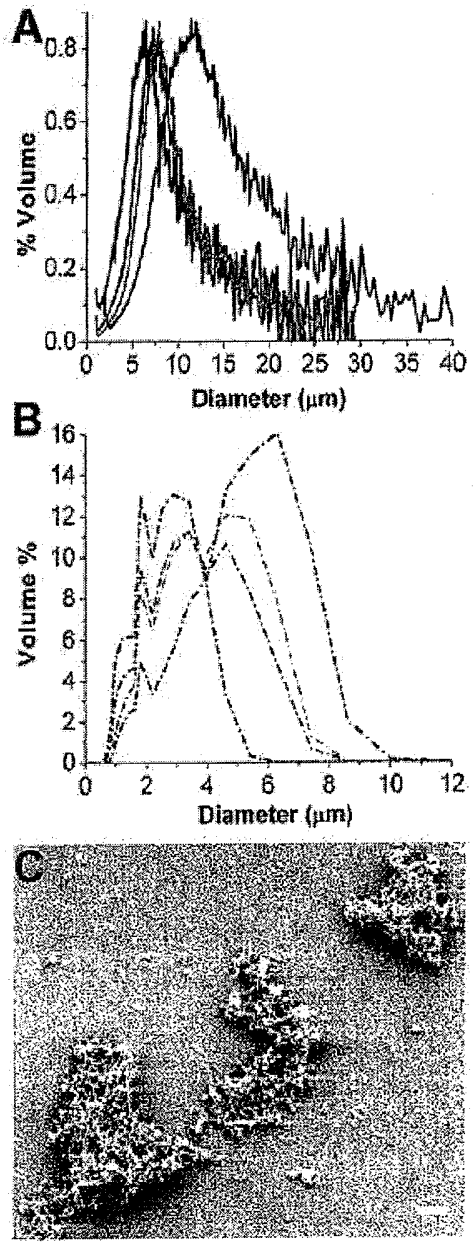

FIG. 8A, FIG. 8B, FIG. 8C, FIG. 8D, FIG. 8E, FIG. 8F

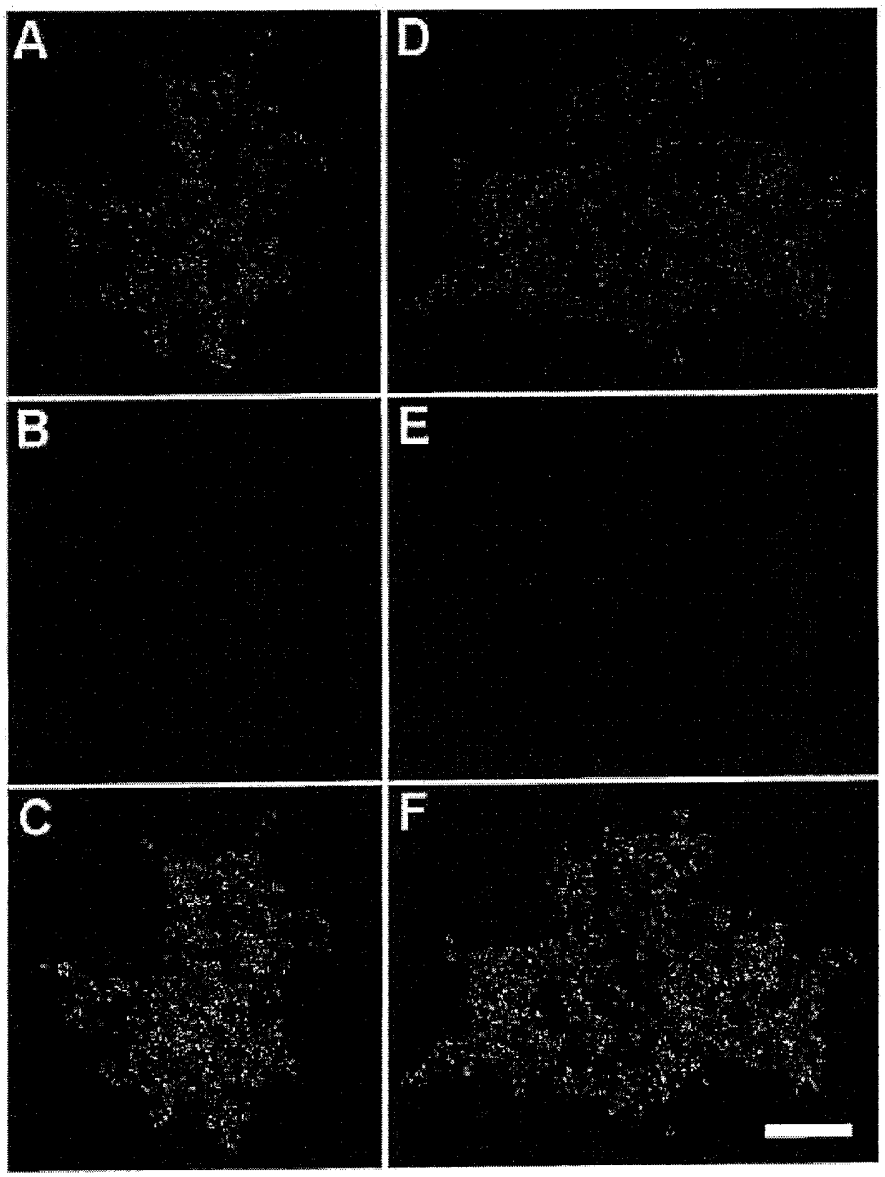

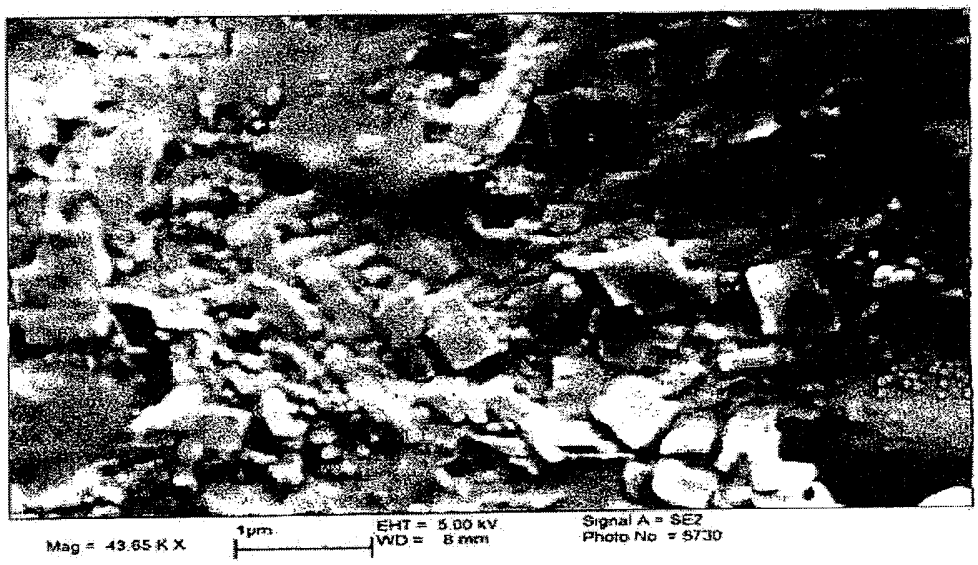

FIG. 9

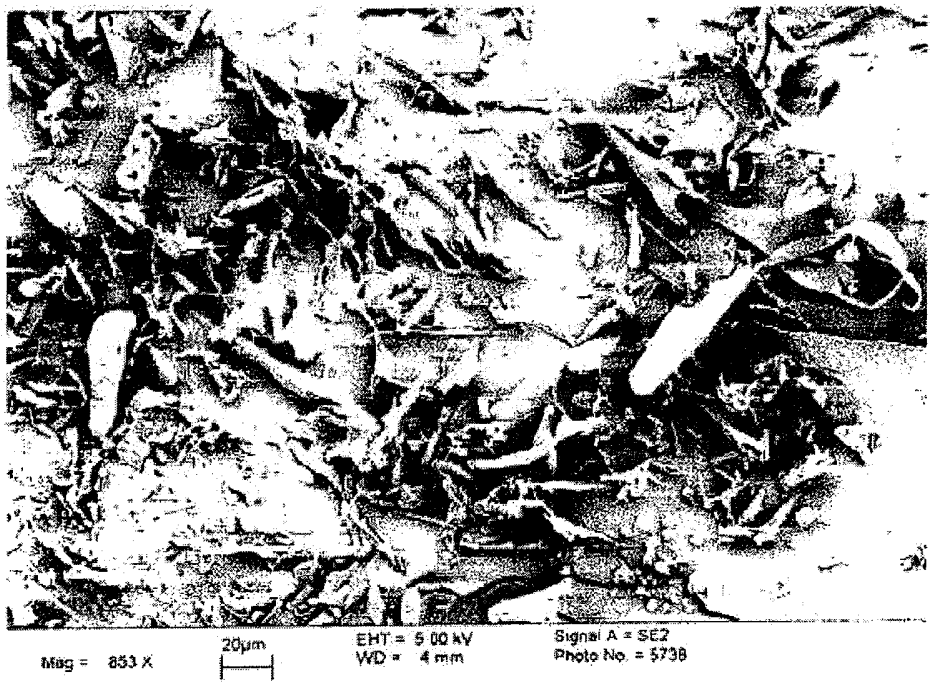

FIG. 10

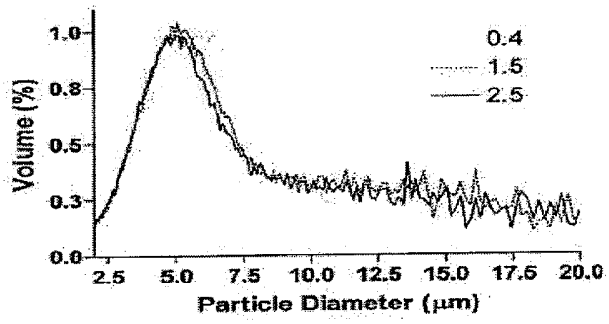
Volume (%)
1.0
0.8
0.5
0.3
0.0
2.5
5.0
7.5
10.0
12.5
15.0
17.5
20.0
Particle Diameter (μm)
0.4
1.5
2.5

FIG. 11

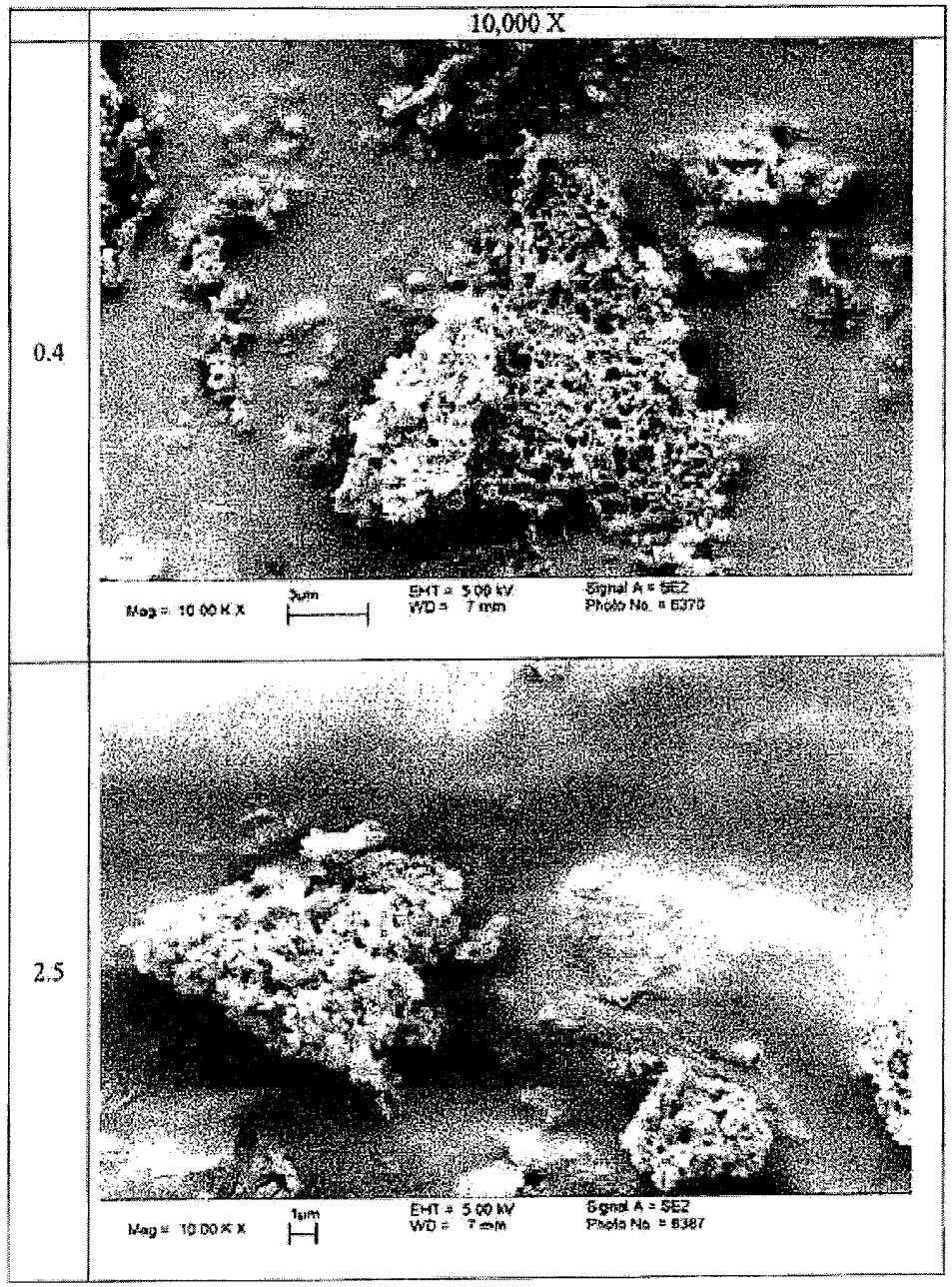
10,000 X
0.4
Mag = 10.00 K X
1µm
EHT = 5.00 kV
WD = 7 mm
Signal A = SE2
Photo No. = 6378
2.5
Mag = 10.00 K X
1µm
EHT = 5.00 kV
WD = 7 mm
Signal A = SE2
Photo No. = 6387

FIG. 12

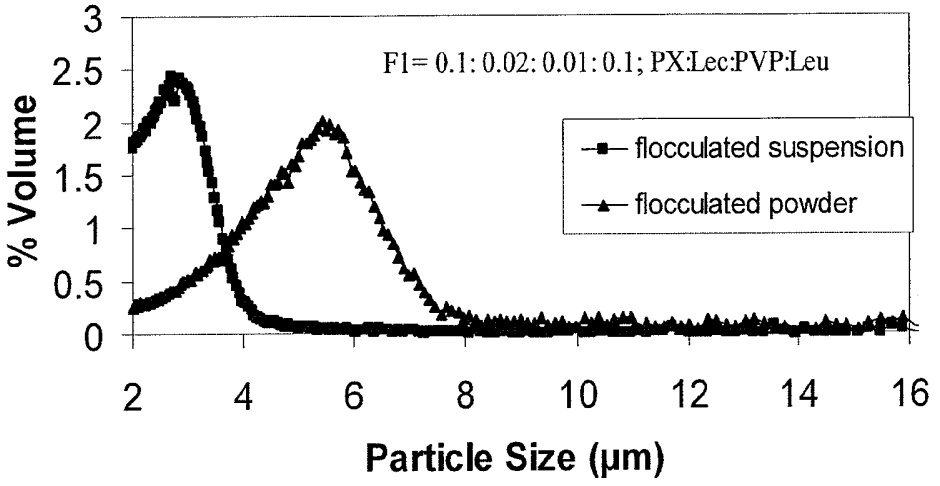
F1= 0.1: 0.02: 0.01: 0.1; PX:Lec:PVP:Leu
flocculated suspension
flocculated powder
% Volume
Particle Size (µm)
0
0.5
1
1.5
2
2.5
3
2
4
6
8
10
12
14
16

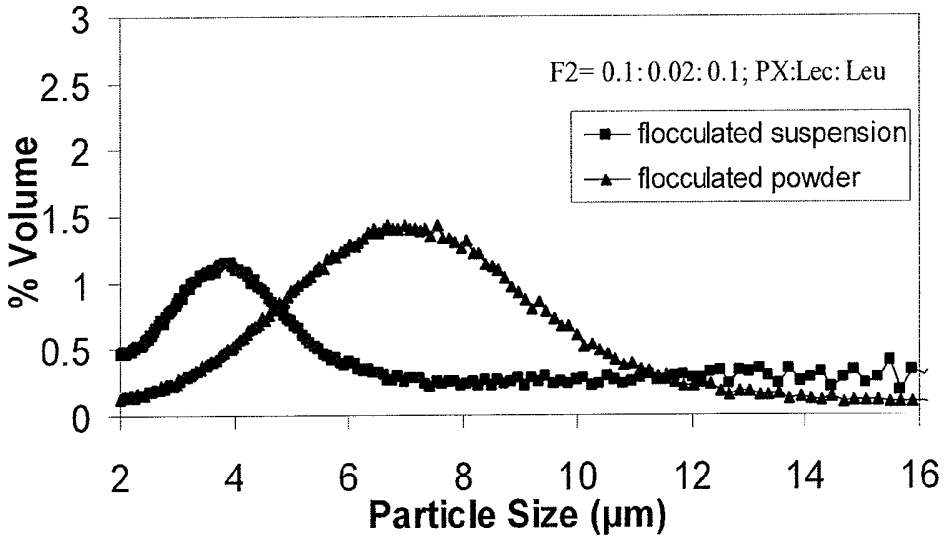
F2= 0.1: 0.02: 0.1; PX:Lec: Leu
flocculated suspension
flocculated powder
% Volume
Particle Size (µm)
0
0.5
1
1.5
2
2.5
3
2
4
6
8
10
12
14
16

FIG. 13

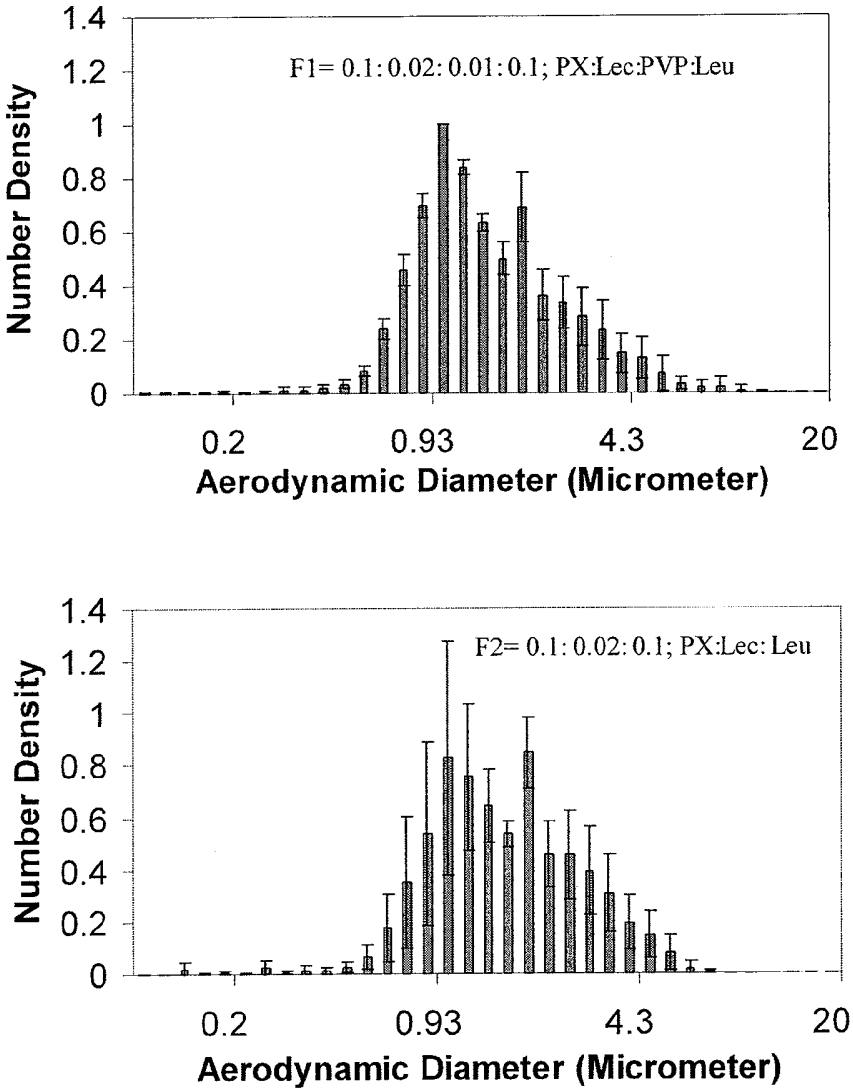
F1= 0.1: 0.02: 0.01: 0.1; PX:Lec:PVP:Leu
Number Density
1.4
1.2
1
0.8
0.6
0.4
0.2
0
0.2
0.93
4.3
20
Aerodynamic Diameter (Micrometer)

F2= 0.1: 0.02: 0.1; PX:Lec: Leu
Number Density
1.4
1.2
1
0.8
0.6
0.4
0.2
0
0.2
0.93
4.3
20
Aerodynamic Diameter (Micrometer)

FIG. 14

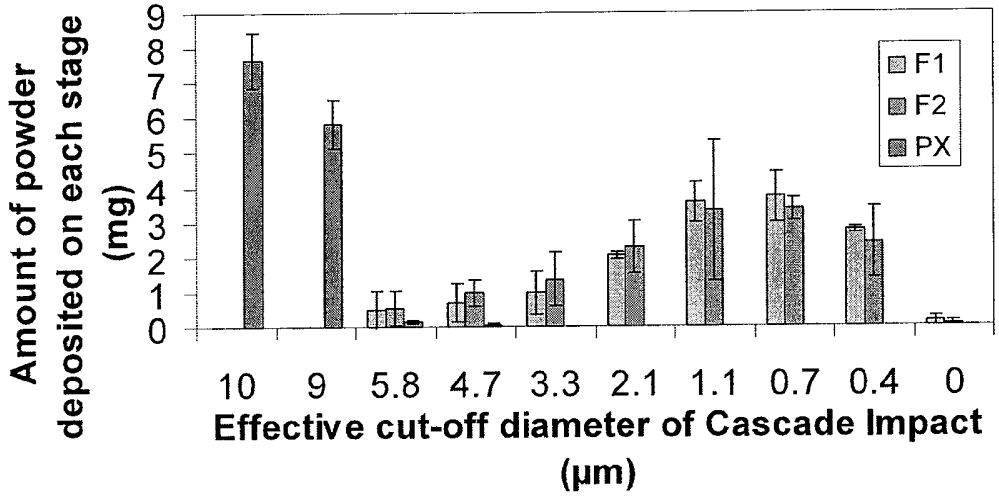

F1 = 0.1: 0.02:0.01: 0.1;PX: Lec: PVP: Leu
F2 = 0.1: 0.02: 0.1; PX: Lec:Leu
PX: Paclitaxel powder as received

FIG. 15

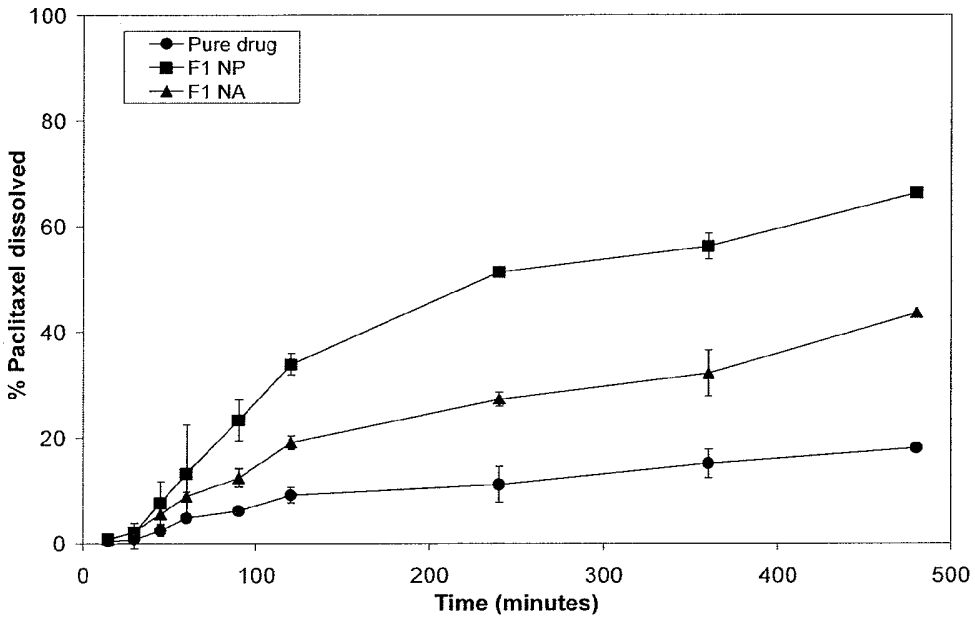
Pure drug
F1 NP
F1 NA
% Paclitaxel dissolved
Time (minutes)
0
20
40
60
80
100
0
100
200
300
400
500

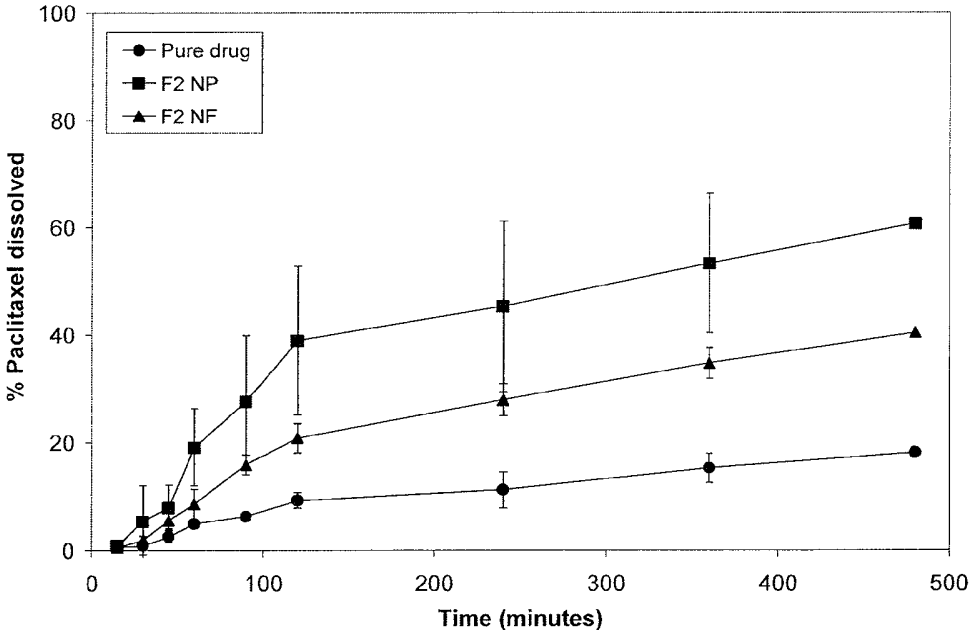
Pure drug
F2 NP
F2 NF
% Paclitaxel dissolved
Time (minutes)
0
20
40
60
80
100
0
100
200
300
400
500

FIG. 16

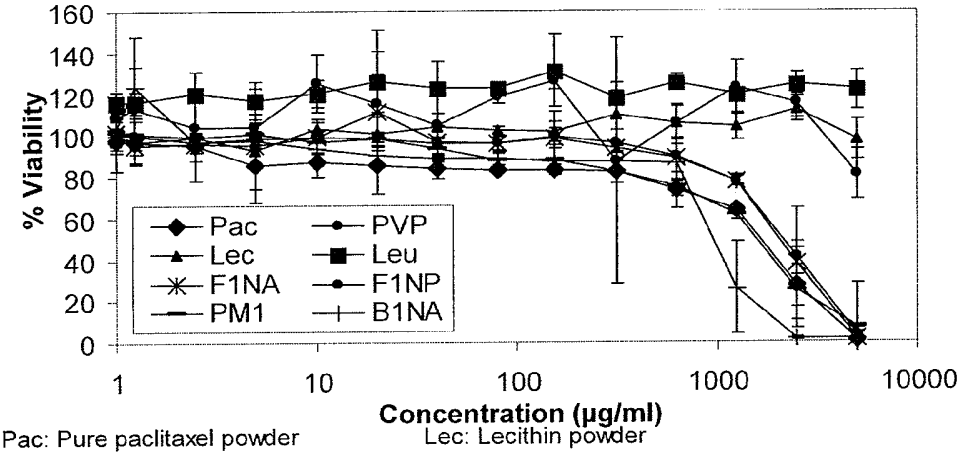

Pac: Pure paclitaxel powder Lec: Lecithin powder
Leu: Leucine powder PVP: PVP K90 powder
PM: Physical mixture of F1 components
(0.1: 0.02: 0.01: 0.1; Pac: Lec: PVP K90: Leu)
B1NA: F1 Blank nanoparticle agglomerates F1NP: F1 nanoparticles
F1NA: F1 nanoparticle agglomerates

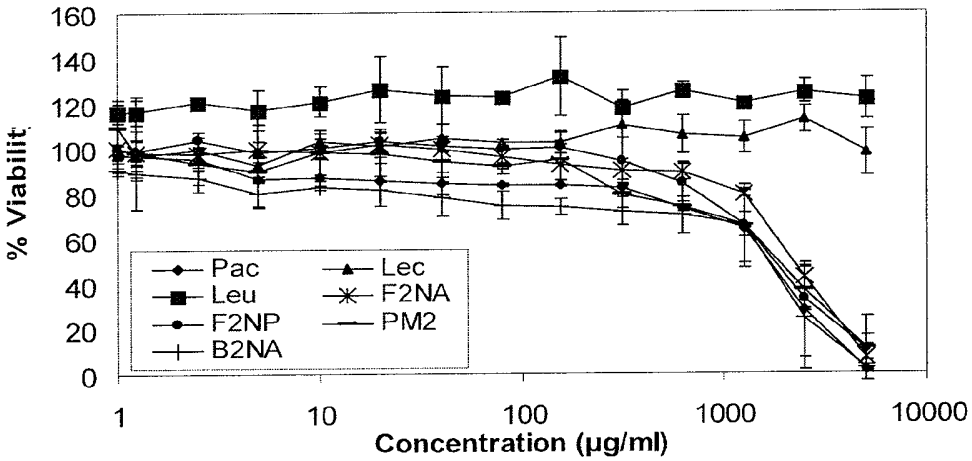

Pac: Pure paclitaxel powder Lec: Lecithin powder Leu: Leucine powder
PM: Physical mixture of F2 components (0.1: 0.02: 0.1; Pac: Lec: Leu)
B2NA: F2 Blank nanoparticle agglomerates F2NP: F2 nanoparticles
F2NA: F1 nanoparticle agglomerates

FIG 17

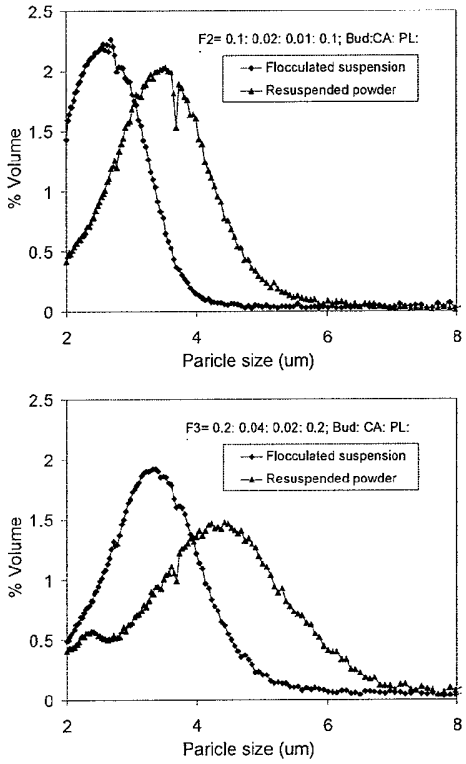
F2= 0.1: 0.02: 0.01: 0.1; Bud:CA: PL:
Flocculated suspension
Resuspended powder
% Volume
Paricle size (um)
F3= 0.2: 0.04: 0.02: 0.2; Bud: CA: PL:
Flocculated suspension
Resuspended powder
% Volume
Paricle size (um)

FIG. 18

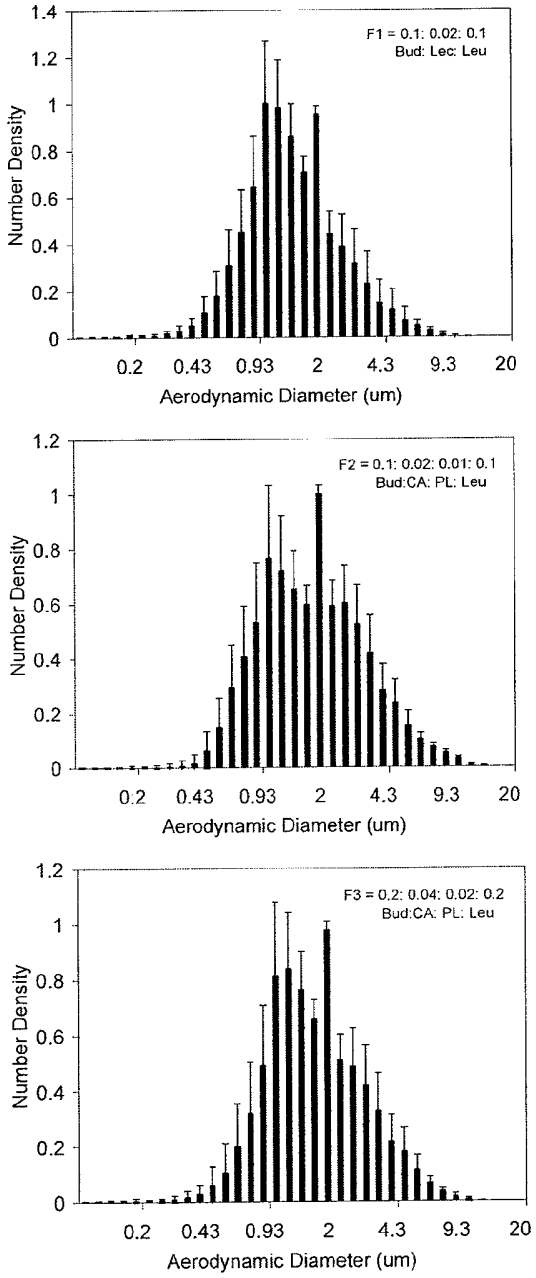
F1 = 0.1: 0.02: 0.1
Bud: Lec: Leu
Number Density
Aerodynamic Diameter (um)
F2 = 0.1: 0.02: 0.01: 0.1
Bud:CA: PL: Leu
Number Density
Aerodynamic Diameter (um)
F3 = 0.2: 0.04: 0.02: 0.2
Bud:CA: PL: Leu
Number Density
Aerodynamic Diameter (um)

FIG. 19

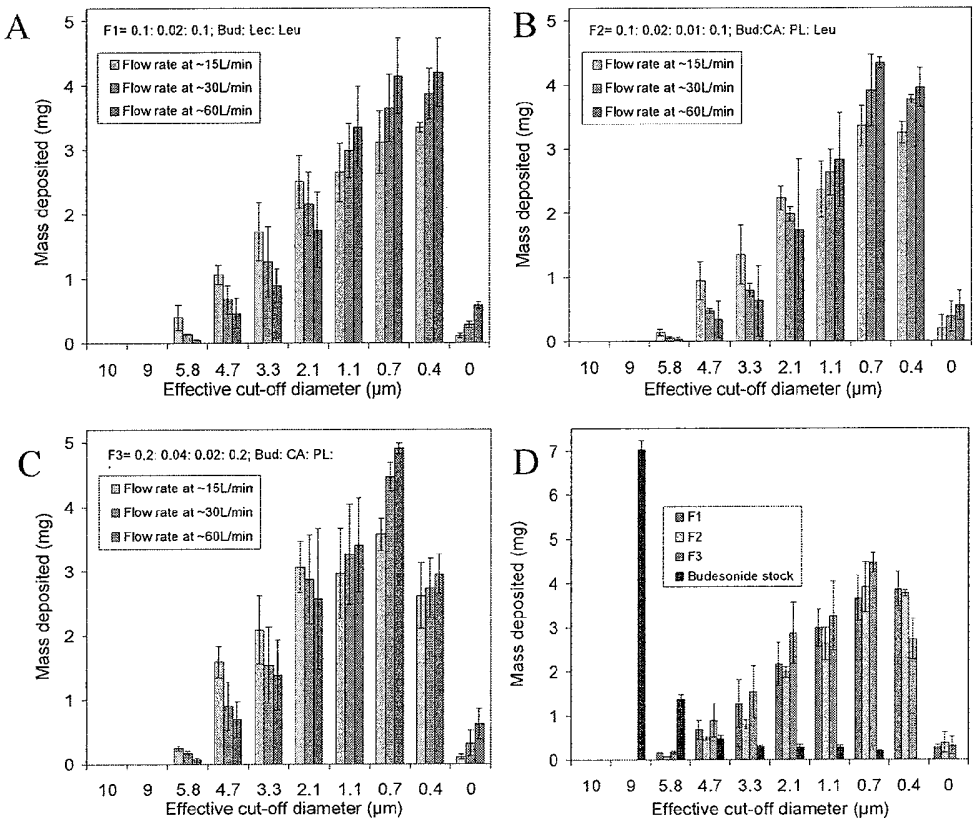
A
F1= 0.1: 0.02: 0.1; Bud: Lec: Leu
Flow rate at ~15L/min
Flow rate at ~30L/min
Flow rate at ~60L/min
Mass deposited (mg)
Effective cut-off diameter (µm)
B
F2= 0.1: 0.02: 0.01: 0.1; Bud:CA: PL: Leu
C
F3= 0.2: 0.04: 0.02: 0.2; Bud: CA: PL:
D
F1
F2
F3
Budesonide stock
10 9 5.8 4.7 3.3 2.1 1.1 0.7 0.4 0

FIG. 20

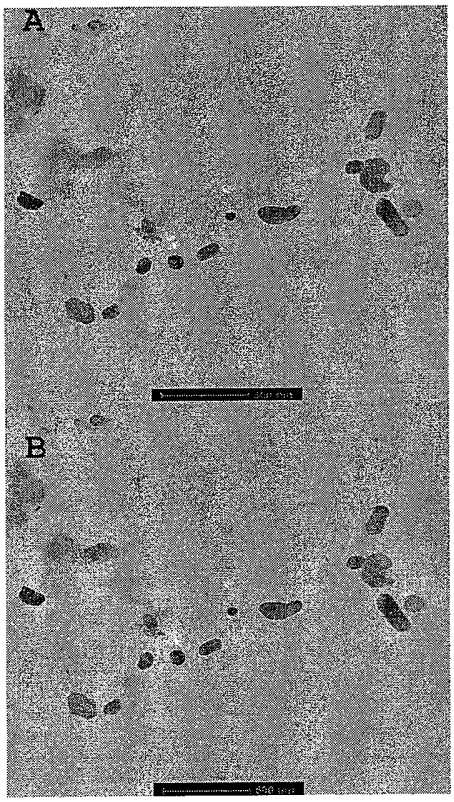

FIG. 21

FIG. 22

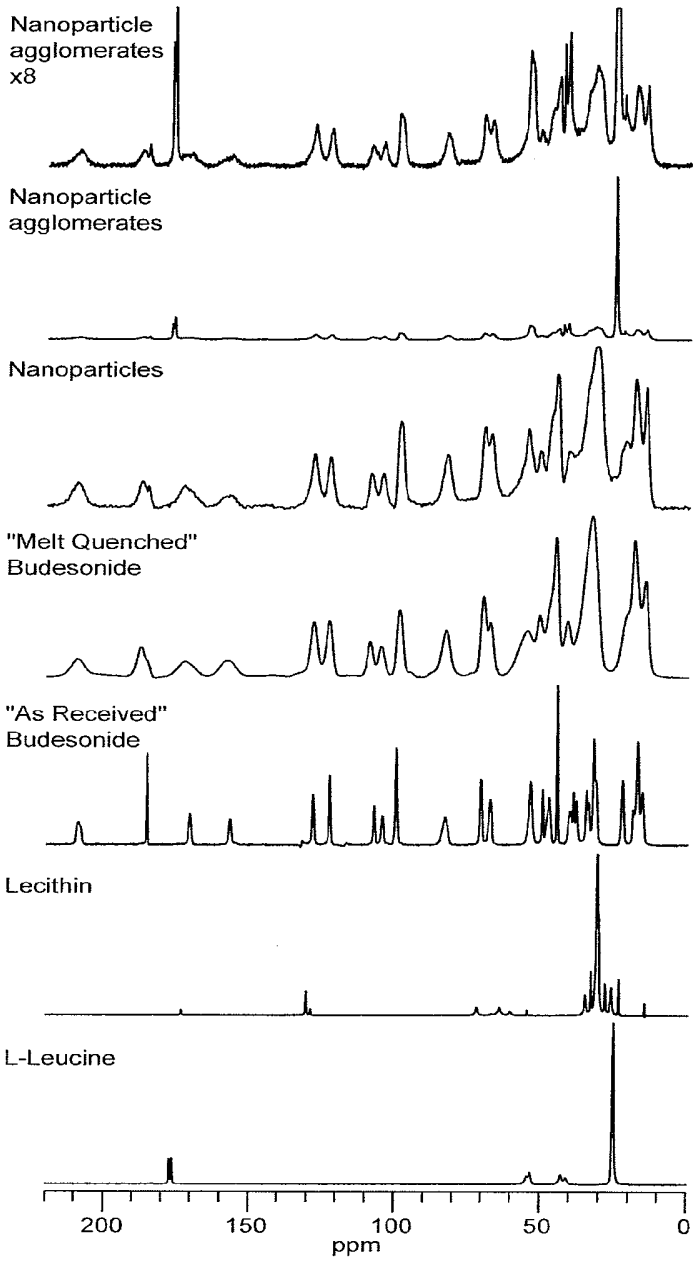
Nanoparticle agglomerates x8
Nanoparticle agglomerates
Nanoparticles
"Melt Quenched" Budesonide
"As Received" Budesonide
Lecithin
L-Leucine
200
150
100
50
0
ppm

FIG. 23

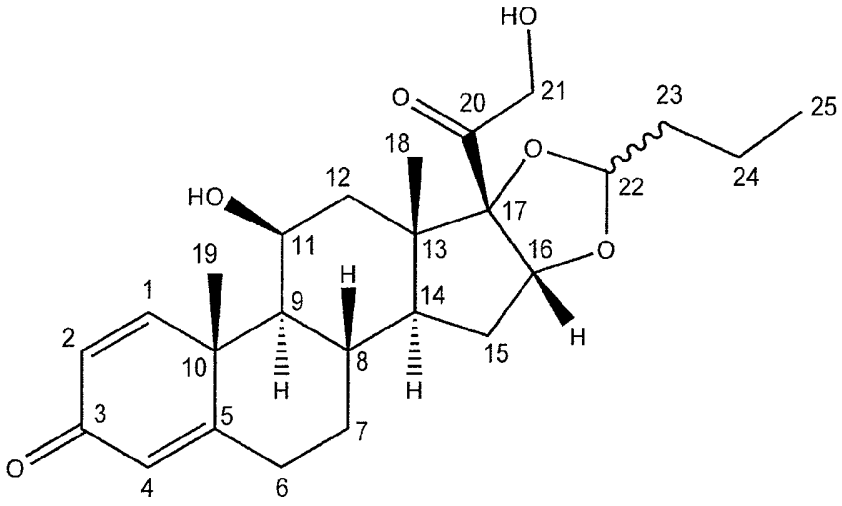
HO
O
20
21
23
25
18
O
12
22
24
HO
17
19
11
13
16
O
1
9
H
14
2
10
8
15
H
H
3
5
7
O
4
6

FIG. 24

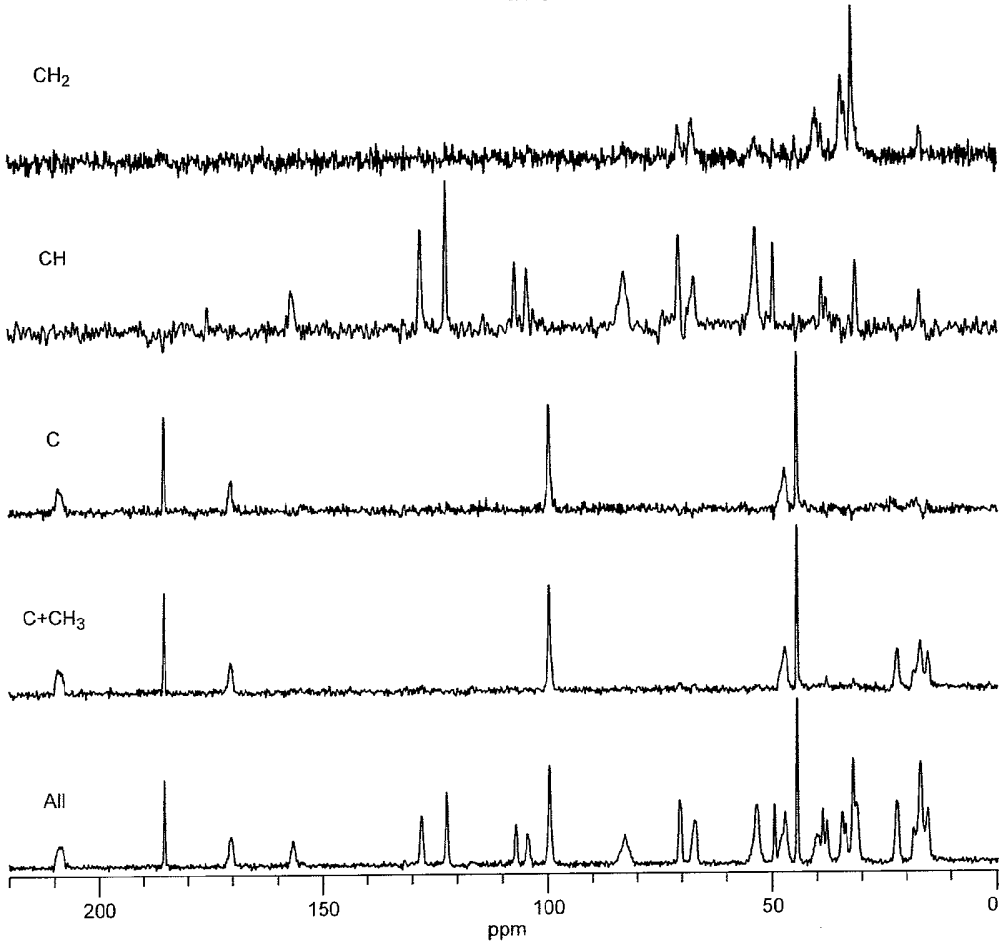

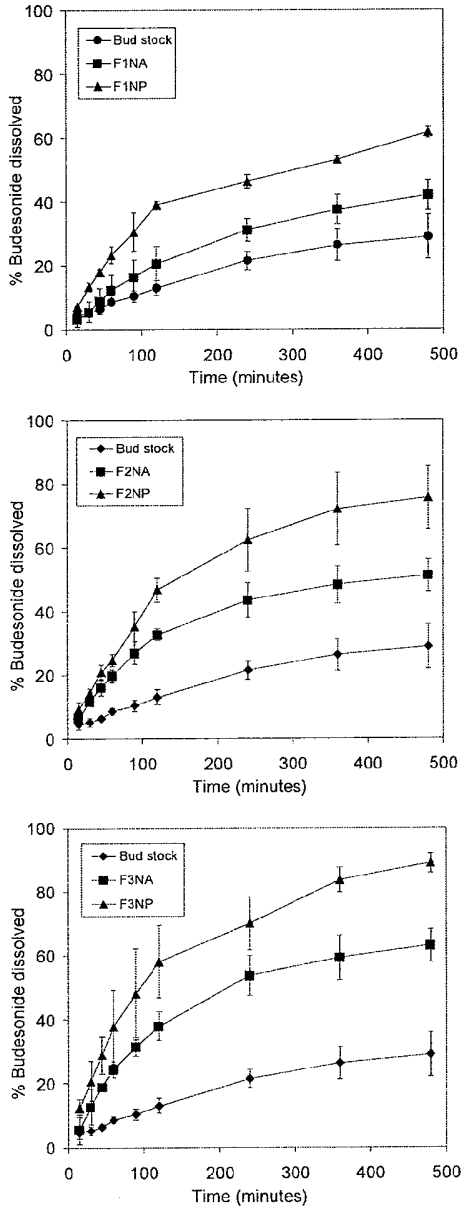
Bud stock
F1NA
F1NP
% Budesonide dissolved
Time (minutes)
Bud stock
F2NA
F2NP
% Budesonide dissolved
Time (minutes)
Bud stock
F3NA
F3NP
% Budesonide dissolved
Time (minutes)

FIG. 25.

FIG. 26

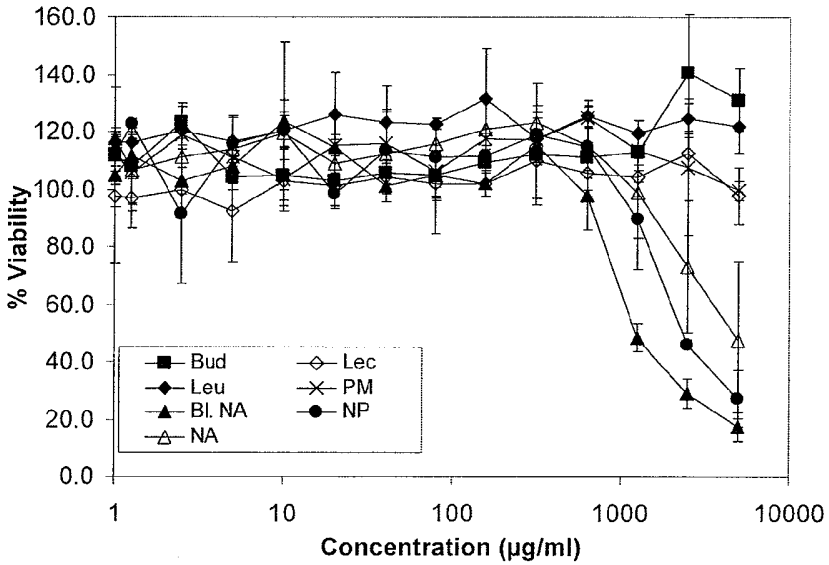

Bud: budesonide Lec: Lecithin stock Leu: Leucine stock
PM: Physical mixture of F1 components (0.1: 0.02: 0.1; Bud: Lec: Leu)
Bl. NA: F1 Blank nanoparticle agglomerates NP: F1 nanoparticles
NA: F1 nanoparticle agglomerates

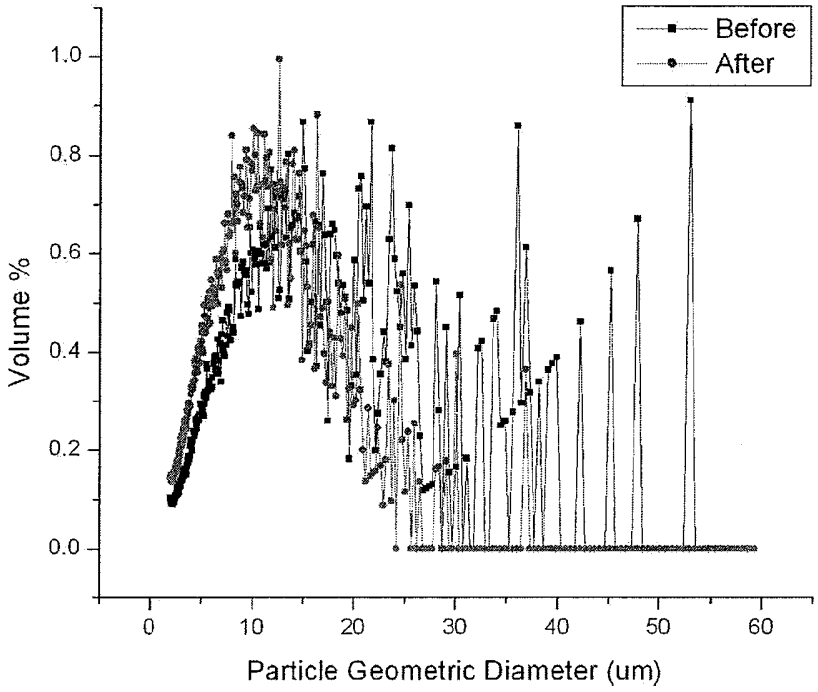
Before
After
Volume %
1.0
0.8
0.6
0.4
0.2
0.0
0
10
20
30
40
50
60
Particle Geometric Diameter (um)

FIG. 27

FIG. 28

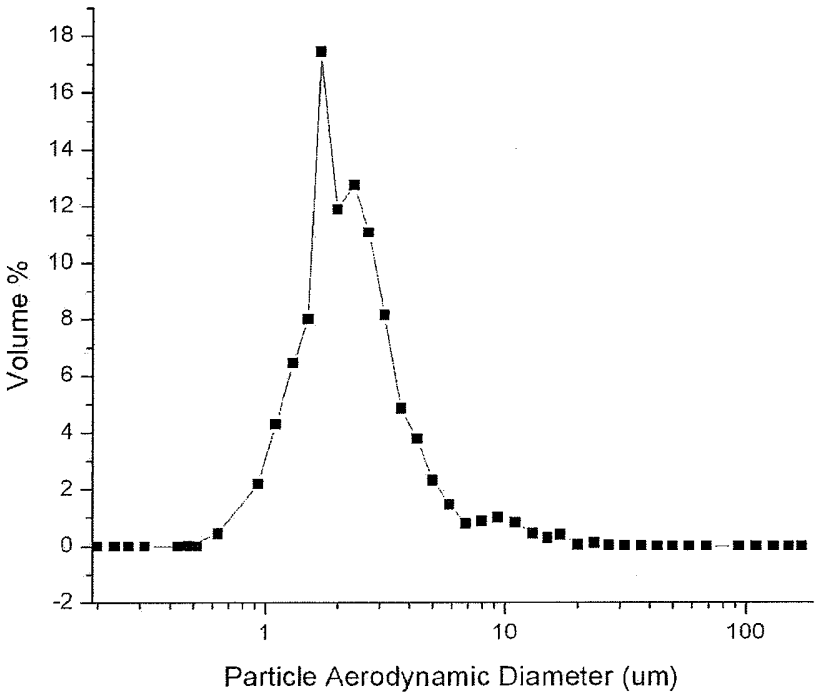
Volume %
18
16
14
12
10
8
6
4
2
0
-2
1
10
100
Particle Aerodynamic Diameter (um)

FIG. 29

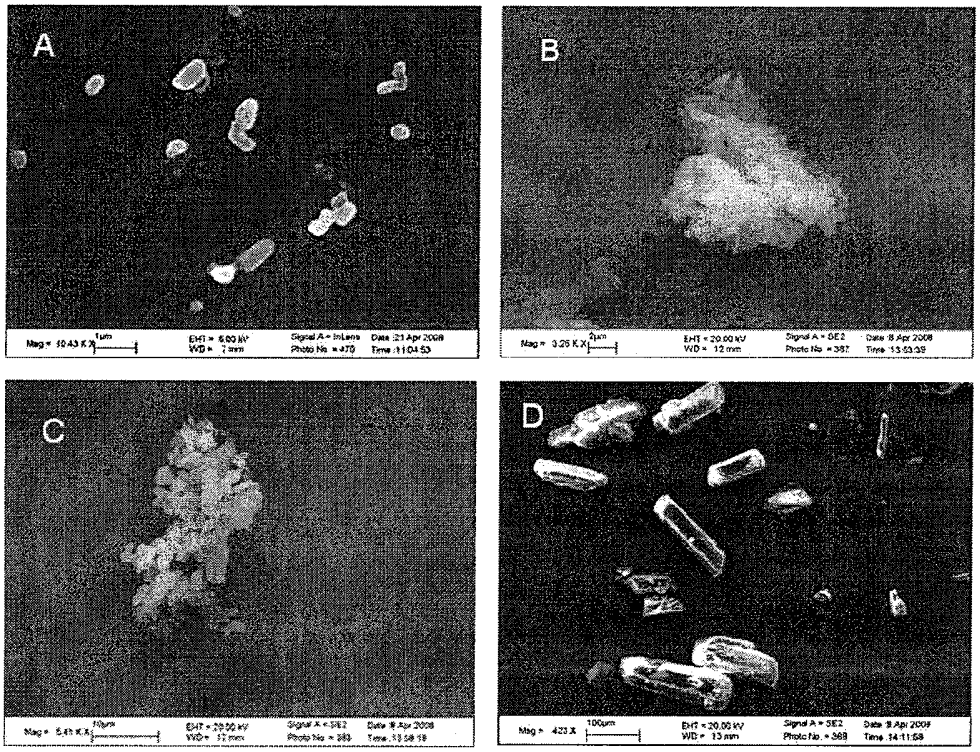

FIG. 30

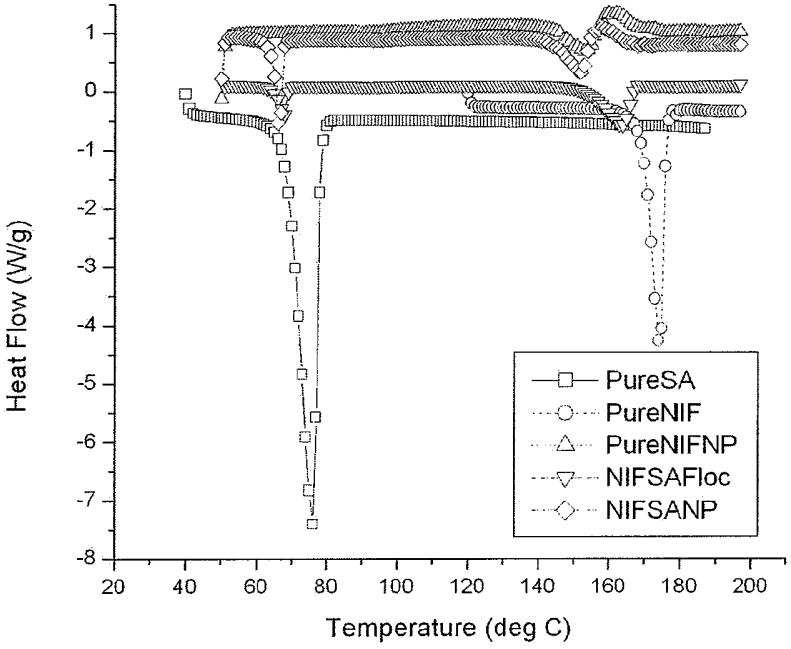
Heat Flow (W/g)
1
0
-1
-2
-3
-4
-5
-6
-7
-8
20
40
60
80
100
120
140
160
180
200
Temperature (deg C)
PureSA
PureNIF
PureNIFNP
NIFSAFloc
NIFSANP

FIG. 31

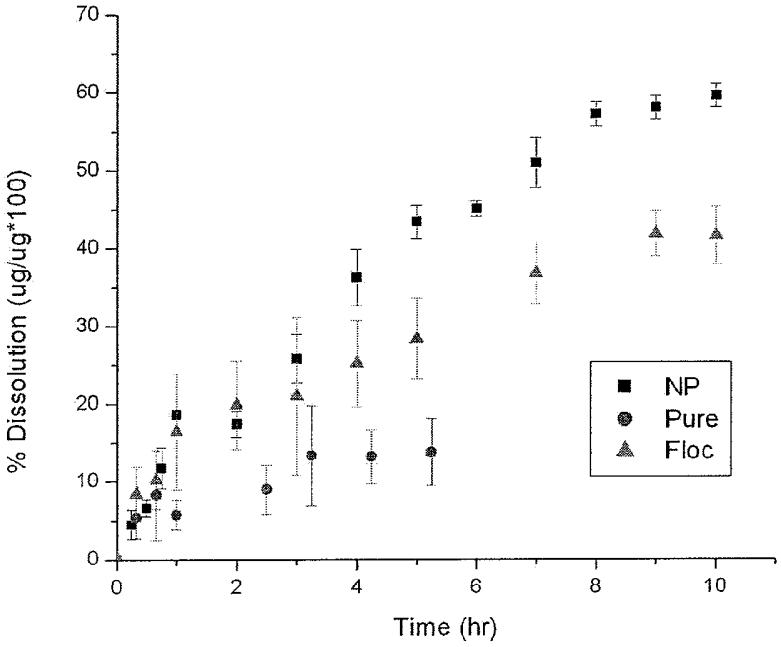
% Dissolution (ug/ug*100)
Time (hr)
NP
Pure
Floc
0
10
20
30
40
50
60
70
0
2
4
6
8
10

FIG. 32

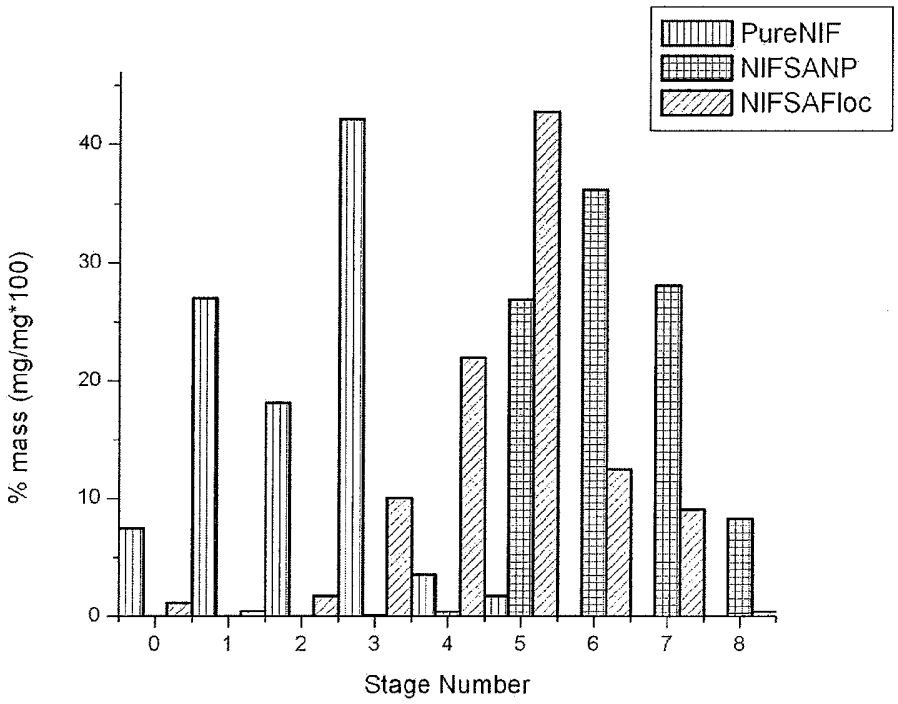
PureNIF
NIFSANP
NIFSAFloc
% mass (mg/mg*100)
0
10
20
30
40
0
1
2
3
4
5
6
7
8
Stage Number

FIG. 33

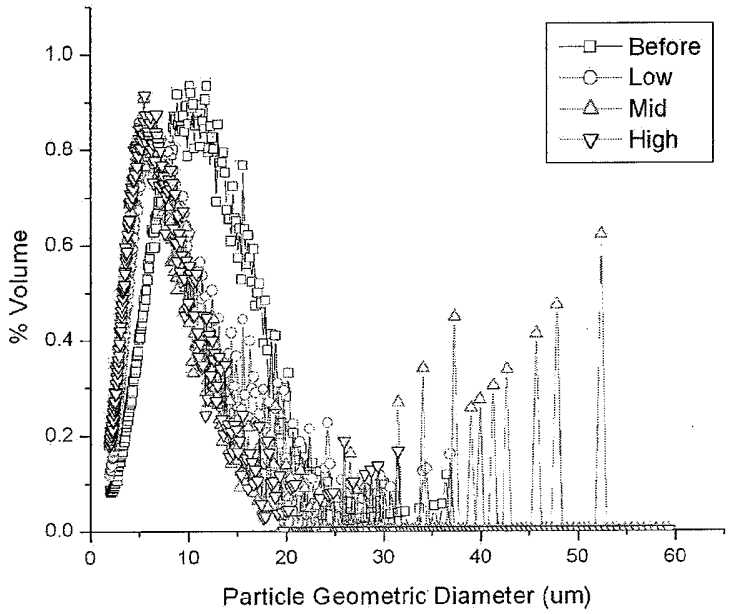
Before
Low
Mid
High
% Volume
1.0
0.8
0.6
0.4
0.2
0.0
0
10
20
30
40
50
60
Particle Geometric Diameter (um)

FIG. 34

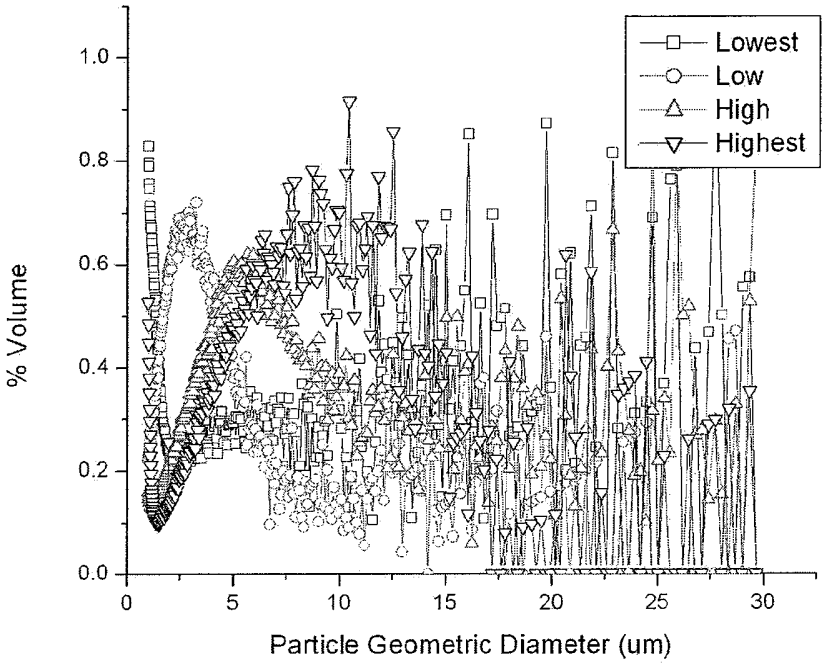
Lowest
Low
High
Highest
% Volume
1.0
0.8
0.6
0.4
0.2
0.0
0
5
10
15
20
25
30
Particle Geometric Diameter (um)

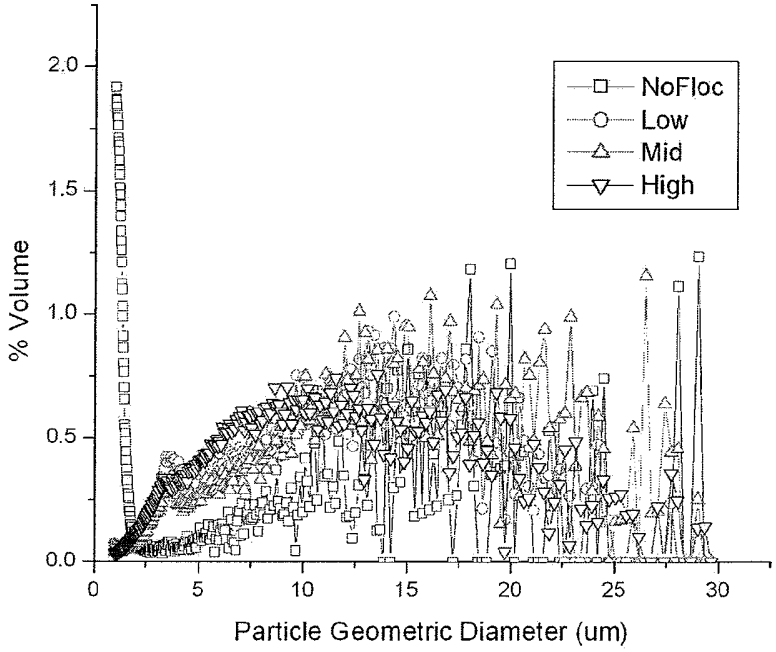
NoFloc
Low
Mid
High
% Volume
Particle Geometric Diameter (um)
0.0
0.5
1.0
1.5
2.0
0
5
10
15
20
25
30

FIG. 35

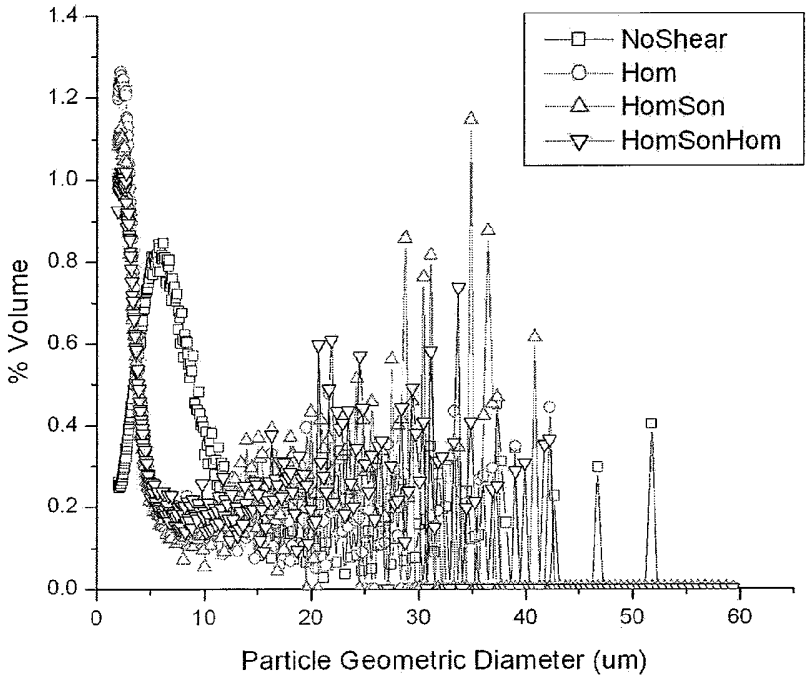
NoShear
Hom
HomSon
HomSonHom
% Volume
Particle Geometric Diameter (um)
0.0
0.2
0.4
0.6
0.8
1.0
1.2
1.4
0
10
20
30
40
50
60

FIG. 36

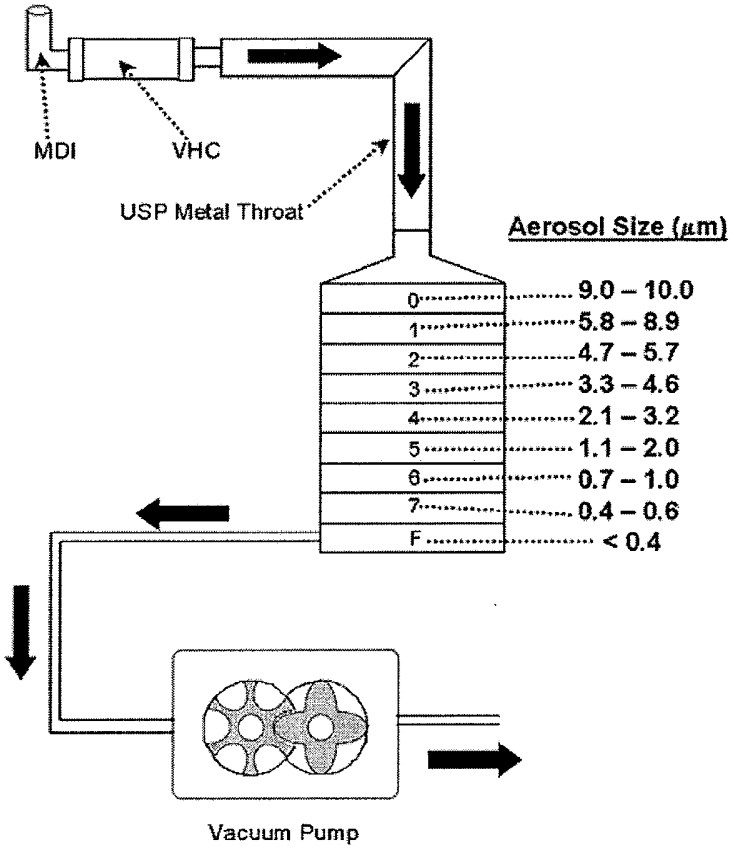
MDI
VHC
USP Metal Throat
Aerosol Size (μm)
0 9.0 – 10.0
1 5.8 – 8.9
2 4.7 – 5.7
3 3.3 – 4.6
4 2.1 – 3.2
5 1.1 – 2.0
6 0.7 – 1.0
7 0.4 – 0.6
F < 0.4
Vacuum Pump

FIG. 37

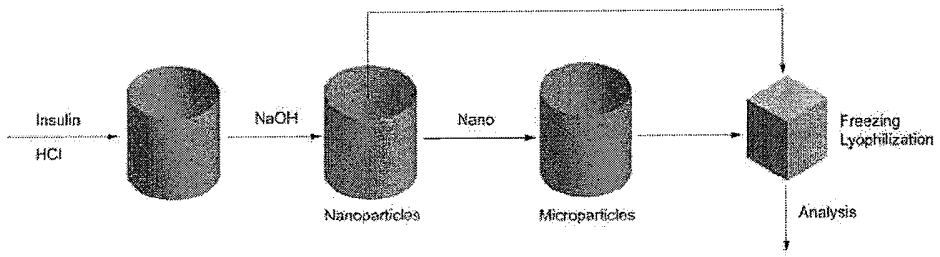
Insulin
HCl
NaOH
Nanoparticles
Nano
Microparticles
Freezing
Lyophilization
Analysis

FIG. 38

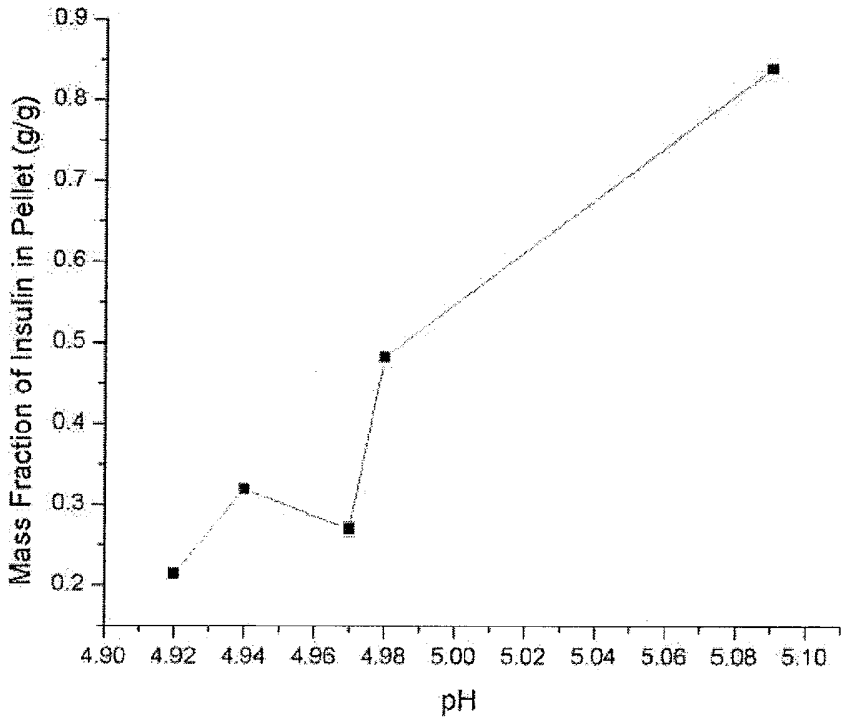
Mass Fraction of Insulin in Pellet (g/g)
0.9
0.8
0.7
0.6
0.5
0.4
0.3
0.2
4.90
4.92
4.94
4.96
4.98
5.00
5.02
5.04
5.06
5.08
5.10
pH

FIG. 39

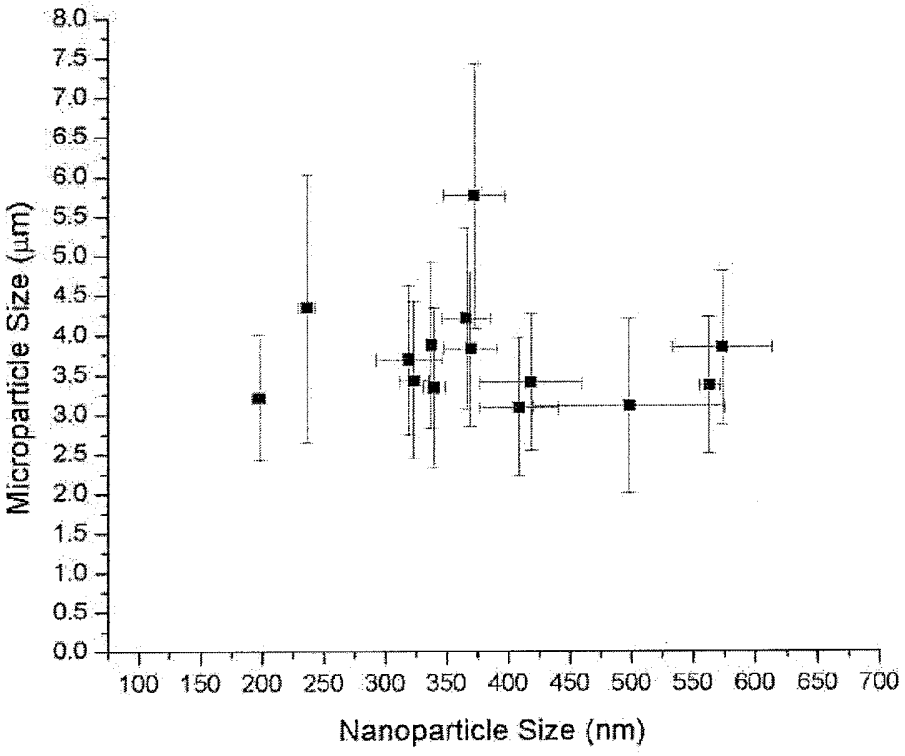
Microparticle Size (μm)
8.0
7.5
7.0
6.5
6.0
5.5
5.0
4.5
4.0
3.5
3.0
2.5
2.0
1.5
1.0
0.5
0.0
100 150 200 250 300 350 400 450 500 550 600 650 700
Nanoparticle Size (nm)

FIG. 40

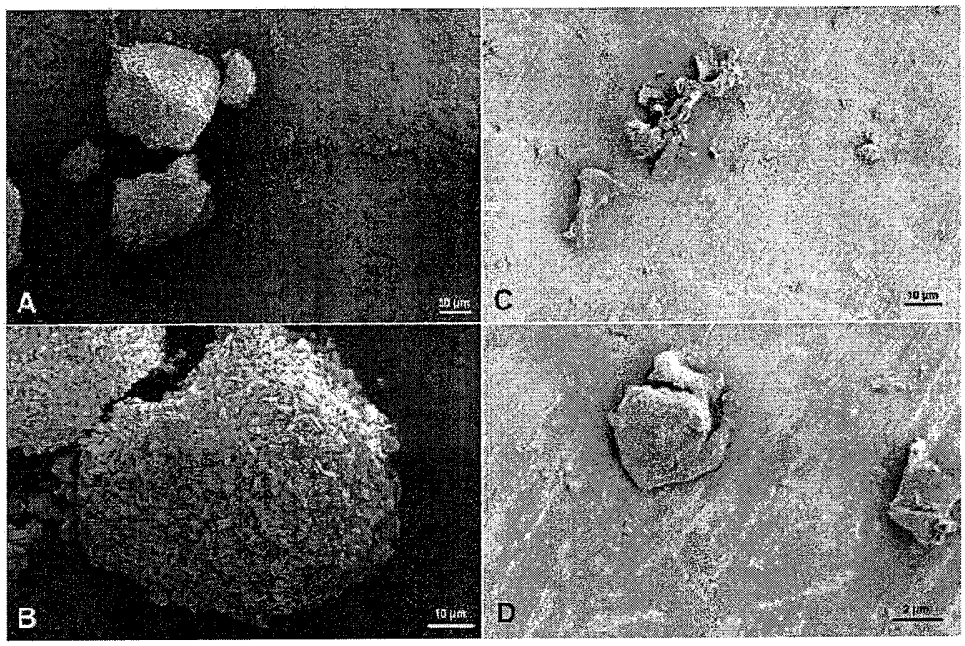

FIG. 41

FIG. 42

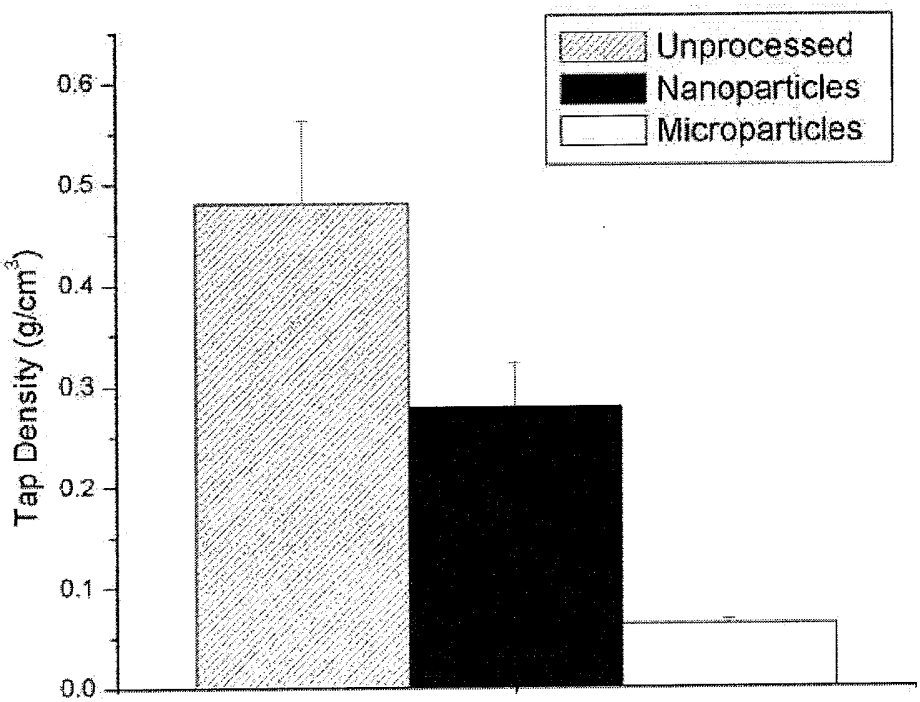
Unprocessed
Nanoparticles
Microparticles
Tap Density (g/cm3)
0.0
0.1
0.2
0.3
0.4
0.5
0.6

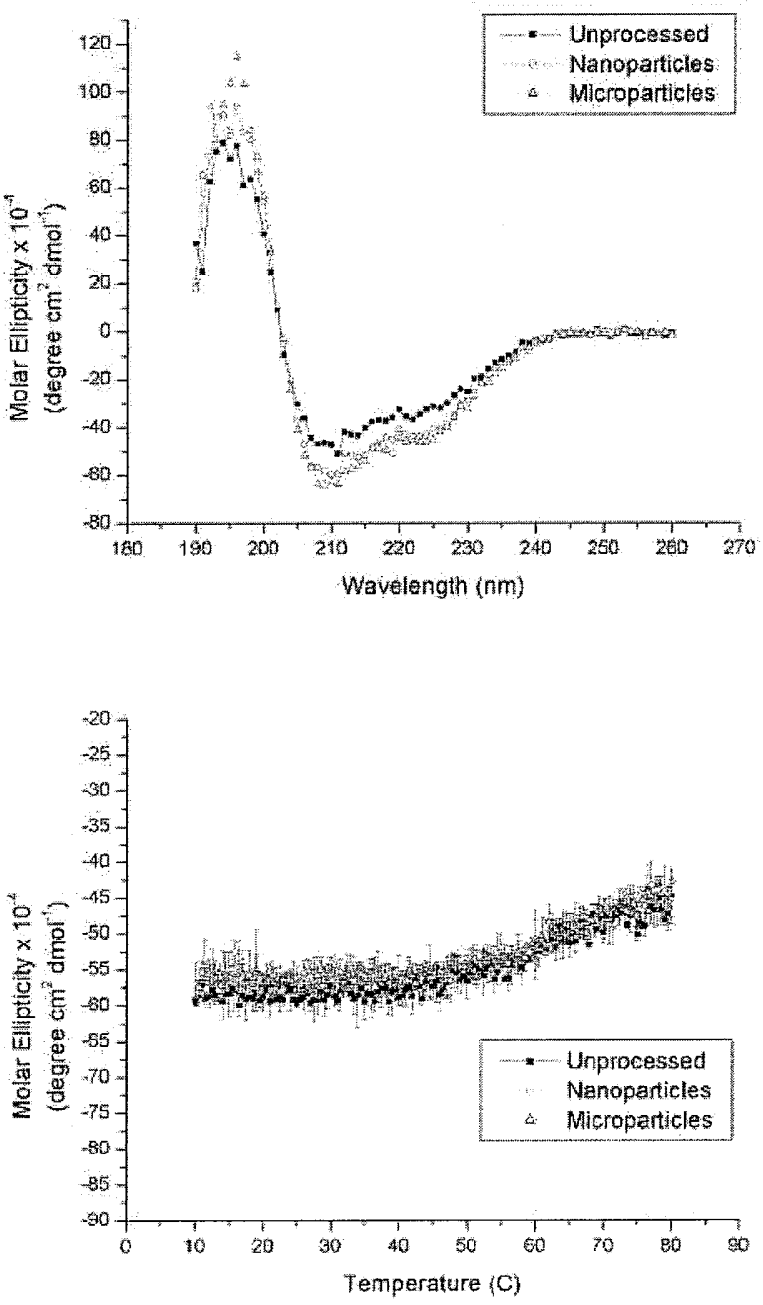
Unprocessed
Nanoparticles
Microparticles
Molar Ellipticity x 10^-4 (degree cm^2 dmol^-1)
Wavelength (nm)
Unprocessed
Nanoparticles
Microparticles
Molar Ellipticity x 10^-4 (degree cm^2 dmol^-1)
Temperature (C)

FIG. 43

FIG. 44

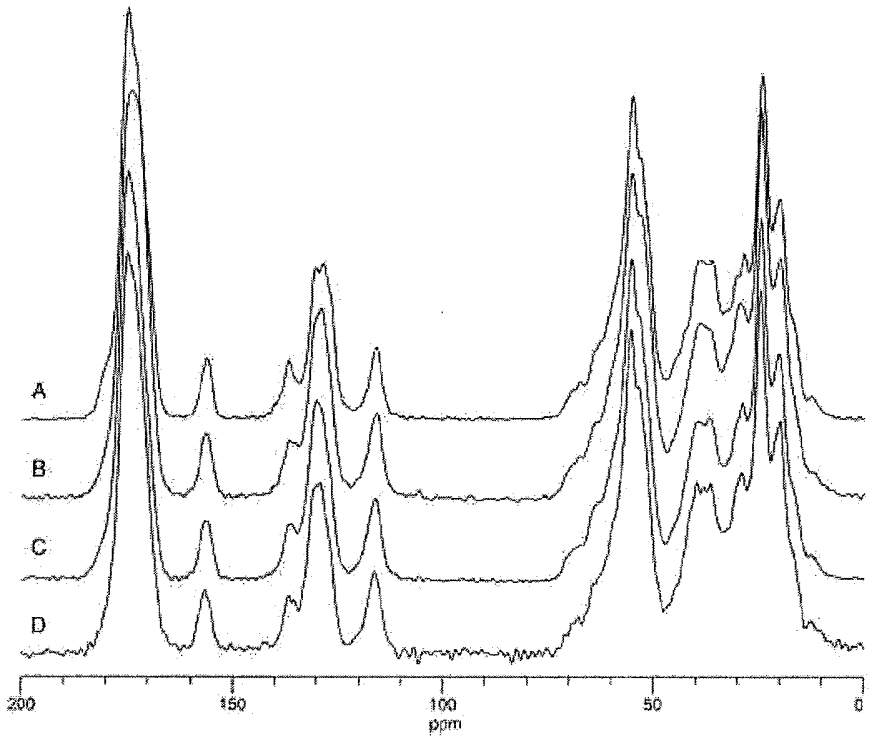

FIG. 45

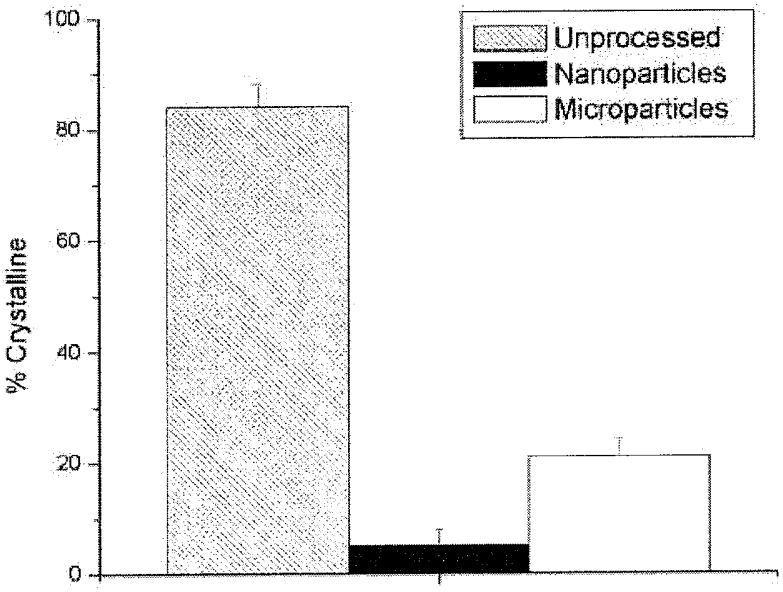
100
80
60
40
20
0
% Crystalline
Unprocessed
Nanoparticles
Microparticles

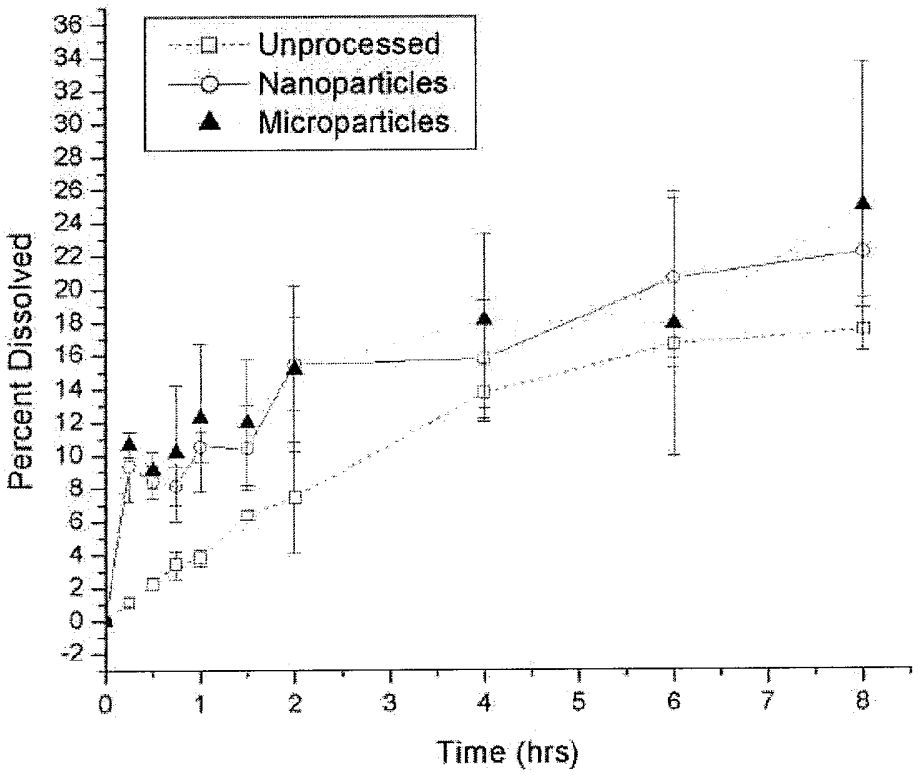
Unprocessed
Nanoparticles
Microparticles
Percent Dissolved
Time (hrs)
36
34
32
30
28
26
24
22
20
18
16
14
12
10
8
6
4
2
0
-2
0
1
2
3
4
5
6
7
8

FIG. 46

INTERNATIONAL SEARCH REPORT

International application No.
PCT/US 09/50565

A. CLASSIFICATION OF SUBJECT MATTER
IPC(8) - A61K 9/26
USPC - 424/469-470
According to International Patent Classification (IPC) or to both national classification and IPC

B. FIELDS SEARCHED

Minimum documentation searched (classification system followed by classification symbols)
USPC: 424/469-470

Documentation searched other than minimum documentation to the extent that such documents are included in the fields searched
USPC: 424/423; 427/2.1; 427/402; 427/458; 428/36.91;428/36.9; 428/426; 623/926 (see search terms below)

Electronic data base consulted during the international search (name of data base and, where practicable, search terms used)
PubWEST (PGPB, USPT, EPAB, JPAB) Google, Google Patent Search , Google Scholar
nanocluster, nanoparticles, nanoparticulate, drug, pharmaceutical, composition, chemotherapy, chemotherapeutic, paclitaxel, steroid, budesonide, hormone, insulin, tocolytic agent, vasodilator agent, calcium channel blocker, dihydropyridine

C. DOCUMENTS CONSIDERED TO BE RELEVANT

Category*	Citation of document, with indication, where appropriate, of the relevant passages	Relevant to claim No.
X --- Y	US 2007/0172653 A1 to (Berkland et al.) 26 July 2007 (26.07.2007) abstract; fig 1, para [0006], [0008]-[0016], [0019]-[0022], [0044]-[0045], [0052]-[0054], [0058], [0079], [0084]-[0085], [0088], [0122]-[0123]	1-4, 13-33, 45-49 ---------- 5-12, 34-44
Y	US 6,441,025 B2 (Li et al.) 27 August 2002 (27.08.2002) abstract; col 1, ln 10-18	5, 34, 36, 38, 40, 42
Y	Lenfers et al. Substantial activity of budesonide in patients with irinotecan (CPT-11) and 5-fluorouracil induced diarrhea and failure of loperamide treatment. Annals of Oncology, 1999, Vol 10: 1251-1253, summary; pg 1251, col 2, para 3-4; pg 1253, col 1, para 3-4	6-7, 12, 35-36, 38, 40, 42
Y	Alabaster et al. Metabolic Modification by Insulin Enhances Methotrexate Cytotoxicity in MCF-7 Human Breast Cancer Cells. Eur J Cancer Clin Oncol, 1981, Vol 17, No 1, pp. 1223-1228, abstract; fig 1, pg 1223, col 2, para 3; pg 1225, col 2, para 4; pg 1228, col 2, para 2	8-9, 37-38, 40, 42
Y	US 5,362,729 A (Cozzi et al.) 8 November 1994 (08.11.1994) col 10, ln 4-11; col 14, ln 11-25	10, 39
Y	Thews et al. Nifedipine improves blood flow and oxygen supply, but not steady-state oxygenation of tumours in perfusion pressure controlled isolated limb perfusion. British Journal of Cancer, 2002, Vol 87, pp 1462-1469; abstract; pg 1463, col 1, para 2-3; pg 1463, col 2, para 2	11-12, 40, 42
Y	Lieberman et al. Pharmaceutical dosage forms-- disperse systems. Informa Health Care, 1996, Vol 2, Ed 2, Fig 3, Table 4; pg 18, para 7; pg 19, para 1-2; pg 29, para 3; pg 166, para 1-3; page 288, para 3	41, 43-44

☐ Further documents are listed in the continuation of Box C. ☐

* Special categories of cited documents:
"A" document defining the general state of the art which is not considered to be of particular relevance
"E" earlier application or patent but published on or after the international filing date
"L" document which may throw doubts on priority claim(s) or which is cited to establish the publication date of another citation or other special reason (as specified)
"O" document referring to an oral disclosure, use, exhibition or other means
"P" document published prior to the international filing date but later than the priority date claimed
"T" later document published after the international filing date or priority date and not in conflict with the application but cited to understand the principle or theory underlying the invention
"X" document of particular relevance; the claimed invention cannot be considered novel or cannot be considered to involve an inventive step when the document is taken alone
"Y" document of particular relevance; the claimed invention cannot be considered to involve an inventive step when the document is combined with one or more other such documents, such combination being obvious to a person skilled in the art
"&" document member of the same patent family

Date of the actual completion of the international search	Date of mailing of the international search report
18 August 2009 (18.08.2009)	08 SEP 2009
Name and mailing address of the ISA/US Mail Stop PCT, Attn: ISA/US, Commissioner for Patents P.O. Box 1450, Alexandria, Virginia 22313-1450 Facsimile No. 571-273-3201	Authorized officer: Lee W. Young PCT Helpdesk: 571-272-4300 PCT OSP: 571-272-7774

Form PCT/ISA/210 (second sheet) (July 2009)